# A Study on Parametric Appraisal of Drilling on Bio-compatible Materials

A THESIS SUBMITTED IN FULFILLMENT OF

THE REQUIREMENT FOR THE AWARD OF THE DEGREE

OF

**Master of Technology (Research)**

**in**

**Mechanical Engineering**

Submitted

by

**Suman Chatterjee**
(Roll No. 612ME301)

Under the Supervision of

**Prof. Siba Sankar Mahapatra**


**Department of Mechanical Engineering**

**National Institute of Technology, Rourkela 769008**

August 2014

*Devoted to my best loving family*


# CERTIFICATE

This to certify that the thesis entitled "**A Study on Parametric Appraisal of Drilling on Bio-compatible Materials**" being submitted by **Suman Chatterjee** for the award of the degree of Master of Technology (Research) (Mechanical Engineering) of NIT Rourkela, is a record of bonafide research work carried out by him under our supervision and guidance. **Mr. Suman Chatterjee** has worked for more than two years on the above problem at the Department of Mechanical Engineering, National Institute of Technology, Rourkela and this has reached the standard fulfilling the requirements and the regulation relating to the degree. The contents of this thesis, in full or part, have not been submitted to any other university or institution for the award of any degree or diploma.

Dr. Siba Sankar Mahapatra
Professor
Department of Mechanical Engineering
National Institute of Technology,
Rourkela

Place: Rourkela
Date:

# *ACKNOWLEDGEMENT*

This thesis is a result of research that has been carried out at **National Institute of Technology, Rourkela**. During this period, I came across with a great number of people whose contributions in various ways helped my field of research and they deserve special thanks. It is a pleasure to convey my gratitude to all of them.

In the first place, I would like to express my deep sense of gratitude and indebtedness to my supervisor **Prof. S.S. Mahapatra** for his advice and guidance from early stage of this research and providing me extraordinary experiences throughout the work. Above all, they provided me unflinching encouragement and support in various ways which exceptionally inspire and enrich my growth as a student, a researcher and a scientist.

I specially acknowledge **Prof. S.S. Mahapatra** for his advice, supervision and crucial contribution as and when required during this research. His involvement with originality has triggered and nourished my intellectual maturity that will help me for a long time to come. I am proud to record that I had opportunity to work with an exceptionally experienced scientist like him.

I am grateful to **Prof. S.K. Sarangi**, Director, **Prof. S.S. Mahapatra**, Head of Mechanical Engineering Department, **Prof. K.P. Maity**, former Head of Mechanical Engineering Department, and **Prof. S. Datta,** Professor Mechanical Engineering Department, National Institute of Technology, Rourkela, for their kind support and concern regarding my academic requirements. I am very much thankful to all my teachers

I express my thankfulness to the faculty and staff members of the Mechanical Engineering Department for their continuous encouragement and suggestions. Among them, **Sri P. K. Pal** deserves special thanks for his kind cooperation in non-academic matters during the research work. I also thankful to **Prof. S.K. Patel,** Professor Mechanical Engineering Department, **Mr.**

**Sudhansu Sekhar Samal,** Technical Assistant Central Workshop Mechanical Engineering Department, for providing me the facility and guidance for performing the experiments.

I am indebted to **Dr. Saurav Dutta, Mr. Kumar Abhishek, Ms. Bijaya Bijeta Nayak, Mr. Chhabi Ram Matawale, Mr. Manas Ranjan Singh, Mr. Rajiv Kumar Yadav, Mr. Chitrasen Samantra, Mr. Chinmaya Prasad Mohanty, Mr. Vikas Sonkar, Mr. Swayam Bikas Mishra** and **Ms. Sanjita Jaipuria** for their support and co-operation which is difficult to express in words. The time spent with them will remain in my memory for years to come.

Special thanks are also due to **Dr. R. Ganesh Narayan, Mr. Arpan Kumar Mondal, Mr. Jiten Basumatary** and **Mr. Pranjol Paul,** Department of Mechanical Engineering, Indian Institute of Technology, Guwahati, for kind support and co-operation during my experimental work.

**My parents** and **My Brother** deserve special mention for their inseparable support and prayers. They are the persons who show me the joy of intellectual pursuit ever since I was a child. I thank them for sincerely bringing up me with care and love. I thank them for being supportive and caring.

Last, but not the least, I thank the one above all of us, the omnipresent God, for giving me the strength during the course of this research work.

*Suman Chatterjee*

## ABSTRACT

Titanium alloy and stainless steel finds widespread applications in different fields such as bio-medical, aerospace and electronics due to their superior physical properties (high strength, toughness, corrosion resistance and durability and low density). Due to their bio-compatibility in nature, they are used in the field of bio-medical engineering such as artificial bone joints, artificial knee joints and in dental fields. Drilling is one of the important machining processes involved in most of the application fields including bio-medical engineering. This study investigates the effect of drilling parameters on performance measures through development of numerical model using finite element approach. The numerical model is validated by experimental study. The parameters included for investigation are spindle speed, feed rate and drill diameter. The experimental plan is made using design of experiment approach, specifically a face centered central composite design of response surface methodology in order to reduce the experimental runs and reduce cost of experimentation. The output performance characteristics considered are burr height at entry, burr height at exit, surface roughness, circularity at entry and circularity at exit. In order to optimize multiple responses simultaneously, the responses are converted into single response using superiority and inferiority ranking (SIR) method. Empirical model relating machining parameters with output responses have been developed using non-linear regression analysis. An improved version of latest evolutionary approach known as Harmony Search (HS) algorithm has been is used to find out best parametric condition subjected to constraints such as circularity at entry and circularity at exit. The study also investigates the effect of high speed laser drilling process of Ti6Al4V and AISI 316 stainless steel during laser drilling. Laser machining is carried out using assistant gas as nitrogen environment using a 2.5 kW $CO_2$ laser. The experimental planning has been done using Taguchi $L_9$ orthogonal design. The machining parameters used for investigation in the study are flushing pressure, laser power and pulse frequency. The output responses investigated are heat affected zone (HAZ), spatter area, circularity and taper of hole. Parametric study on drilling process helps in providing guidelines to the practitioners for securing the implant material in an adequate manner.



Keywords: Harmony Search (HS) algorithm; Laser Drilling; Numerical Modeling; Superiority and Inferiority Ranking (SIR) Method

## Table of Contents

## List of Figures

## List of Tables

## Glossary of Terms

| | |
|---|---|
| % | Percentage |
| µ | Micron |
| µm | Micro Meter |
| 3D | Three Dimensional |
| ABC | Artificial Bee Colony |
| Al | Aluminium |
| ANN | Artificial Neural Network |
| ANOVA | Analysis of Variance |
| BA | Bat Algorithm |
| $B_{en}$ | Burr Height at Entry |
| $B_{ex}$ | Burr Height at Exit |
| bw | Bandwidth |
| $bw_{max}$ | Maximum Bandwidth |
| $bw_{min}$ | Minimum Bandwidth |
| CAD | Computer Aided Design |
| cc | Cubic Centimeter |
| CCD | Central Composite Design |
| $C_{ent}$ | Circularity at Entry |
| $C_{exit}$ | Circularity at Exit |
| CFRP | Carbon Fibre Reinforcement Plastic |
| CNC | Computer Numerical Control |
| $CO_2$ | Carbon Dioxide |
| Cr | Chromium |
| CS | Cuckoo Search |
| $D_1$ | Diameter One |
| $D_2$ | Diameter One |
| $D_{ent}$ | Diameter at Entry |
| $D_{exit}$ | Diameter at Exit |
| df | Degree of Freedom |
| DOE | Design of Experiment |
| EDS | Energy Dispersive Spectroscopy |
| Exp. | Experimental |
| F value | Fishers Value |
| FE | Finite Element |
| Fe | Iron |
| FEA | Finite Element Analysis |
| FEM | Finite Element Method |
| FRP | Fibre Reinforcement Plastic |
| g | Gram |
| GA | Genetic Algorithm |
| gn | Generation |
| GPa | Giga Pascal |
| HAZ | Heat Affected Zone |
| HM | Harmony Memory |
| HMCR | Harmony Memory Considering Rate |
| HMS | Harmony Memory Size |
| HS | Harmony Search |
| Hz | Hertz |
| Ibs | Pounds |

| | |
|---|---|
| I-flow | Inferiority Flow |
| I-matrix | Inferiority Matrix |
| K | Kelvin |
| kN | Kilo Newton |
| kW | Kilo Watt |
| l | Litre |
| m | Meter |
| MADM | Multi Attribute Decision Making |
| Mb | Mega Byte |
| MCDM | Multi Criteria Decision Making |
| min | Minute |
| mm | Millimeter |
| MPa | Mega Pascal |
| MPI | Multi-Response Performance Index |
| MS | Mean Square |
| $N_2$ | Nitrogen Gas |
| NC | Numeric Controller |
| Nd:Yag | Neodymium-Doped Yttrium Aluminium Garnet |
| NI | Number of Iteration |
| Ni | Nickel |
| $O_2$ | Oxygen Gas |
| Pa | Pascal |
| PAR | Pitch Adjusting Rate |
| $PAR_{max}$ | Maximum Pitch Adjusting Rate |
| $PAR_{min}$ | Minimum Pitch Adjusting Rate |
| PC | Principal Component |
| PCA | Principal Component Analysis |
| PSO | Particle Swarm Optimization |
| p-value | Probability Value |
| PVD | Physical Vapour Deposition |
| $R^2$ | Co-Efficient of Determination |
| $R_a$ | Surface Roughness |
| RE | Relative Error |
| rpm | Revolution Per Minute |
| RSM | Response Surface Methodology |
| SA | Simulated Annealing |
| SEM | Scanning Electron Microscopy |
| SFLA | Shuffled Frog Leaping Algorithm |
| S-flow | Superiority Flow |
| Sim. | Simulation |
| SIR | Superiority and Inferiority Ranking |
| S-matrix | Superiority Matrix |
| SS | Sum of Square |
| Ti | Titanium |
| TiN | Titanium Nitrate |
| TOPSIS | Technique for Order Preference by Similarity to Ideal Solution |
| TS | Tabu Search |
| V | Vanadium |
| viz. | Such as |
| W | Watt |

| | |
|---|---|
| WC | Tungsten Carbide |
| WPCA | Weighted Principal Component Analysis |

# CHAPTER 1

# BACKGROUND AND MOTIVATION

# CHAPTER 1

# BACKGROUND AND MOTIVATION

## 1.1. Introduction

Materials which are designed to replace and perform as living tissue inside the living organisms are known as biocompatible materials. An ideal biomaterial exhibits properties like high biocompatibility, mechanical strength, wear and fatigue resistance and low elastic modulus. To achieve all these properties in a single material, it is somewhat difficult. Due to their excellent mechanical properties and good biocompatibility, some metals are used as biomaterials. As the metallic bonds in these materials are essentially non-directional, the position of the metallic ions can be changed without destroying the crystal structure. This results in a plastically deformable solid. The principal demerit of metals is tendency of corrosion in an in-vivo environment (Oldani and Dominguez 2012). The corrosion of metals leads to several consequences such as weakening of the implant, erosion of the implant materials and harmful effect on the organs and tissues near the surroundings.

Some of the metallic biomaterials conveniently used for replacement of hard tissues such as dental implants, spinal fixation devices, and total knee and hip joints are titanium alloys and stainless steel.

## 1.2. Titanium alloys

Titanium and titanium alloys are extensively used in manufacturing industries due to their excellent properties such as high strength to weight ratio and corrosion resistance even at high temperature (Boyer 1996). Among all the alloys, Ti6Al4V is widely used for most of the daily as well as bio-medical applications. Ti6Al4V is a combination of alpha-beta alloy having chemical composition of 6% aluminium, 4% vanadium and remaining titanium material. Aluminium stabilizes and strengthens the alpha phase raising the beta-transus temperature (Tamirisakandala et al. 2005) as well as reducing the density of the alloy. The vanadium is a beta stabilizer that provides a greater amount of ductile beta phase during hot working. Ti6Al4V is considered superior to other titanium alloys and suitable for aerospace applications due to favorable mechanical properties such as low density, high strength, fracture resistance, chemical inertness and excellent corrosion resistance (Gorsse and Miracle 2003; Biswas and Majumdar 2009). Ti6Al4V alloy is also used in bio-medical engineering, turbine blade manufacturing, bone supplement in bone

grafting, automobile and chemical industries (Boyer 1996; Alonso et al. 2003; Geetha et al. 2009; Jha et al. 2010).

In early 1930s, the titanium was first time used for implantation purpose. It was noted that the titanium have good bioactive behaviour due to formation of hydrated oxide layer on the surface of implant leading to incorporation of natural human bone (Li et al. 1994; Oldani and Dominguez 2012). Table 1.1 shows the properties of Ti6Al4V.

Table 1.1: Properties of Ti6Al4V (ASM Aerospace Specification Metals, Inc.)

| **Properties** | **Metric** |
|---|---|
| Density | 4.43 g/cc |
| Hardness, Rockwell C | 36 |
| Tensile strength, Ultimate | 950 MPa |
| Modulus of Elasticity | 113.8 GPa |
| Poisson's Ratio | 0.342 |
| Thermal conductivity | 6.7 W/m-K |

### 1.3. Stainless steel

Austenitic stainless steel (AISI 316) is widely used in the field of aerospace, automobile and medical engineering. Due to their favorable machinability and mechanical properties such as non-magnetic nature, non-heat treatable, high strength, low heat conductivity, low density and chemical properties such as chemically inert, superior pitting corrosion resistance, they are extensively used in many engineering applications. The favourable properties make it a preferred material for applications in making medical devices and implants materials especially in joint replacement of hip and knees, bone screws and plate for fracture fixation. Table 1.2 shows the properties of AISI 316.

Table 1.2: Properties of AISI 316 (ASM Aerospace Specification Metals, Inc.)

| **Properties** | **Metric** |
|---|---|
| Density | 8 g/cc |
| Hardness, Rockwell C | 79 |
| Tensile strength, Ultimate | 580 MPa |
| Modulus of Elasticity | 193 GPa |
| Poisson's Ratio | 0.27-0.30 |
| Thermal conductivity | 16.3 W/m-K |

### 1.4. Drilling

Drilling as well as micro-drilling (diameter < 0.5 mm) of Ti6Al4V and AISI 316 is a challenging task due to high strength-to-density ratio, toughness, fracture resistance characteristics, cutting temperature (due to low thermal conductivity), chemically reactive in nature at high temperature, creating strong adhesion to tool surface by the work piece

(Boyer et al. 1994; Welsch 1993; Lin et al., 1995; Mohanty 2011). As high temperature is generated near the cutting edges of the tool during drilling process, rapid wear of cutting tools occurs (Dornfeld et al. 1999, Mohanty 2011; Cantero et al. 2005; Rahim and Sharif 2006; Gandarias et al. 2008; Riester et al. 2008; Caydas et al. 2011; Soreng 2011; Taruma et al. 2012;). This phenomenon leads to formation of burrs and tool failure during drilling operation.

**1.5. Laser drilling**

Laser drilling operation is a non-conventional drilling process where laser is used for making holes. Since there is no contact between tool and the work materials in laser drilling, it eliminates the problems of chatter and vibration during machining (Chryssolouriset al. 1988). The standard lasers used for the laser machining process are ruby laser, Nd:YAG (Neodymium Yttrium Aluminum Garnet) and carbon dioxide ($CO_2$) gas. Lasers are sustainable alternative for machining of materials such as metals, composites, ceramics, and polymers (Majumdar and Manna 2011; Jeon and Lee 2012). In laser drilling, high energy infrared laser beam is focused on a spot in the work piece (generally varies between 0.1-2.0 mm in diameter) resulting in melting, vaporization, chemical degradation throughout the depth of the material. Deep holes with small diameters can be drilled with little thermal or mechanical damage to the material. Its wide range of applications includes in field of medical, aeronautics, automobiles and manufacturing industries. The current challenge is to investigate the effects of laser process parameters such as laser power, pulse frequency and flushing pressure on the process outputs like heat affected zone (HAZ), taper of the kerf and quality of the surface during laser drilling (Akman et al. 2009; Leone et al. 2010; Pandey and Dubey 2012).

**1.6. Need for research**

Through exhaustive literature survey (Chapter 2), it is noticed that limited research work has been directed to study the effect of drilling parameters on quality of holes while drilling of materials like Ti6Al4V and AISI 316. Metal removal is one of the major concerns in case of micro-drilling operation. The burr formation at entry side of drilled hole affects the quality of hole. The drill bits in micro-drilling are fractured by small impact of tool and work piece because bending occurs due to their slender shape. Drilling of materials like titanium alloys and stainless steel is a challenging task due to work hardening of the materials and rubbing of tools against the hardened zone causing

rapid tool wear (Bellows and Kohls 1982; Guo and Caslaru 2011; Kudla 2011; Karum and Ozcelik 2014).

The following are the research gap noticed after the literature survey:

- Few studies have been reported to analyze the effect of drilling parameters on output responses viz. thrust, torque and circularity of holes numerically on drilling of Ti6Al4V and AISI 316.
- Few experimental investigations have been attempted to analyze the effect of micro-drilling on the materials like Ti6Al4V and AISI 316.
- Limited number of studies has reported the effect of flushing pressure in laser drilling.
- Few attempts have been made in which $CO_2$ laser is used for drilling of metals like Ti6Al4V and AISI 316.

In the present study, simulation of drilling operation of bio-compatible materials has been carried out to analyze the effect of drilling parameters such as spindle speed, feed rate and drill diameter on the output responses such as thrust force, torque and circularity at entry and exit of the drilled hole. To check the adequacy of the developed numerical model, comparison between simulation and experimental results for few sets has been made. A multi-objective optimization scheme for drilling responses such as burr height at entry and exit and surface roughness has been proposed using superiority and inferiority ranking (SIR) method for conversation of multiple responses into a single equivalent response. An empirical relation between multiple response characteristic known as R-flow value and process parameters has been developed. In order to obtain best parametric setting, a recently developed meta-heuristic algorithm known as harmony search (HS) algorithm is used to explore the optimization space effectively. To investigate the challenges in laser drilling, the study investigates the effect of laser process parameters such as laser power, pulse frequency and flushing pressure on the responses like heat affected zone (HAZ), taper of the kerf and quality of the surface in the machining process using $CO_2$ laser cutting machine.

### 1.7. Research Objectives

The objectives of this dissertation rest on of research gap found through exhaustive literature survey presented in Chapter 2. Literature suggests that titanium alloy (Ti6Al4V) and stainless steel (AISI 316) have been proven to be good materials for metal implants. To use these biocompatible materials, there is a need to adopt a machining process like drilling. Precisely, the dissertation presents for developing a better understanding of

phenomenon involved in conventional and non-conventional drilling of bio-compatible materials.

To this end, the objective for this research work objectives are as follows:

- To develop a finite element based model for studying the effect of control parameters during drilling of bio-compatible materials.
- To study the effect of control parameters on output responses during drilling of bio-compatible materials.
- To conduct a parametric analysis of high speed laser during drilling of bio-compatible materials.

### 1.8. Structure of the Thesis

The dissertation is organized as follows:

CHAPTER 1: Background and Motivation

This chapter introduces the concept of drilling and its growth in terms of applications in diverse fields of applications. The chapter also provides the summary of problem statement to be addressed in this research.

CHAPTER 2: Literature Review

This chapter reviews related literature to provide background information on the issues to be considered in the thesis and emphasize the relevance of the present study. The search was restricted on those articles for which full text is available. The study is categorized into three parts such as numerical analysis of drilling process, drilling of metallic materials and laser drilling process.

CHAPTER 3: Numerical Approach for the Drilling Process

In this chapter, numerical analysis has been performed using FEM based software DEFORM-3D™. The modeling has been done for the estimation of the responses such as thrust force, torque, circularity at entry and exit during drilling of Ti6Al4V and AISI 316.

CHAPTER 4: Experimental investigation of Drilling Process

In this chapter, study of control parameters on process responses during drilling of Ti6Al4V and AISI 316 has been carried out. A method known as SIR-TOPSIS (superiority and inferiority ranking aggregated with technique for order preference by similarity to ideal solution) has been proposed for converting multiple responses into single equivalent response. Harmony search (HS) algorithm has been implemented for optimization of the single equivalent response.

CHAPTER 5: Experimental Investigation of Laser Drilling Process

This chapter investigates the influence of process parameters like flushing pressure (Pa), laser power (W) and pulse frequency (Hz) on taper, heat affected zone (HAZ), spatter area and circularity of the laser drilled hole. This study also presents the suitability of different materials during laser drilling using $CO_2$ laser having capacity of 2.5 kW.

CHAPTER 6: Executive Summary and Conclusions

This chapter presents the brief summary of findings, major contribution to research work and future scope of the research.

The dissertation enclosed with the references and list of publications.

**1.9. Conclusions**

The present chapter highlights the necessity of drilling analysis in field of manufacturing, aerospace and automobile industry and biomedical engineering. The chapter also focuses on the need of study of drilling of metallic alloys using laser drilling and the research objectives with layout of the thesis.

# CHAPTER 2

# LITERATURE REVIEW

# CHAPTER 2

# LITERATURE REVIEW

## 2.1. Introduction

The current chapter highlights the development and problems associated with various aspects related to drilling of bio-compatible materials. One of the major challenges that appear during drilling is the rapid tool wear due to toughness of the material and poor thermal conductivity. In case of laser drilling, the major challenge is the reduction of taper of the kerf. Table 2.1 provides the source and number of citations from each source to analyze the trend of research in this direction. The majority of the citations are taken from peer-reviewed journals for which full text is available.

Table 2.1: List of Publications Cited

| Publications | Citations |
|---|---|
| Acta Biomaterialia | 2 |
| Advanced Materials Research | 4 |
| Applied Mechanics and Materials | 1 |
| Applied Mathematics and Computation | 1 |
| Biomaterials | 1 |
| Books | 8 |
| Ceramics International | 1 |
| CIRP Annals-Manufacturing Technology | 7 |
| CIRP Journal of Manufacturing Science and Technology | 1 |
| Computer Methods in Applied Mechanics and Engineering | 1 |
| Computer-Aided Design | 1 |
| Computers and Industrial Engineering | 1 |
| Construction Innovation: Information, Process, Management | 1 |
| Engineering Applications of Artificial Intelligence | 1 |
| European Journal of Operational Research | 1 |
| Expert Systems with Applications | 1 |
| Indian Journal of Engineering and Materials Sciences | 1 |
| International Journal of Applied Metaheuristic Computing | 1 |
| International Journal for Numerical Methods in Biomedical Engineering | 1 |
| International Journal of Advanced Manufacturing Technology | 16 |
| International Journal of Fatigue | 1 |
| International Journal of Machine Tools and Manufacture | 9 |
| International Journal of Machining and Machinability of Materials | 1 |
| International Journal of Precision Engineering and Manufacturing | 1 |
| Journal of Dental Research | 4 |

| | |
|---|---|
| Journal of Intelligent Manufacturing | 2 |
| Journal of Japan Institute of Light Metals (Japan) | 1 |
| Journal of Macromolecular Science - Chemistry | 1 |
| Journal of Materials Processing Technology | 12 |
| Journal of Materials Science: Materials in Medicine | 1 |
| Journal of Mechanical Science and Technology | 1 |
| Journal of Micromechanics and Microengineering | 1 |
| Journal of the Mechanical Behavior of Biomedical Materials | 2 |
| Journal of the Royal Society Interface | 1 |
| Keikinzoku | 1 |
| Materials and Design | 1 |
| Materials and Manufacturing Processes | 6 |
| Materials Science and Engineering: Part A | 1 |
| Measurement | 3 |
| Optics and Laser Technology | 3 |
| Optics and Lasers in Engineering | 1 |
| Procedia CIRP | 1 |
| Procedia Engineering | 1 |
| Proceedings of the World Congress on Engineering | 1 |
| Revista Facultad de Ingenieria | 1 |
| Robotics and Computer-Integrated Manufacturing | 1 |
| Science and Technology of Advanced Materials | 1 |
| Solid State Phenomena | 1 |
| Thesis | 1 |
| Transactions of Nonferrous Metals Society of China | 1 |
| Third WSEAS International Conference on Visualization, Imaging and Simulation | 1 |
| **Total** | **116** |

### 2.2. Classification of Literatures

The literature review gives enough confidence to identify a pertinent gap or methodological weaknesses in the existing literature to solve the research problem. The literature on drilling of bio-material can be broadly classified in two ways - one based on drilling process and other one is laser drilling process which is illustrated in Figure 2.1. Next sections provide brief discussion on these issues. Finally, chapter is concluded by summarizing the advancement in drilling process and possible literature gap so that relevance of the present study can be emphasized.

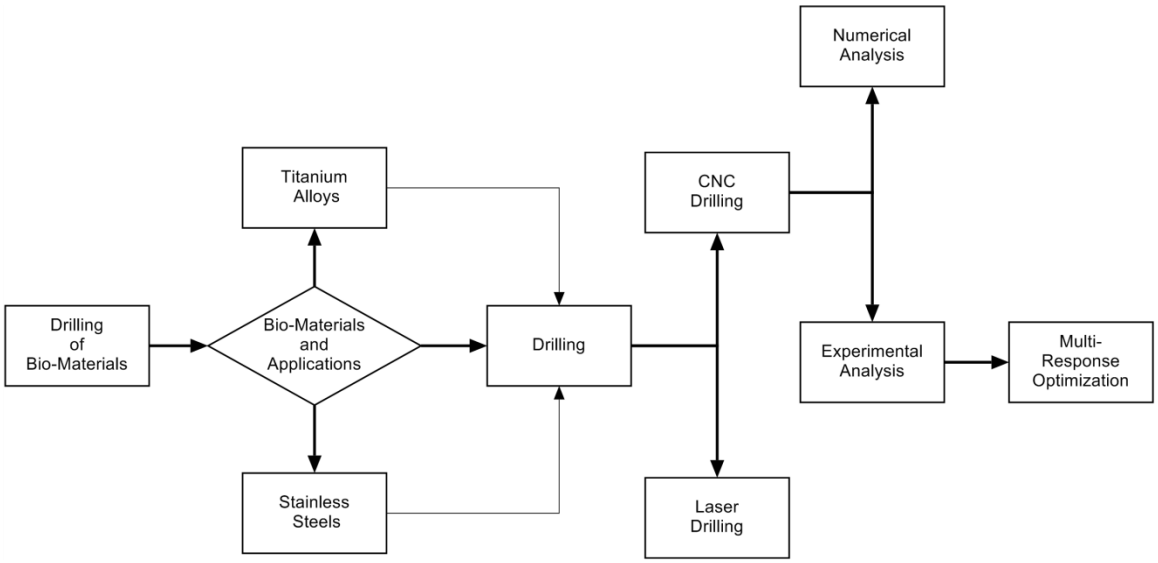

Figure 2.1: Taxonomic framework for drilling of bi-compatible materials

### 2.3. Bio-compatible Materials

Biocompatible material (Bio-material) is a synthetic or natural material used to transplant parts of living body and works in familiar contact with living tissues (Homsy et al. 1970; Hench and Ethridge 1982). Grafting of bone is a surgical technique used to substitute bone in order to repair or replace damaged or fractured bones. The surgical technique is an enormously complex procedure and poses a substantial health risk of the patient (Hench 1998; Cao and Hench 1996). Boyer (1996) has mentioned that the principal metallic bio-materials are aluminium, cobalt-chromium alloys, stainless steel, titanium and its alloy. Titanium alloy (Ti6Al4V) and stainless steel (AISI 316) are the good alternatives for implants (Navarro et al. 2008). Titanium alloy (Ti6Al4V) has been basically used in aerospace applications (Denizard et al. 2008) due to their excellent properties such as low density, high strength, non-toxicity and non-corrosive in nature. The corrosion resistance property makes it useful for biomedical applications (Murr et al. 2009; Krishna et al. 2008; Denizard et al. 2008 and Gepreel and Niinomi 2013). The corrosion resistance property is occurring due to formation of self-organized oxide layers on the surface of alloys (Minagar et al. 2012; Fleck and Eifler 2010). It is acknowledged that titanium and its alloying elements like niobium, molybdenum, zirconium, tantalum, silicon and tin are bio-compatible in nature (Wang et al. 2004; Li et al 2010; Gittens et al. 2011; Alghamdi et al. 2013). Yang and Ren (2010) have suggested that austenitic stainless steels are best suited for the medical applications due to high strength, good plasticity, wear and corrosion resistance, stable austenitic structure and bio-

compatibility. Dewidar et al. (2007) have proposed a fabrication technique to develop a porous 316 austenitic stainless steel for bone implantation The presence of porosity in the material leads to growth in new bone tissues. Table 2.2 shows some of the synthetic bio-materials and their bio-medical applications.

Table 2.2: List of some synthetic materials used for bio-medical applications (Ratner 2004 and Mohanty 2011).

| **Bio-medical applications** | **Materials** |
|---|---|
| **Skeleton System** | |
| Joint replacements (knee, hip) | Titanium, Ti6Al4V alloy, stainless steel, polyethylene |
| Bone plate for fracture fixation | Stainless steel, cobalt-chromium alloy |
| Bone defect repair | Hydroxyl-apatite |
| Artificial tendon and ligament | Teflon, Dacron |
| Dental implant for tooth fixation | Titanium, Ti6Al4V alloy, stainless steel, polyethylene, titanium, alumina, calcium phosphate |
| **Cardiovascular System** | |
| Blood vessel prosthesis | Dacron, Teflon, polyurethane |
| Heart valve | Reprocessed tissue, stainless steel, carbon |
| Catheter | Silicone rubber, Teflon, polyurethane |

### 2.4. Drilling Operation

Drilling is a commonly adopted machining operation in industrial as well as surgical processes. Drilling is one of major conventional machining processes mainly used for joining of the components (Lee et al 2009). Drilling operation generally produces burrs on the surfaces causing deformation of holes. Burr on holes degrades the quality of the products, reduces the surface finish, distorts the holes and creates assembling issues. Drilling operation widely performed aerospace and biomedical science where the thrust force (Bouzakis et al. 2009) and circularity of holes are important issues to be looked into. The circularity of holes in drilling, expressed as the ratio of minimum Farret diameter to maximum Farret diameter (Ghoreishi et al. 2002), depends on machining parameters and cutting tool configurations (Shyha et al. 2010). Less chip formation near the hole edges and good surface finish on the hole surface are desirable during drilling, (Sakurai et al. 1992; Sakurai et al. 1992, Bhowmick and Alpas 2008). It is advisable to find optimum parametric setting to attain less chip/burr formation, high circularity and minimum surface roughness (Rajmohan and Palanikumar et al. 2012; Myers and Montgomery 1995). The twist drill possesses a complex geometry as compared to other cutting tools used for machining processes. Kurt et al. (2009) have pointed out that the work piece, drill geometry and the drill bit material are important parameters that influence circularity of the drilled hole. This is to be noted that burrs at entry and exit side

of the drilled hole is formed due to the plastic deformation of the work piece during drilling operation (Pilny et al. 2012). Yoon et al. (2011) have developed a response surface methodology (RSM) model for analyzing the shape factors of tools in micro-drilling process. Kilickap (2010) have developed the mathematical model for estimating burr height and surface roughness during drilling of Al-7075 using RSM concept. Many studies have been made for predicting the burr size in drilling operation using RSM and Taguchi technique (Karnik et al. 2008; Cicek et al. 2013). Mandal et al. (2011), Kivak et al. (2012) and Asilturk and Neseli (2012) have proposed Taguchi's experimental design approach for minimizing tool wear, surface roughness, and thrust force in drilling operation.

Drilling of titanium alloys is a challenging task due to its high strength (strength-to-density ratio), corrosion resistance and fracture resistive characteristics (Boyer et al. 1994). In comparison to machining of other materials, machining of titanium and its alloys is a difficult process due to low modulus of elasticity and conductivity because it possesses high strength at elevated temperature (Lutjering and Wiliams 2003; Ramesh et al 2008; Ramesh et al. 2008). Arrazola et al. (2009) and Armendia et al. (2010) have reported that titanium alloys have poor machinability through extensive experimental studies at various machining conditions. Due to high heat generation (because of low thermal conductivity), it is difficult to drill the Ti6Al4V alloy as it leads to rapid tool wear occurring at the tip of tool-work piece interface (Perez et al. 2000; Leyens and Peters 2003; Cantero et al. 2005). As it is chemically reactive with most of the tool materials, a strong adhesion wear occurs resulting in tool failure. Cantero et al. (2005) have performed dry drilling on Ti6Al4V with TiN coated carbide drill bit at different machining conditions for continuous drilling of workpiece to study the tool wear. Hong and Ding (2001) have conducted machining operation under cryogenic environment using liquid nitrogen as coolant to reduce tool temperature in machining of Ti6Al4V. The effects of cutting conditions and drill geometry on formation of burr during drilling of Ti6Al4V with solid carbide and high-speed cobalt drill-bits had been studied by Dornfeld et al. (1999) and Ko et al. (2003). It is concluded that drill geometry has greater influence on burr size. Deburring generally leads to extra machining operations which is time consuming and costly proposition. In some cases, it is difficult to perform for getting good finish (Aurich et al. 2009). Therefore, there is need to find a operation related setup that can produce less burr and good surface finish. It is proposed that performance of machining operation of titanium alloys can be enhanced by selecting improved cutting tool materials

and coated tools (Corduan et al. 2003; Andriya et al. 2012). Titanium nitrate (TiN) coated tungsten carbide tools are used mostly in metal cutting process due to their high wear resistance, hardness and chemical stability (Corduan et al. 2003).

AISI 316 stainless steel is extensively used in the field of aerospace, automobile and medical engineering field. Due to their favorable machinability and mechanical properties, it is preferred for various applications. Austenitic stainless steels find large application in day-to-day life like house hold goods (cutlery, sinks, tubing, springs, nuts, bolts etc.), air craft fittings, and aerospace components (bushings, shafts, valves, special screws etc.) due to its high strength, corrosion and oxidation resistance (Chow et al. 2008). Therefore, attention must be paid to study its machinability characteristics since stainless steel possesses low thermal conductivity, high mechanical and micro structural sensitivity to strain and stress rate (Lee et al. 2009). Cicek et al. (2013) have studied the parametric effect of process parameters on drilling operation of AISI 304 using cryo-treated tool to minimize the surface roughness and roundness error using Taguchi method. For minimization of burr height and burr thickness, Gaitonde et al. (2008) and Gaitonde et al. (2008) have proposed design of experiment (DOE) approach to obtain optimum parametric setting for drilling of AISI 316. The study reveals that the drill diameter and lip clearance angle have major contribution in development burr. To predict the drilling responses such as burr thickness and burr height during drilling austenitic stainless steel, Karnik et al. (2008) and Karnik and Gaitonde (2008) have proposed artificial neural network (ANN) model.

**2.5. Numerical Analysis of Drilling Operation**

Marasi (2013) has developed a finite element (FE) model in Deform-2D to study the effect of drilling parameters on thrust forces. Poutord et al. (2013) have examined the effect of drilling parameters on thrust force and torque in drilling of Ti6Al4V and carbon fiber reinforced polymers (CFRP) using tungsten carbide (WC) drill bit (Grade K20). Similarly, Gao et al. (2012) and Sha et al. (2013) have analyzed the effect of drilling parameters on quality of holes while drilling CFRP using finite element model. Singh et al. (2008) have proposed a finite element (FE) model using ProE (FEM software package with CAD input capability) to analyze the effect of input variables on process output such as thrust force and torque while drilling of fiber reinforced plastics (FRP) in dry condition. The model assists to understand the influence of tool geometry on change in temperature of drill tool and work piece, Bagci and Ozcelik (2006) have proposed a FE model using AdvantEdge to analyze drilling operation using coated carbide drills.

Kyratsis and Bilalis (2011) has proposed a computer aided design (CAD) based three dimensional model using DRILL3D to evaluate the thrust force during drilling operation. A design of experiment (DOE) approach has been used to generate simulation scenarios eliminating unnecessary experimental runs.

Gardner and Dornfeld (2006) states that DEFORM-3D is a robust FEM simulation tool as compared to other FEM based software for complex machining processes like drilling operation. To study the performance of the cutting process parameters during turning of AISI 316 and inconel 718 using uncoated and coated carbide tools, Outerio et al. (2008) has developed finite element model using DEFORM-3D software. Gao et al. (2011) have investigated the effect drilling parameters on cutting forces and temperature using stainless steel as work piece. Constantin et al. (2010) has investigated the various machining processes viz. turning, milling and drilling in different FE based software to understand the effectiveness of the software. Karpat et al. (2008) have analyzed the effect of tool geometry on cutting force in turning using a finite element model. Wang et al. (2012) have proposed a finite element model using AdvantEdge software to study the influence of magnitude of honed cutting edge of K-Grade carbide drills on the cutting force and torque. To study the effect of geometrical parameters of twist drill bit on torque, cutting force and chip removal in drilling of stainless steel, Gao et al. (2011) have proposed a FE model using Pro/E and DEFORM-3D. Similarly, Muhammad et al. (2012) have analyzed the effect of various work materials on torque, cutting force and chip removal in drilling using a FE model. Sun et al. (2012) have proposed a finite element model to evaluate effect of rotational speed and feed speed on thrust force and torque. Abouridouane et al. (2013) have proposed finite element (FE) based model for micro-drilling of carbon steels (C05, C45 and C75) using carbide twist drills. Qi et al. (2014) have proposed a finite element model to measure the stress developed region in the bone using surgical tools such as twist drill bit and hollow drill bit during drilling (orthopedic surgery applications).

**2.6. Multi-response Optimization**

Design of experiment (DOE) approach has been extensively used by the researchers to systematically analyze the effect of process parameters on performance output with less number of experimental runs (Montegomery 2003). However, the DOE approaches can optimize a single response. When multiple responses need to be optimized simultaneously, the approaches break down. Therefore, a large number of techniques have been suggested for multi-response optimization by combining desirability function

approach (Singh et al. 2013), utility concept (Fereirra et al. 2001) and grey relation analysis (Tosun 2006) along with DOE. Most of the techniques rest on converting multiple responses into an equivalent single response. However, the responses may themselves be correlated. In order to obtain an equivalent single response in correlated multiple response case, weighted principal component analysis (WPCA) technique has been used in optimization of a drilling process (Liao 2006; Routara et al. 2010; Siddiquee et al. 2010). Mandal et al. (2011), Kivak et al. (2012) and Asilturk and Neseli (2012) have used Taguchi method for optimization of drilling parameters considering process responses such as tool wear, surface roughness and thrust force. Rajmohan and Palanikumar (2014), Kilickap and Huseyinoglu (2010), Valarmathi et al. (2012) and Velumani et al. (2013) have adopted response surface methodology (RSM) approach for developing empirical relationship between the drilling parameters and performance characteristics by conducting reasonable number of experimental runs. Meena and Azad (2012), Kumar et al. (2013) and Lin and Yeh (2012) have proposed various multi-response optimization techniques using different multi-criteria decision making (MCDM) methods. However, superiority and inferiority (SIR) ranking method, an effective MCDM method possessing the strengths of most MCDM methods, has not been used for converting multiple responses into an equivalent single response (Tong et al. 2007; Xu 2001; Marzouk 2008; Tam et al. 2004). SIR method provides the decision makers a systematic, flexibility and realistic approach to effectively rank the alternatives even in imprecise environment.

In the pursuit of searching global optimal parameters in optimization of machining processes, various evolutionary techniques have been adopted recently. Cus and Balic (2003) have used genetic algorithm (GA) to obtain optimum cutting conditions in CNC turning operation. Zain et al. (2010) have applied GA to minimize surface roughness in end milling process considering machining variables such as rake angle, feed rate and cutting speed. Haq et al. (2006) have used particle swarm optimization (PSO) to obtain optimal machining tolerances in a clutch assembly. Baskar et al. (2005) have employed PSO for optimization of milling operation. Kolahan and Liang (1996) and Kolahan and Liang (2000) have proposed a tabu-search algorithm for optimization of hole making process. Although a large number of evolutionary optimization techniques exist in the literature, still search is going on to obtain an algorithm which can improve solution quality, avoid premature convergence and reduce computational burden. In comparison to other algorithms, harmony search (HS) algorithm possesses the capability of finding

optimal solution with less memory requirement and computational time by adjusting only few parameters (Manjarres et al. 2013; Cobos et al. 2013; Weyland 2010; Mahdavi et al. 2007; Lee et al. 2005).

### 2.7. Laser Drilling Operation

Drilling of materials like stainless steel and titanium alloys is difficult due to work hardening and rubbing of tools against the hardened zone causing rapid tool wear (Yeo et al. 1994; Tansel et al. 1998). Laser drilling is an alternative way for micro-drilling. Since there is no contact between tool and the work materials, the problem of chatter and vibration during machining can be eliminated (Chryssolouris et al. 1988). The standard lasers used for the laser machining process are ruby laser, Nd:YAG (Neodymium Yttrium Aluminum Garnet) and carbon dioxide ($CO_2$) gas. Low et al. (2000) have studied the spatter deposition during laser drilling of Nimonic 263 alloy using a fibre-optic delivered 400 W Nd:YAG laser. Ghoreishi et al. (2000) have investigated the influence of control variables on hole taper and circularity in laser percussion drilling using stainless steel as work piece. A comparison between stainless steel and mild steel reveals that pulse frequency has significant influence on the quality of hole in drilling of stainless steel. Brajdic et al. (2008) have investigated the effect of laser drilling parameters on hole quality in deep drilling of through holes made on stainless steel with the superposed radiation of two pulsed Nd:YAG lasers. It is found that heat affected zone (HAZ) severely influence the quality of hole, Nagesh et al. (2013) have directed their efforts in improving the quality of laser drilled holes in thermoset based composites. The results indicate that the heat affected zone can be reduced employing lower laser power whereas taper angle can be reduced adopting higher laser power.

Shelton and Shin (2010) have attempted $CO_2$ laser machining on the materials such as AISI 422, AISI 316, Inconel 718 and Ti6Al4V to study the effect of process parameters on the machining responses such as work piece micro structure, edge burrs and surface finish. Yan et al. (2012) have used a $CO_2$ laser for drilling of thick aluminum sheets with a view to minimize hole taper and spatter area. Taweel et al. (2009) have proposed a Taguchi method for laser drilling of Kevlar-49 using $CO_2$ laser. Implementation Taguchi method helps to systematically analyze the effect of each parameter on quality of laser drilled hole such as taper, kerf width and dross height. Shuja and Yilbas (2014) have employed $CO_2$ laser for drilling of coated carbon steel material to study the effect of assisting gas on the quality of drilled holes surface.

## 2.8. Conclusions

A comprehensive study on existing literature reveals that an extensive study on drilling of bio-compatible materials is required. To understand the literature gap and source of the problem, the surveyed literature is classified into four sections such as bio-compatible materials, drilling operation, numerical analysis of drilling operation and laser drilling. The chapter illustrates the machining problems that arise during drilling of titanium alloys and stainless steel. The researchers have proposed various numerical and experimental approaches to overcome burr formation and surface roughness during drilling. The chapter also describes various optimization techniques used to obtain optimum parametric setting that minimizes the surface roughness and burr height and maximizes the circularity of drilled hole. Present chapter also emphasizes to understand the effect of $CO_2$ laser parameters on spatter area, HAZ, taper of the kerf and circularity of the drilled hole during laser drilling of metals. The literature indicates that $CO_2$ laser can be effectively used for laser drilling of metals.

The proposal for the current research is derived from identifying the literature gap. Specifically, the present research work proposes a numerical model for drilling of difficult-to-machine materials to analyze the effect of drilling parameters such as feed rate, spindle speed and drill diameter on the output responses such as circularity at entry and exit, burr height and surface roughness. As the responses are more than one, there is need to obtain optimum parametric setting for simultaneous optimization of all the responses. Therefore, an attempt has been made to develop a hybrid approach using HS algorithm with SIR method for optimization of the multiple responses. The research work also focuses on implementing $CO_2$ gas for laser drilling of alloys such as Ti6Al4V and AISI 316.

# CHAPTER 3

# NUMERICAL APPROACH FOR THE DRILLING PROCESS

# CHAPTER 3

# NUMERICAL APPROACH FOR THE DRILLING PROCESS

## 3.1. Introduction

Materials such as metallic alloys, composites, glasses and ceramics are extensively used in various engineering applications due to their properties like high stiffness, specific strength and toughness (Singh et al. 2013). However, these materials pose extreme difficulties while machining for providing useful shapes. Drilling is an important machining operation used for production of different types of parts applied in the field of manufacturing, aerospace and automotive industry. Drilling is also used in the field of biomedical engineering for production of parts and implantation of bones. The quality of the drilled hole depends on drilling (spindle) speed, feed and drilling diameter. Drilling of austenitic stainless steel (AISI 316) and titanium ally (Ti6Al4V), widely used in field of areospace industries and bio-medical engineering (bio-compatibility in nature), is really difficult because these materials exhibit severe work hardening needing high cutting forces and generating high localizied temperatures near the machined surface and cutting edges. As a result, machining of these materials invariably leads to poor surface integrity and short tool life (Arrazola et al. 2009; Outeiro et al. 2002). Therefore, it is desirable to investigate the machinability of Ti6Al4V and AISI 316 because of potentaility of applications. As actual drilling opearation on these materials is somewhat diffciult, an alternative rote of developing a simulation model based on finite element method has been developed to understand the effect of process parameters on machinability.

## 3.2. Numerical model

Marasi (2013) has developed a finite element (FE) model in Deform 2D to study the effect of drilling parameters on thrust force. Poutord et al. (2013) have examined the effect of drilling parameters on thrust force and torque in drilling of Ti6Al4V and carbon fiber reinforced polymers (CFRP) using tungsten carbide (WC) drill bit (Grade K20). To understand the complexity of drilling operation, many studies have proposed finite element models to analyze the tool temperature, cutting forces, torque, and tool wear (Singh et al. 2008; Kadirgama et al. 2008; Bagci and Ozcelik 2006; Kyratsis et al. 2011). Cantero et al. (2005) have studied tool wear, hole quality, mechanical properties and strength of tool during dry drilling of Ti6Al4V to decide on appropriate machining parameters.

Since complex mechanism is involved in machining, prediction of performance characteristics in machining becomes a tedious process. Numerous numerical models based on finite element approach have been proposed to get insight into machining processes. Pittala and Monno (2011) have predicted temperature of work piece during face milling operation of Ti6Al4V using finite element based software such as DEFORM 2D and DEFORM 3D. Abouridouane et al. (2012) have successfully employed DEFORM 3D finite element computational model to analyze size effect in micro-drilling of ferritic-pearlitic carbon steel. Strenkowski et al. (2002) and Strenkowski et al. (2004) have developed a three dimensional model based on finite element analysis for predicting tool forces and chip flow in drilling operation using DEFORM 3D software. Working with DEFORM 3D is basically divided into two stages (i) pre-processor stage where the parameters inputted to develop the 3D model and (ii) second stage consists of simulation and analysis of results. Flow chart of the process helps to understand the analysis process in details shown in Figure 3.1. All the required details for the numerical analysis are to be included in the pre-processor such as machining type, process condition, tool and work piece details and the results are to be noted from the post processor stage. If the error occurs, it is necessary to proceed through the pre-processor again.

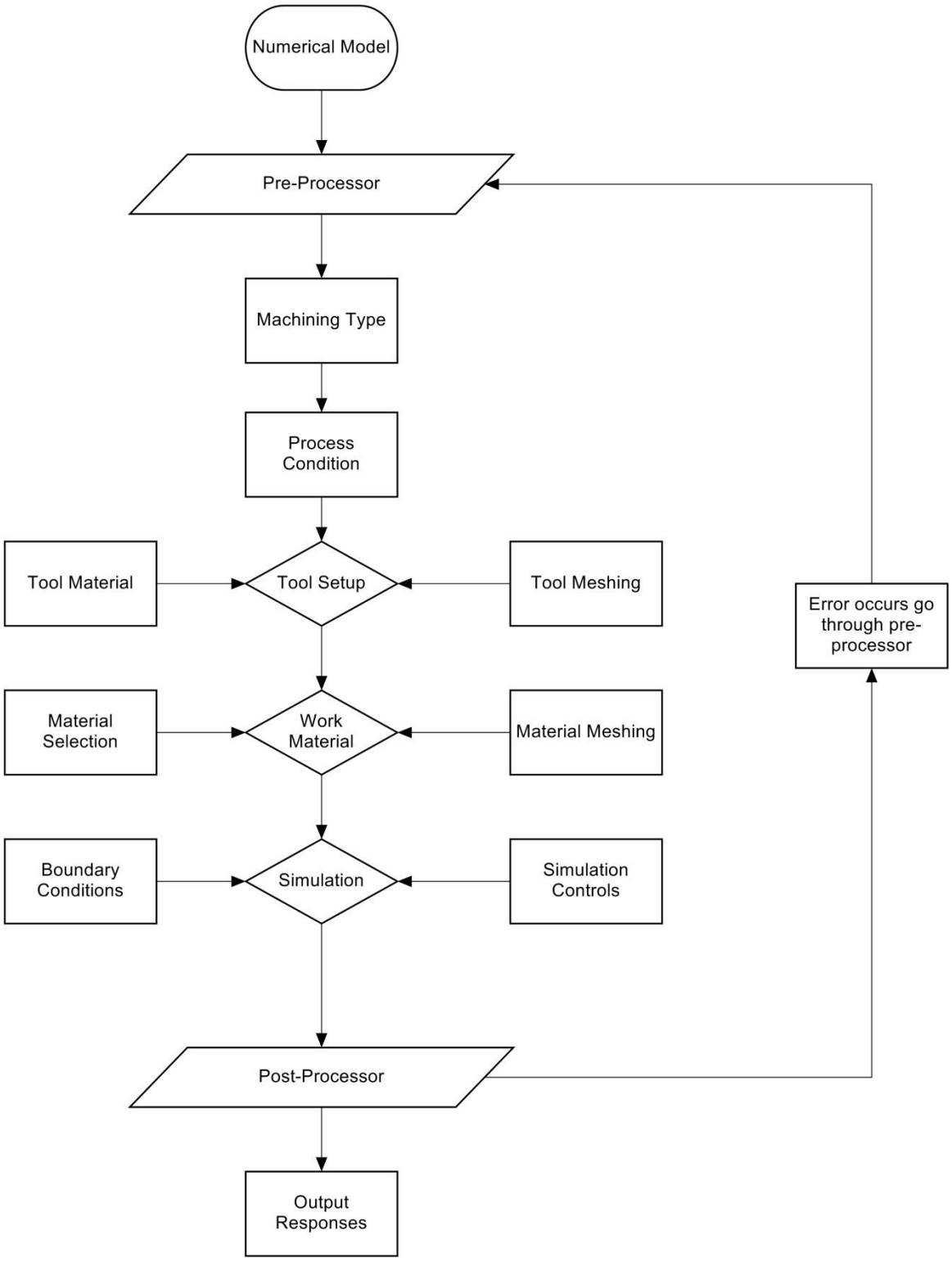


Figure 3.1: Flow chart for numerical analysis

### 3.2.1. Pre-processor steps

The pre-processor steps for numerical analysis in DEFORM 3D (Gao et al. 2012; DEFORM manual) are as follows for the drilling analysis of AISI 316.

- The machining process parameters such as spindle speed, feed rate and drill bit diameter, surrounding temperature and coolant supply along with machining type are described in the pre-processor stage to build the computational model.
- Since the dry drilling of titanium alloy is considered, air as coolant is assumed and the default coolant setting is used.
- To develop a drill bit, dimensioning of drill bit is to be mentioned in tool setup as per Table 3.1.

Table 3.1: Specifications of drill bit

| | | | |
|---|---|---|---|
| Diameter (mm) | 5 | 6 | 7 |
| Width (mm) | 1.2 | 1.35 | 1.5 |
| Helix and Cone Angle | $40^0$ | $40^0$ | $40^0$ |
| Point Angle | $135^0$ | $135^0$ | $135^0$ |
| Number of Flutes | 2 | 2 | 2 |
| Tool Material | Tungsten Carbide | Tungsten Carbide | Tungsten Carbide |
| TiN Coating (mm) | 5 µm | 5 µm | 5 µm |

- The tool materials, coating layer and work piece material are defined by loading the data from the library of the software (Table 3.1). If the material file is not present in the library then all the physical and mechanical properties are required to be mentioned.
- Dimensioning of work piece has been done as per Table 3.2, in work-material section.

Table 3.2: Workpiece specifications

| | |
|---|---|
| Work piece Material | AISI 316 |
| Width (mm) | 5 |
| Work piece Diameter (mm) | 65 |

- Before submitting the developed numerical model for simulation, meshing of tool and work piece has been performed. The element is defined as tetrahedral shape of size ratio of 1:4 and 1:7 for tool and work piece respectively. The mesh number of 10,000 and 15,000 for the tool and work piece respectively has been defined. The Figures 3.2 (a) and (b) show the images of the meshed tool and work piece respectively. DEFORM™ uses Langrangian meshing because it has the capability of re-meshing at each and every step when deformation occurs in drilling simulation. Langrangian meshing has the advantage of restarting the simulation from the point

where the model has stopped if the model stops at any condition (DEFORM manual).

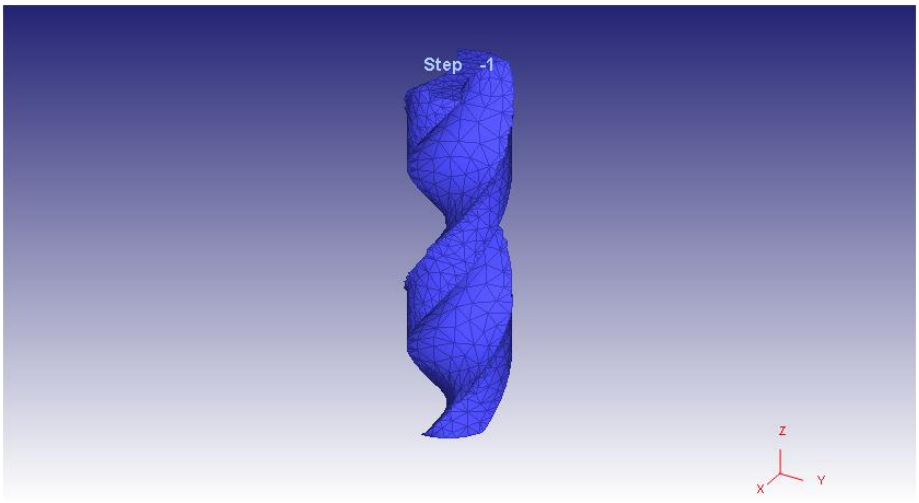


Figure 3.2 (a): Meshed tool

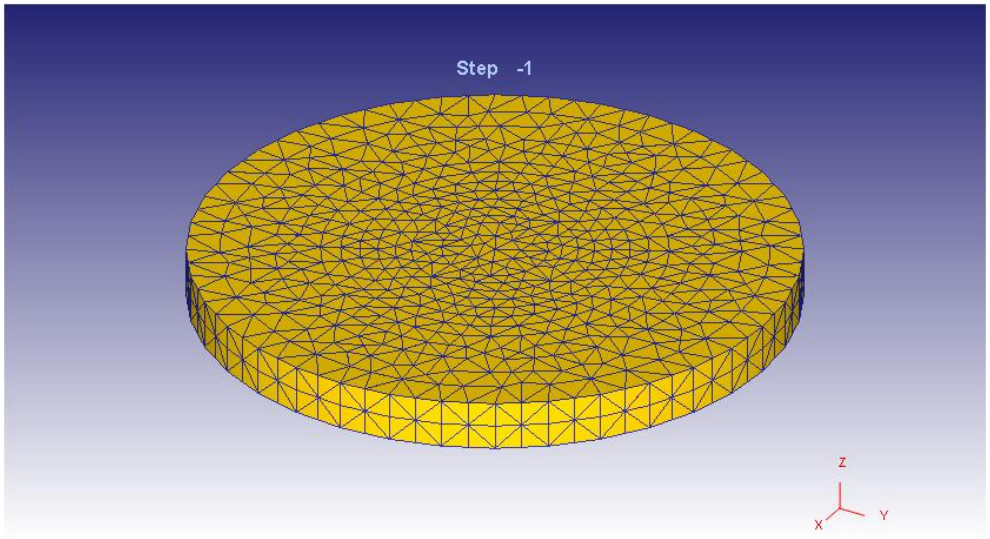


Figure 3.2 (b): Meshed work piece at step 1 before drilling

- Boundary condition for the work piece is defined. The work piece is fixed in all directions (x, y and z-axes) to get best drilling condition.
- Defining the number of steps (iterations) for the operation is set to be 20,000 to complete the operation.
- Next step is to checking and generating of data base. If database is not developed, go to the pre-processor stage and repeat the above mentioned steps from the beginning till database are developed and analysis is completed.

- After completion of above steps, the model is submitted for simulation. The Figure 3.3 shows the tool work piece setup before drilling analysis.

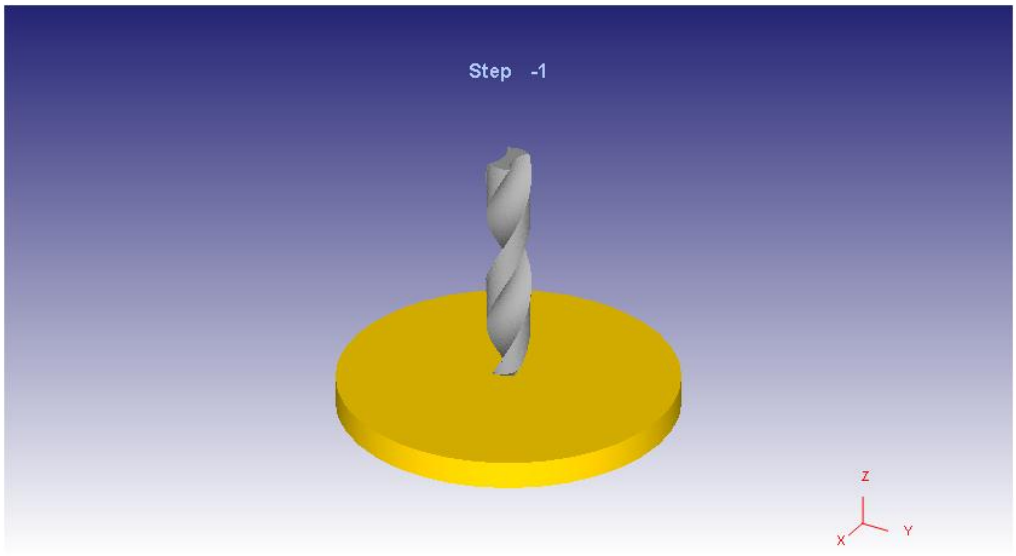


Figure 3.3: Tool work piece setup before drilling analysis

### 3.2.2. Post-processor steps

After inputting all data in pre-processor stage and generating a good database, the next step is to submit the developed model in simulation control. After completing the simulation, the post-processor is accessed to evaluate the simulated model to estimate the drilling responses. To analyze the simulated results, following steps need to be followed:

- Once the simulation is completed, the results are stored in file in the DEFORM 3D database directory.
- Select '**.**DB file' the file from the sub-directory.
- Submit the file in the DEFORM 3D post processor to analyze the simulated results.
- Run the simulated process to obtain the results. Select single object mode from the menu bar which helps to find the circularity at entry and exit. Figure 3.4 shows the measurement of the circularity at entry for AISI 316 at 600 rpm spindle speed, 30 mm/min feed rate and 7 mm drill diameter. The simulation images are imported to image processing toolbox of MATLAB 12.0 to measure the circularity at entry and exit of the drilled hole (Table 3.6). Circularity is defined in terms of ratio of minimum ferret diameter ($D_1$) to maximum ferret diameter ($D_2$) (Ghoreishi et al. 2002).

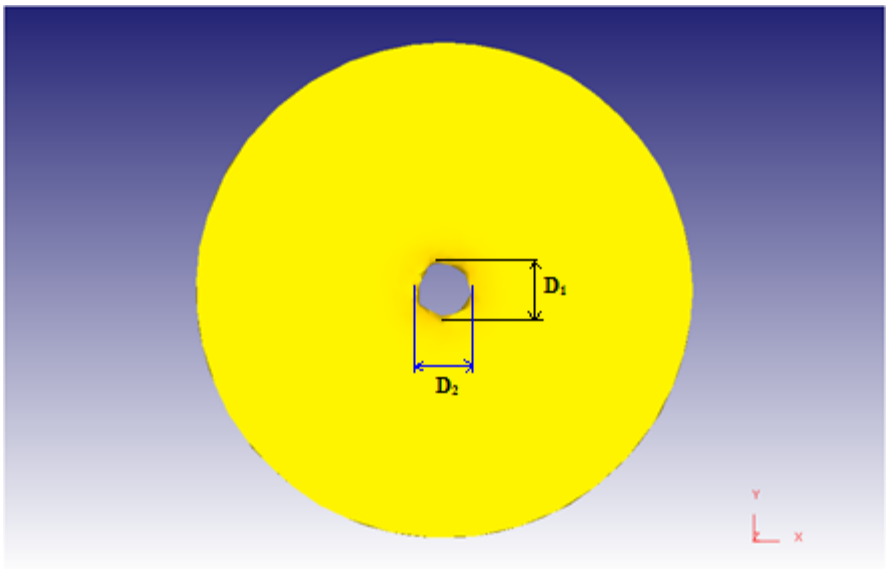


Figure 3.4: Measurement of circularity at entry for AISI 316 at 600 rpm spindle speed, 30 mm/min feed rate and 7 mm drill diameter

- Select the graph load stroke from the menu bar to note thrust force and torque (Figure 3.5 and Figure 3.6). For each response, the average of the obtained results is taken into account and listed in Table 3.7.

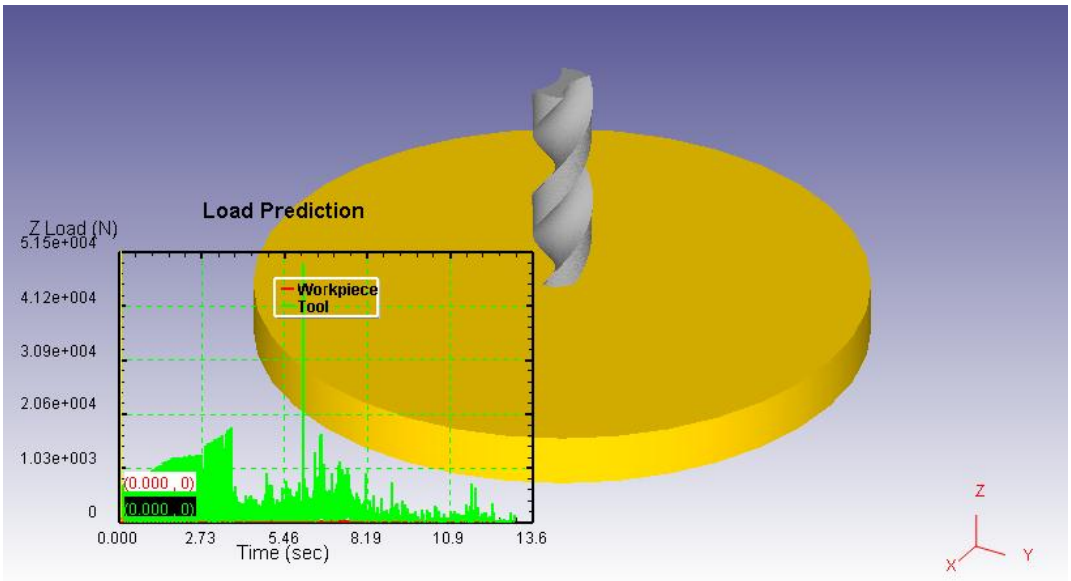


Figure 3.5: Thrust force prediction for AISI 316 at 600 rpm spindle speed, 30 mm/min feed rate and 7 mm drill diameter

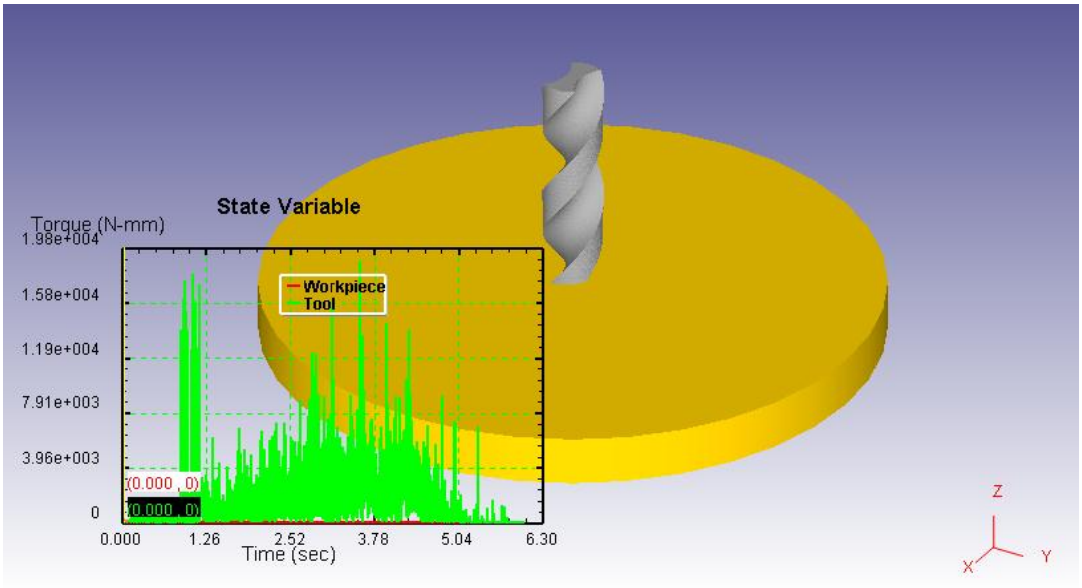


Figure 3.6: Torque prediction for AISI 316 at 600 rpm spindle speed, 30 mm/min feed rate and 7 mm drill diameter

Similarly, the all the steps mentioned in section 3.2.1 (pre-processor steps and section 3.2.2 (post-processor steps) are repeated for the drilling analysis of titanium alloy (Ti6Al4V) to predict the drilling output responses such as circularity, thrust force and torque. The results are tabulated in Table 3.7.

### 3.3. Experimental details

Statistical design of experiments (DOE) approach for designing experimental strategy can reduce experimental time and cost by reducing experimental runs and obtain maximum process related information. Further, simulation of drilling of Ti6Al4V by finite element analysis (FEA) can supplement understanding of the process. Combination of DOE and FEA can help to achieve proper parametric setting to overcome the difficulties arises in machining of Ti6Al4V and AISI 316.

Response surface methodology (RSM) is basically a collection of statistical and mathematical techniques useful for developing, improving and optimizing process (Montegomery 2009). Kyratsis et al. (2011) have used response surface methodology to design the experimental and simulation strategies to study parametric effect of drilling operation on thrust force. It deals with the situation where several input variable potentially influence the performance measure or quality of the product or process. The performance measure or quality is known as response. The response surface methodology comprises regression surface fitting to obtain approximate responses, design of experiments to obtain minimum variances of the responses and optimization

using the approximated responses. To develop an appropriate approximating model between the response 'Y' and independent variables {$X_1$, $X_2$, ……., $X_n$} in statistical modeling, the relationship is written in the form of

$$Y = f(X_1, X_2 ..... X_n) + \varepsilon \quad (3.1)$$

where the form of the true response function Y is unknown and ε is a term that represents other sources of variability not accomplished in Y. Usually, it includes the effects like measurement error on response, background noise, other variables and so on. Usually, ε is treated as statistical error often assumed be normally distributed with mean zero and variance $\sigma^2$.

The variables $X_1$, $X_2$, …. , $X_n$ are usually called the natural variables because they are expressed in natural units of measurements. In RSM, it is convenient to transform the natural variables into coded variables $x_1$, $x_2$, …, $x_n$, which are usually defined to be dimensionless with mean zero and the same standard deviation. In terms of the coded variables, the response function will be written as f ($x_1$, $x_2$, …, $x_n$) and the surface generated using this function is known as response surface. Since the form of relationship between the response and the independent variable is unknown, a suitable approximation is made for developing functional relationship between Y and a set of independent variables. Usually, a second order model is utilized as shown below.

$$Y = \beta_0 + \sum_{j=1}^{k} \beta_j x_j + \sum_{j=1}^{k} \beta_{jj} x_j^2 + \sum_{i=1}^{k} \sum_{j=2}^{k-1} \beta_{jj} x_i x_j \quad (3.2)$$

The coefficients β's used in the above model can be calculated by means of least squares technique.

The simulation analysis is performed using DEFORM 3D considering a circular work piece having thickness of 5 mm and 65 mm diameter. PVD coated tungsten carbide (WC) drill bit of diameter 5, 6 and 7 mm is used. The analysis is based on the steps mentioned in the previous section. Three input parameters such as spindle speed (A) in rpm, feed rate (B) in mm/min and drill bit diameter (C) in mm are considered. The actual control parameters are converted into coded value using equation 3.3 as shown below (Padhee et al. 2012).

$$\text{Coded value } (x) = \frac{X - \frac{X_{max} + X_{min}}{2}}{\frac{X_{max} - X_{min}}{2}} \quad (3.3)$$

x is in coded form and $X_{max}$ and $X_{min}$ are the actual maximum and minimum parametric setting. Table 3.1 shows actual and coded machining parameters. Experimental design is developed by Design Expert 7.0 V software (State-Ease Inc., USA) based on face centered central composite design. Table 1.1 and 1.2 shows the material properties of the Ti6Al4V and AISI 316 (Aerospace Specification Metals Inc.)

Table 3.3: Machining parameters

| **Factors** | **Levels (coded)** | | |
|---|---|---|---|
| | -1 | 0 | +1 |
| A – Spindle speed (RPM) | 400 | 500 | 600 |
| B – Feed rate (mm/min) | 30 | 40 | 50 |
| C – Drill diameter (mm) | 5 | 6 | 7 |

Table 3.6 shows the design matrix and responses obtained via. simulation for AISI 316 stainless steel. The experimental runs consist of twenty sets of coded conditions. It comprises of a $2^3$ full factorial design, six center points and six star points with axial distance of one. Drilling simulation results for Ti6Al4V is shown in Table 3.7.

Table 3.6: The simulation layout for drilling of AISI 316

| **Experiment Number** | **A** | **B** | **C** | **Circularity at entry** | **Circularity at exit** | **Thrust, kN** | **Torque, kN-mm** |
|---|---|---|---|---|---|---|---|
| 1 | -1 | -1 | -1 | 0.88605 | 0.88817 | 2 | 8.14 |
| 2 | 1 | -1 | -1 | 0.87977 | 0.88115 | 1.84 | 3.32 |
| 3 | -1 | 1 | -1 | 0.8691 | 0.92889 | 1.53 | 4.85 |
| 4 | 1 | 1 | -1 | 0.83258 | 0.91841 | 1.38 | 4.62 |
| 5 | -1 | -1 | 1 | 0.83258 | 0.88737 | 1.31 | 8.62 |
| 6 | 1 | -1 | 1 | 0.89557 | 0.92341 | 1.93 | 10.2 |
| 7 | -1 | 1 | 1 | 0.92666 | 0.93308 | 1.63 | 3 |
| 8 | 1 | 1 | 1 | 0.89786 | 0.85707 | 1.38 | 6.42 |
| 9 | -1 | 0 | 0 | 0.92568 | 0.92564 | 1.51 | 5.76 |
| 10 | 1 | 0 | 0 | 0.84859 | 0.90019 | 1.59 | 5.57 |
| 11 | 0 | -1 | 0 | 0.82446 | 0.92936 | 1.89 | 7.23 |
| 12 | 0 | 1 | 0 | 0.86798 | 0.86765 | 1.57 | 4.35 |
| 13 | 0 | 0 | -1 | 0.84827 | 0.98026 | 1.07 | 5.15 |
| 14 | 0 | 0 | 1 | 0.83817 | 0.92111 | 1.42 | 6.72 |
| 15 | 0 | 0 | 0 | 0.88445 | 0.92534 | 1.67 | 7.05 |
| 16 | 0 | 0 | 0 | 0.88445 | 0.92534 | 1.67 | 7.05 |
| 17 | 0 | 0 | 0 | 0.88445 | 0.92534 | 1.67 | 7.05 |
| 18 | 0 | 0 | 0 | 0.88445 | 0.92534 | 1.67 | 7.05 |
| 19 | 0 | 0 | 0 | 0.88445 | 0.92534 | 1.67 | 7.05 |
| 20 | 0 | 0 | 0 | 0.88445 | 0.92534 | 1.67 | 7.05 |

Table 3.7: The simulation layout for drilling of Ti6Al4V

| Experiment Number | A | B | C | Circularity at entry | Circularity at exit | Thrust, kN | Torque, kN-mm |
|---|---|---|---|---|---|---|---|
| 1 | -1 | -1 | -1 | 0.8489 | 0.808 | 1.1 | 3.29 |
| 2 | 1 | -1 | -1 | 0.8612 | 0.965 | 0.864 | 4.05 |
| 3 | -1 | 1 | -1 | 0.8574 | 0.952 | 1.357 | 6.08 |
| 4 | 1 | 1 | -1 | 0.7977 | 0.921 | 1.07 | 2.20 |
| 5 | -1 | -1 | 1 | 0.8944 | 0.933 | 1.429 | 10.7 |
| 6 | 1 | -1 | 1 | 0.8935 | 0.910 | 1.06 | 6.89 |
| 7 | -1 | 1 | 1 | 0.9371 | 0.918 | 1.716 | 12.8 |
| 8 | 1 | 1 | 1 | 0.9054 | 0.940 | 1.003 | 13.9 |
| 9 | -1 | 0 | 0 | 0.9522 | 0.921 | 1.629 | 4.56 |
| 10 | 1 | 0 | 0 | 0.8959 | 0.927 | 1.186 | 6.25 |
| 11 | 0 | -1 | 0 | 0.8315 | 0.883 | 1.142 | 5.64 |
| 12 | 0 | 1 | 0 | 0.8629 | 0.883 | 1.442 | 4.37 |
| 13 | 0 | 0 | -1 | 0.8935 | 0.899 | 1.095 | 8.35 |
| 14 | 0 | 0 | 1 | 0.8637 | 0.970 | 1.47 | 14.2 |
| 15 | 0 | 0 | 0 | 0.9623 | 0.958 | 1.691 | 5.82 |
| 16 | 0 | 0 | 0 | 0.9623 | 0.958 | 1.691 | 5.82 |
| 17 | 0 | 0 | 0 | 0.9623 | 0.958 | 1.691 | 5.82 |
| 18 | 0 | 0 | 0 | 0.9623 | 0.958 | 1.691 | 5.82 |
| 19 | 0 | 0 | 0 | 0.9623 | 0.958 | 1.691 | 5.82 |
| 20 | 0 | 0 | 0 | 0.9623 | 0.958 | 1.691 | 5.82 |

### 3.4. Validation of simulation

To check the adequacy of the numerical simulation, some set of drilling experiments are performed with same process parametric setting used for the numerical simulation. The experiments are performed on a CNC milling machine (MAXMILL) supplied by MTAB Engineers, India having FANUC controller, 3.7 kW spindle motor, positional accuracy of 0.01mm, vertical (Z axis) travel of 250mm, load on table of 200kg, rapid feed of 10 m/mm and maximum speed of 10000 rpm. The circular shaped Ti6Al4V grade-5 and AISI 316 having dimension of 65 mm diameter and 5 mm thickness supplied by Mishra Dhatu Limited, Hyderabad, India is used as work piece. The twist drill bits of tungsten carbide (TiN PVD coated) supplied by WIDIA-RUBIG, Germany are used in the experiment. Drilling experiments are conducted with a back-up plate (Perfex). The experimental data has noted down in Table 3.8 and 3.9.

### 3.5. Results and discussions

To check the adequacy of the numerical analysis performed, comparison of the simulated and experimental results for drilling is made for the responses such as circularity at entry ($C_{ent}$), circularity at exit ($C_{exit}$), thrust and torque. The relative error (RE) between the experimental and simulated responses is calculated using equation 3.4 as shown in Tables 3.8 and 3.9. The mean relative error (%) for the responses

obtained (Table 3.8) are 4.7, 2.51, 8.91 and 4.62 for $C_{ent}$, $C_{exit}$, thrust and torque respectively for drilling of AISI 316. Similarly, the mean relative error (%) for the responses obtained (Table 3.9) are 5.05, 2.95, 4.71 and 4.67 for circularity at entry, circularity at exit, thrust and torque respectively for drilling of Ti6Al4V. It indicates that finite element model can predict the responses with reasonable degree of accuracy.

$$\text{Relative error}(\%) = \frac{|\text{Experimental value} - \text{Simulated value}|}{\text{Experimental value}} \times 100 \quad (3.4)$$

Table 3.8: The Experimentation for drilling of AISI 316

| Exp. No. | Circularity at entry | | R.E. | Circularity at exit | | R.E. | Thrust, kN | | R.E. | Torque, kN-mm | | R.E. |
|---|---|---|---|---|---|---|---|---|---|---|---|---|
| | Exp. | Sim. | | Exp. | Sim. | | Exp. | Sim | | Exp | Sim | |
| 2 | 0.930 | 0.880 | 5.38 | 0.902 | 0.881 | 2.33 | 2.006 | 1.84 | 8.28 | 8.55 | 8.14 | 4.80 |
| 6 | 0.952 | 0.896 | 5.88 | 0.898 | 0.923 | 2.78 | 1.950 | 1.93 | 1.03 | 9.90 | 10.20 | 3.00 |
| 12 | 0.920 | 0.868 | 5.65 | 0.889 | 0.868 | 2.36 | 1.775 | 1.57 | 11.55 | 4.46 | 4.35 | 2.40 |
| 20 | 0.901 | 0.884 | 1.89 | 0.902 | 0.925 | 2.55 | 1.455 | 1.67 | 14.78 | 7.68 | 7.05 | 8.20 |
| Average R.E. (%) | | | 4.70 | | | 2.51 | | | 8.91 | | | 4.62 |

Table 3.9: The Experimentation for drilling of Ti6Al4V

| Exp. No. | Circularity at entry | | R.E. | Circularity at exit | | R.E. | Thrust, kN | | R.E. | Torque, kN-mm | | R.E. |
|---|---|---|---|---|---|---|---|---|---|---|---|---|
| | Exp. | Sim. | | Exp. | Sim. | | Exp. | Sim. | | Exp. | Sim | |
| 3 | 0.94 | 0.857 | 8.83 | 0.931 | 0.952 | 2.26 | 1.351 | 1.357 | 0.44 | 5.96 | 6.08 | 2.01 |
| 7 | 0.95 | 0.937 | 1.37 | 0.948 | 0.918 | 3.16 | 1.864 | 1.716 | 7.94 | 11.89 | 12.8 | 7.65 |
| 12 | 0.95 | 0.863 | 9.16 | 0.940 | 0.883 | 6.06 | 1.516 | 1.442 | 4.88 | 4.74 | 4.37 | 7.81 |
| 17 | 0.97 | 0.962 | 0.82 | 0.961 | 0.958 | 0.31 | 1.791 | 1.691 | 5.58 | 5.75 | 5.82 | 1.22 |
| Average R.E. (%) | | | 5.05 | | | 2.95 | | | 4.71 | | | 4.67 |

**Note: Exp. = experimentation, Sim. = simulation and R.E. = relative error**

To check the adequacy of developed numerical (simulated) model, the experimental results are compared with simulation values for different output responses such as circularity at entry and exit, thrust and torque for drilling of Ti6Al4V and AISI 316 shown in Figures 3.7 and 3.8 respectively. The graphs (Figure 3.7 and 3.8) show that the experimental results are comparatively closer to simulated results.

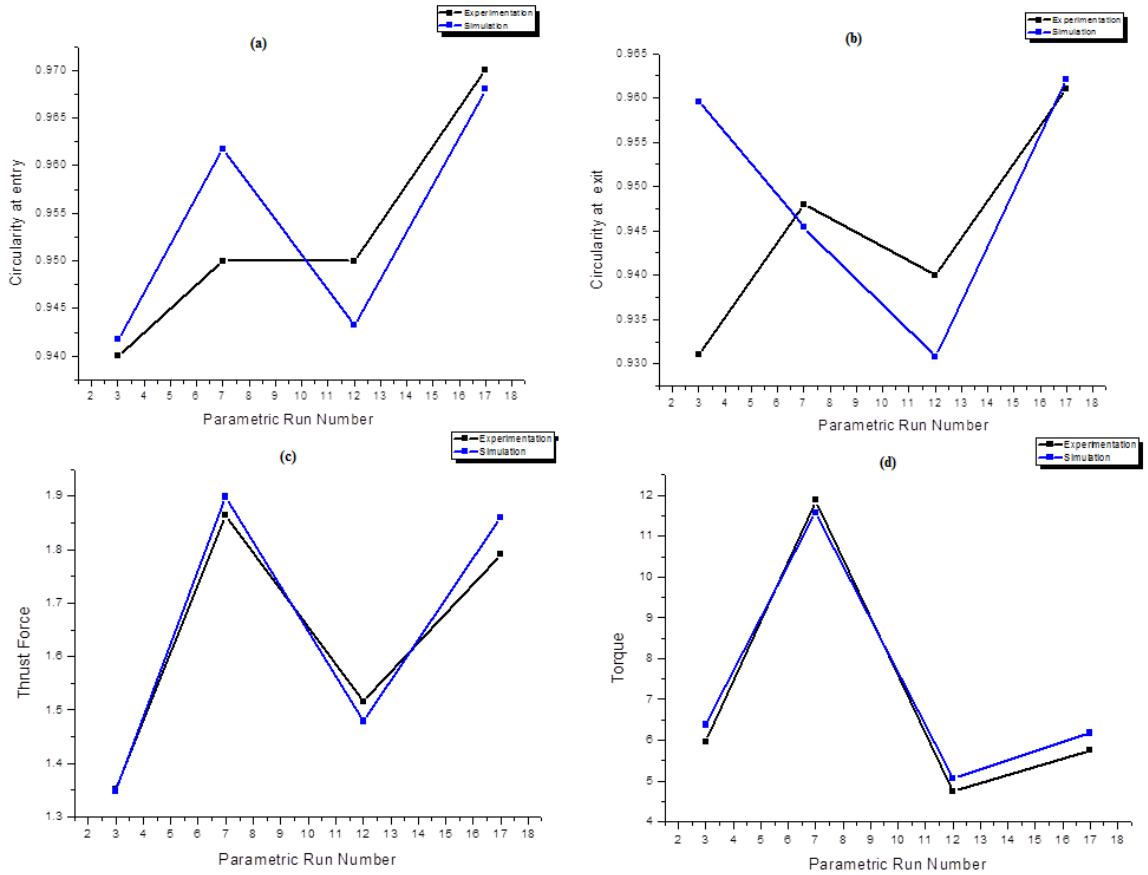


Figure 3.7: Comparison of simulation and experimental results for drilling of Ti6Al4V

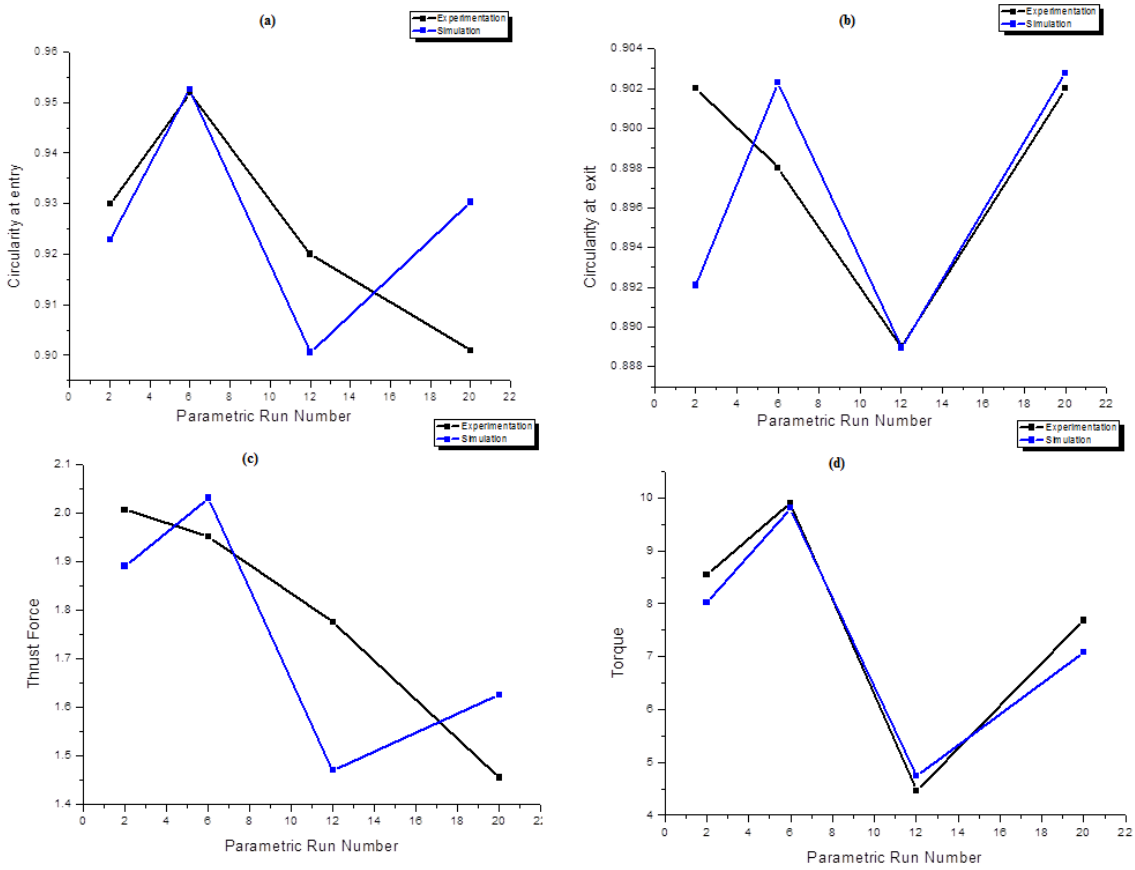


Figure 3.8: Comparison of simulation and experimental results for drilling of AISI 316

### 3.6. Conclusions

In the present chapter, FEM based numerical analysis has been performed for the drilling process using DEFORM 3D 6.1.V. Drilling experiments has been performed with same parametric level and the results obtained are closer to the results obtained by numerical analysis. The obtained mean relative error (%) is less than 10% shows the adequacy of the developed numerical model. The mean relative error (%) for the responses obtained are 5.05, 2.95, 4.71 and 4.67 for circularity at entry, circularity at exit, thrust and torque respectively for the simulation of drilling of Ti6Al4V. The mean relative error for the responses obtained are 4.7, 2.51, 8.91 and 4.62 for circularity at entry, circularity at exit, thrust and torque respectively for the simulation of drilling of AISI 316. The results also indicate that FE model can predict the responses with reasonable degree of accuracy.

# CHAPTER 4

# EXPERIMENTAL INVESTIGATION OF DRILLING PROCESS

# CHAPTER 4

# EXPERIMENTAL INVESTIGATION OF DRILLING PROCESS

## 4.1. Introduction

Drilling is a machining operation which uses a drill-bit to cut or enlarge a hole of circular cross-section in solid materials. The drill-bit is pressed against the workpiece and rotated at rate varying from tens to thousands of revolutions per minute. The forces acting at the cutting edge against the workpiece lead to cutting off chips from the hole as it is drilled. Drilling operation is one of the important machining processes used for making holes and assembling the parts. It is observed that tool wear occurs fast with carbide tools when hard materials are drilled. To avoid such type of condition, TiN coated PVD tools are used (Lin and Shyu 2000; Kilickap and Huseyinoglu 2010; Chen and Liu 2000; Lee et al. 2009; Arrazola et al. 2009; Armendia et al. 2010). Therefore, it is vital to study the machining behaviour coated drill bits when hard materials are drilled.

The influence of control parameters on process output characteristics need to be explored. Once the impact of control parameters are established, it is necessary to obtain best process state leading to optimization of multiple performance characteristics. For selecting the best appropriate alternatives from the present criteria leads to the concept of multi-criteria, multi-attribute, multi-disciplinary and multi-objective problems which include both managerial and technical criteria for the decision makers (Wadhwa et al. 2009). For selecting the best alternatives, there is a requirement of certain logical mathematical tool for the decision makers. In recent times, a large number of multi-attribute decision making (MADM) techniques have been proposed having their own merits and demerits. Superiority and Inferiority (SIR) method (Xu 2001) is a multi-criteria decision making (MCDM) method which has the flexibility of using both cardinal as well as non-cardinal data. When multiple performance characteristics are dealt, it is convenient to convert all characteristics into an equivalent characteristic (response). In this direction, the present chapter uses superiority and inferiority ranking integrated with technique for order preference by similarity to ideal solution (SIR-TOPSIS) approach to convert multiple responses into single response. An empirical relation between process parameters and the equivalent single response is developed using non-linear regression technique. Finally, harmony search (HS) algorithm has been proposed for optimization of the single equivalent response.

### 4.2. SIR-TOPSIS method

Superiority and inferiority ranking (SIR) method, introduced by Xu (2001), is one of the multi criteria decision making (MCDM) approach for ranking the products and alternatives in an effective way. The method uses the combined information of both the flows (superiority flow and inferiority flow). It can be viewed as an advancement and extension of PROMTHEE method (Xu 2001). The method can process both the ordinal and cardinal values. The effectiveness of the alternatives is understood by their superiority and inferiority scores which are attained by generalized criteria introduced in PROMTHEE method. SIR method is capable of analyzing different criteria without transforming them into a single scale (Tam et al. 2004). It possesses the strength to analyze the experts judgment systematically on their decision factors and alternatives to provide a more realistic and rational solution for their judgment.

#### 4.2.1. Superiority and inferiority matrices

The multicriteria problems are expressed in a set of alternatives ($A_1$, $A_2$, …., $A_m$) and criteria ($g_1$, $g_2$, ….., $g_n$), $g_j(A_i)$ is the criteria value of the $i^{th}$ alternative $A_i$ of the $j^{th}$ criterion $g_j$. The $g_j(.)$ is defined by real-value function (j = 1, 2, 3, ….., n; i = 1, 2, 3, …..,m) and is expressed in a decision matrix D is shown below:

$$D = \begin{pmatrix} g_1(A_1) & .... & g_j(A_1) & .... & g_n(A_1) \\ .... & .... & .... & .... & .... \\ g_1(A_i) & .... & g_j(A_i) & .... & g_n(A_i) \\ .... & .... & .... & .... & .... \\ g_1(A_m) & .... & g_j(A_m) & .... & g_n(A_m) \end{pmatrix}$$

Assuming $g(A)$ and $g(A')$ as a criteria values of $A$ and $A'$ with respect to $g$, the difference between two criteria is calculated to estimate the intensity of the preference values $A$ over $A'$ using the equation 4.1.

$$P(A,A') = f(d) = f(g(A) - g(A')) \quad (4.1)$$

where $P(A,A')$ represents the intensity of preferences $A$ over $A'$ and $f(d)$ is a converting non-decreasing function from R (real numbers) to [0, 1] such that $f(d) = 0$ for $d \leq 0$. Such type of functions known as generalized criterion. There were six type of general criterion proposed by Brans et al. (1986) listed in Table 4.1 below. p and q values in the table represent preference and indifference thresholds respectively. The generalized criteria are selected by decision makers as per the intensity of the preference and preference structure depending upon the parameters. Table 4.1 illustrates the type and shape of the

criteria (Xu 2001; Marzouk 2008). Type I represents the special case of type II where q = 0.

Table 4.1: Generalized criteria list

| **Generalized criteria** | | |
|---|---|---|
| Type I True criteria<br>$f(d)=\begin{cases}1 \text{ if } d>0\\0 \text{ if } d\le 0\end{cases}$ | Type II Quasi criteria<br>$f(d)=\begin{cases}1 \text{ if } d>q\\0 \text{ if } d\le q\end{cases}$ | Type III Criterion with linear preference<br>$f(d)=\begin{cases}1 & \text{if } d>p\\ d/p & \text{if } 0<d\le p\\ 0 & d\le 0\end{cases}$ |
| Type IV Level criterion<br>$f(d)=\begin{cases}1 & \text{if } d>p\\ 1/2 & \text{if } q<d\le p\\ 0 & d\le q\end{cases}$ | Type V Criterion with linear preference and indifference area<br>$f(d)=\begin{cases}1 & \text{if } d>p\\ (d-q)/(p-q) & \text{if } q<d\le p\\ 0 & d\le q\end{cases}$ | Type VI Gaussian criterion<br>$f(d)=\begin{cases}1-\exp\left(-d^2/2\sigma^2\right) & \text{if } d>0\\ 0 & \text{if } d\le 0\end{cases}$ |

The superiority index $S_j(A_j)$ and inferiority index $I_j(A_j)$ of each alternative $A_i$ with respect to jth criterion are calculated as follows (equation 4.2 and 4.3):

$$S_j(A_j)=\sum_{k=1}^{m} P_j(A_i,A_k)=\sum_{k=1}^{m} f_j\left(g_j(A_i)-g_j(A_k)\right) \tag{4.2}$$

$$S_j(A_j)=\sum_{k=1}^{m} P_j(A_i,A_k)=\sum_{k=1}^{m} f_j\left(g_j(A_i)-g_j(A_k)\right) \tag{4.3}$$

The superiority and inferiority indices used to establish two matrices superiority matrix (S-matrix) and inferiority matrix (I-matrix) respectively are shown below.

$$S=\begin{pmatrix} S_1(A_1) & .... & S_j(A_1) & .... & S_n(A_1)\\ .... & .... & .... & .... & ....\\ S_1(A_i) & .... & S_j(A_i) & .... & S_n(A_i)\\ .... & .... & .... & .... & ....\\ S_1(A_m) & .... & S_j(A_m) & .... & S_n(A_m)\end{pmatrix} \text{ or } S=\left(S_j(A_i)\right)_{m\times n}$$

$$I=\begin{bmatrix} I_1(A_1) & .... & I_j(A_1) & .... & I_n(A_1)\\ .... & .... & .... & .... & ....\\ I_1(A_i) & .... & I_j(A_i) & .... & I_n(A_i)\\ .... & .... & .... & .... & ....\\ I_1(A_m) & .... & I_j(A_m) & .... & I_n(A_m)\end{bmatrix} \text{ or } I=\left(I_j(A_i)\right)_{m\times n}$$

S matrix shows the superiority and I matrix shows the inferiority information of each alternative on their respective criterion respectively.

### 4.2.2. Calculation of S-flow and I-flow

To attain global preference indices S-flow (superiority flow) $\phi^{>}(.)$ and I-flow $\phi^{<}(.)$ (inferiority flow) i.e. global intensity (superiority and inferiority) of each alternative, standard MCDM aggregation method is used.

Assume V as the aggregation function then S-flow and I-flow of each alternatives $A_i$ can be expressed by equation 4.4 (Xu 2001):

$$\phi^{>}(A_i) = V\left[S_1(A_i),.....,S_j(A_i).....,S_n(A_i)\right] \text{ and } \phi^{<}(A_i) = V\left[I_1(A_i),.....,I_j(A_i).....,I_n(A_i)\right] \tag{4.4}$$

where S-flow $\phi^{>}$ and I-flow $\phi^{<}$ must assume higher and smaller values respectively to represent $A_i$ is preferable (Xu, 2001).

When any MCDM aggregation approach such as YYY is coupled with SIR method then it is termed as SIR-YYY method. For performing MCDM approach, the weightage of the responses should be known. Weights used are expressed by $w_j (j = 1,2,3,.....,n)$ and sum of weights are equal to one.

$$\sum_{j=1}^{n} w_j = 1 \quad (w_j \geq 0) \tag{4.5}$$

For aggregation purpose, SIR-TOPSIS method is proposed (Xu, 2001; Marzouk, 2007). The traditional TOPSIS (Hwang and Yoon, 1981) and other TOPSIS such as BBTOPSIS (Rebai, 1993) can be employed to find superiority (S-flow) and Inferiority (I-flow) flows. It (SIR-TOPSIS) can be calculated using the following equations 4.6 and 4.7:

The $A_I^+$ (positive ideal solution) is the maximum positive value and $A_I^-$ (negative ideal solution) is minimum ideal value (Xu 2001) for the superiority matrix $S = [S_j[A_i]]_{m\times n}$ can be expressed by equation 4.6 and 4.7

$$A_S^+ = (\max S_1(A_i),.....,\max\ S_n(A_i)) = \left(S_1^+,.....,S_n^+\right) \tag{4.6}$$

$$A_S^- = (\min S_1(A_i),.....,\min\ S_n(A_i)) = \left(S_1^-,.....,S_n^-\right) \tag{4.7}$$

S-flow is expressed by equation 4.8

$$\varphi^{>}(A_i) = S^-(A_i)/\left(S^-(A_i) + S^+(A_i)\right), \tag{4.8}$$

where,

$$S^{+}(A_i)=\left\{\sum_{j=1}^{n}\left|w_j\left(S_j(A_i)-S_j^{+}\right)\right|^{\lambda}\right\}^{1/\lambda} \quad \text{and} \quad S^{-}(A_i)=\left\{\sum_{j=1}^{n}\left|w_j\left(S_j(A_i)-S_j^{-}\right)\right|^{\lambda}\right\}^{1/\lambda} \tag{4.9}$$

and $\lambda$ is the Minkowski distance (Xu 2001)

Similarly, the $A_I^{+}$ (ideal solution) and $A_I^{-}$ (negative ideal solution) for the inferiority matrix $I=[I_j[A_i]]_{m\times n}$ can be expressed by equations 4.10 and 4.11.

$$A_I^{+}=(\max I_1(A_i),.....,\max I_n(A_i))=\left(I_1^{+},.....,I_n^{+}\right) \tag{4.10}$$

$$A_I^{-}=(\min I_1(A_i),.....,\min I_n(A_i))=\left(I_1^{-},.....,I_n^{-}\right) \tag{4.11}$$

I-flow is expressed by $\varphi^{<}(A_i)$

$$\varphi^{<}(A_i)=I^{-}(A_i)/\left(I^{-}(A_i)+I^{+}(A_i)\right), \tag{4.12}$$

where,

$$I^{+}(A_i)=\left\{\sum_{j=1}^{n}\left|w_j\left(I_j(A_i)-I_j^{+}\right)\right|^{\lambda}\right\}^{1/\lambda} \quad \text{and} \quad I^{-}(A_i)=\left\{\sum_{j=1}^{n}\left|w_j\left(I_j(A_i)-I_j^{-}\right)\right|^{\lambda}\right\}^{1/\lambda} \tag{4.13}$$

To obtain the single equivalent response, r-flow is calculated using equation 4.14.

$$r-flow=\frac{\varphi^{>}}{\varphi^{>}+\varphi^{<}} \tag{4.14}$$

### 4.3. Harmony search (HS) algorithm

Harmony search (HS) algorithm is a new music (jazz) based meta-heuristic optimization algorithm developed by Lee and Geem (2005). HS algorithm is a music inspired optimization algorithm using the concept of developing a perfect state of harmony by improvising musical process. The objective is to optimize the process parameters by creating the perfect quality of music combination by adjusting the bandwidth, pitch and the best harmony memory to get global optimal value. The concept behind HS is to simulate the memory of the musicians to obtain best memory. In HS, the well trained musician plays the music by creating new harmony. When a musician plays music, he or she may play a pitch of her or his memory creating music by adjusting the pitch rate randomly and playing new notes (Yang 2009). There are three main components which need to be formalized (Omran and Mahdavi 2008) i.e. harmony

memory, pitch and randomization of notes. In an objective function, the variables are considered as pitch of musical instruments and the solution is termed as harmony vector. The aesthetic harmony developed by the algorithm is stored as best fitness value of the objective functions in its memory. The process of attaining best harmony goes on by adjusting of pitch and bandwidth continuously till best harmony is achieved by replacing the worst harmony. The main merit of the algorithm is that it has few mathematical equations and less number of parameters to be adjusted. Although the algorithm is very easy to handle but the major demerit is that it is sometimes difficult to do fine tuning of the solutions (Mahdavi 2007). To overcome such type demerits, several attempts have been made to improve the algorithm (Mahdavi 2007; Omran and Mahdavi 2008; Yang 2009). By introducing PAR (pitch adjusting rate) and the bw (bandwidth) in the algorithm, imperative parameters in performing the tuning of optimized solution vectors, have the potential in improving the convergence rate of algorithm. In basic HS algorithm, PAR and bw are kept fixed.

The main drawback of this method appears in the number of iterations the algorithm needs to find an optimal solution. Small PAR values with large bw values can cause to poor performance of the algorithm and considerable increase in iterations needed to find optimum solution. Although small bw values in final generations increase the fine-tuning of solution vectors but in early generations bw must take a bigger value to enforce the algorithm to increase the diversity of solution vectors. Furthermore large PAR values with small bw values usually cause the improvement of best solutions in final generations when the algorithm converges to optimal solution vector. The key difference between improved and traditional harmony search method is in the way of adjusting PAR and bw. To improve the performance of the HS algorithm and eliminate the drawbacks lies with fixed values of PAR. The algorithm has been successfully applied in various benchmark problems along design and process optimization with reasonable degree success (Lee and Geem 2005; Mahdavi 2007; Omran and Mahdavi 2008). Following are the steps involved in HS algorithm (Lee and Geem 2005; Mahdavi 2007; Omran and Mahdavi 2008; Yang 2009; Mohammed 2013).

**I. Initialization of the algorithm**

Define the objective function to be minimized for the optimization problem as f(x) subjected to $x_i \varepsilon X_i$ i=1,2,….N where **x** is the set of each decision variable $x_i$, N is the number of decision variable, $X_i$ is the set of possible range of values for

each decision variable i.e. ${}_{L}x_i \leq X_i \leq {}_{U}x_i$,. ${}_{L}x_i$ and ${}_{U}x_i$ are the lower and upper bounds for each variable. The HS algorithm parameters such as harmony memory size (HMS) i.e. the number of solution vectors in the harmony memory, pitch adjusting rate (PAR), harmony memory considering rate (HMCR) and maximum number of iterations or stopping criterion are initialized.

**II. Initiating the harmony memory**

Randomly generate vectors to fill the HM matrix as solution vectors depending on HMS.

$$HM=\begin{bmatrix} x_1^1 & \cdots & x_N^1 \\ \vdots & \ddots & \vdots \\ x_1^{HMS} & \cdots & x_N^{HMS} \end{bmatrix}$$

**III. Improvisation of new harmony**

A new harmony vector, $x' = (x_1', x_2' \ldots\ldots x_N')$, is generated based on three rules: (1) memory consideration, (2) pitch adjustment and (3) random selection. Generating a new harmony is called improvisation. In the memory consideration, the value of the first decision variable $(x_1')$ for the new vector is chosen from any of the values in the specified HM range $x' = (x_1'^1 - x_1'^{HMS})$. Values of other decision variables $(x_2', x_3' \ldots\ldots x_N')$ are chosen in the same manner. The HMCR, which varies between 0 and 1, is the rate of choosing one values from the historical values stored in the HM while (1-HMCR) is the rate of randomly selecting one value from the possible range of values.

$$x_i' \leftarrow \begin{cases} x_i' \in \{x_i^1, x_i^2 \ldots\ldots, x_i^{HMS} & \text{with probability HMCR} \\ x_i' \in X_i & \text{with probability } (1 - \text{HMCR}) \end{cases} \quad (4.15)$$

Every component obtained by the memory consideration is examined to determine whether it should be pitch adjusted. This operation uses the PAR parameter for pitch adjustment.

$$\text{Pitch adjusting decison for } x_i' \leftarrow \begin{cases} \text{Yes} & \text{with probability PAR} \\ \text{No} & \text{with probability } (1 - \text{PAR}) \end{cases} \quad (4.16)$$

The value of (1-PAR) sets the rate of doing nothing. If the pitch adjustment decision for $x_i'$ is Yes, $x_i'$ is replaced as follows:

$$x_i' \leftarrow x_i' \pm \text{rand}() * bw \quad (4.17)$$

where, bw is an arbitrary bandwidth and rand( ) is a random number between 0 and 1.

In order to improve the global search capability of the HS algorithm, PAR and bw are dynamically adjusted with generation number. The PAR will be adjusted linearly using the equation

$$\mathrm{PAR(gn)} = \mathrm{PAR_{min}} + \frac{\mathrm{PAR_{max}} - \mathrm{PAR_{min}}}{\mathrm{NI}} \times \mathrm{gn} \tag{4.18}$$

PAR(gn) is the pitch adjustment rate for each generation, NI is number of solution vector generations (number of iterations), gn is generation number, and $\mathrm{PAR_{min}}$ and $\mathrm{PAR_{max}}$ minimum and maximum pitch adjustment rate.

Value of bw is decreased exponentially, higher value of bw maximize the diversity of the solutions and lower the value of bw helps to tune the final solution.

$$\mathrm{bw(gn)} = \mathrm{bw_{max}} \times \mathrm{e}^{(\mathrm{c} \times \mathrm{gn})} \tag{4.19}$$

$$\mathrm{c} = \frac{\ln\left(\frac{\mathrm{bw_{min}}}{\mathrm{bw_{max}}}\right)}{\mathrm{NI}} \tag{4.20}$$

where bw(gn) is the bandwidth for each generation, $\mathrm{bw_{min}}$ and $\mathrm{bw_{max}}$ are minimum and maximum bandwidth respectively.

**IV. Updating the new harmony**

If the new Harmony vector, $\mathrm{x'} = (\mathrm{x'_1}, \mathrm{x'_2} \ldots \ldots \mathrm{x'_N})$ is better than the worst in the HM, judged in terms of the objective function value, the new harmony is included in the HM and the exising worst harmony is removed from the HM.

**V. Stopping criteria**

If the stopping criterion (maximum number of improvisations) is satisfied, computation is terminated. Otherwise, Steps III and IV are repeated.

### 4.4. Experimental details

The experiments are performed on a CNC milling machine (MAXMILL supplied by MTAB Engineers, India) having FANUC controller. The detailed specifications of the CNC machine are listed in Table 4.2. The circular shaped Ti6Al4V grade 5 and AISI 316 having dimension of 65 mm diameter and 5 mm thickness has been used as work piece for drilling operation. Three input parameters such as spindle speed (A) in rpm, feed rate (B) in mm/min and drill bit diameter (C) in mm are considered (Table 3.3).

Table 4.2: Machine specifications

| Specification | Description |
|---|---|
| X Axis travel (Longitudinal Travel) | 300 mm |
| Y Axis travel (Cross Travel) | 250 mm |
| Z Axis travel (Vertical Travel) | 250 mm |
| Clamping Surface | 500 × 350 mm |
| Repeatability | ± 0.005 mm |
| Positional Accuracy | 0.010 mm |
| Coolant Motor | RKM 02505 |
| Motor Power | 0.37 kW |
| Tank Capacity | 110 ltr (Filter and Tray) |

Figure 4.1: Experimental setup for drilling experiment

The actual control parameters are converted into coded value using equation 3.3 as discussed in previous chapter in section 3.3. Table 3.3 (section 3.3) shows actual and coded machining parameters. Face centered central composite design, a response surface methodology (RSM) approach, has been used for obtaining design layout for conducting experiments (Kosaraju and Anne 2013; Pradhan 2013). The details of experimental design are discussed in previous chapter in section 3.3 (Table 3.4).

In drilling operation, the quality of the hole is of foremost important. Circularity is one of the important metrological parameters used to check the roundness of circular parts or features. The circularity of the hole is measured by using the ratio of minimum ($r_1$) to maximum ($r_2$) Feret's diameters of the hole (Ghoreishi et al. 2002). The diameters are measured using optical microscope (RADIAL INSTRUMENT with Samsung camera setup, 30-X magnification Figure 4.2). Farets's diameter is obtained by joining tangents to the maximum points of the surface. The images of hole so acquired are used in image processing toolbox of MATLAB 12.0 to measure the Farret's diameter (Figure 4.5) to

obtain the circularity at entry ($C_{ent}$) and circularity at exit ($C_{exit}$) as listed in Tables 4.3 and 4.4 for Ti6Al4V and AISI 316 respectively. The toolmaker microscope Carl Zeiss (Figure 4.3), Germany (having resolution up to 0.0001 and of 30X magnifications) has been used to measure burr height at entry ($B_{en}$) and burr height at exit ($B_{ex}$) (Figure 4.6). The surface finishes (surface roughness, $R_a$) of the drilled holes are measured by surface roughness tester SJ-210 (supplied by Mitutoyo America Corporation, USA Figure 4.4).

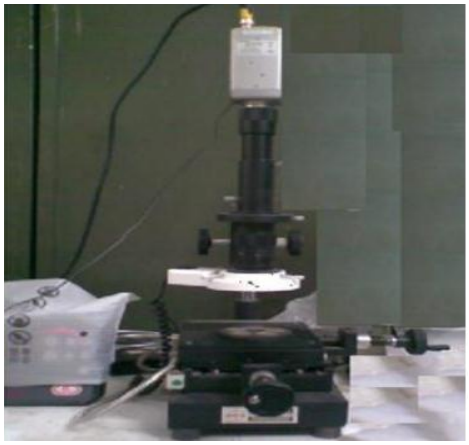

Figure 4.2: RADIAL INSTRUMENT with Samsung camera setup, 30-X magnification

Figure 4.3: Tool maker's microscope

Figure 4.4: Surface roughness tester SJ-210

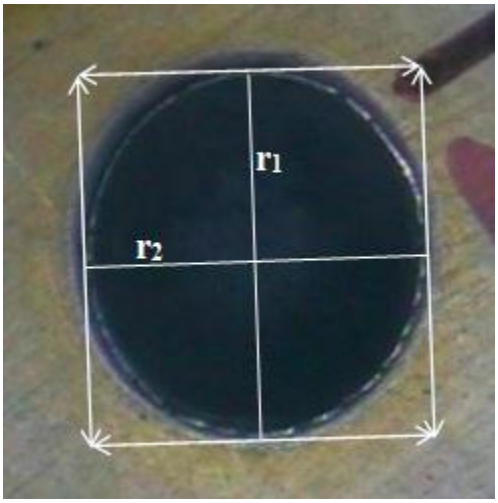


Figure 4.5: Drilled hole at speed of 500 rpm, feed rate of 50mm/min and at drill bit of 6 mm diameter

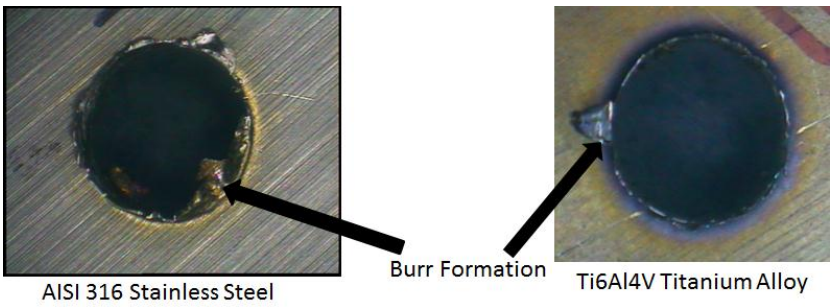


Figure 4.6: Burr formation after drilling of AISI 316 and Ti6Al4V work pieces

Table 4.3: Drilling responses for Ti6Al4V

| Exp. No. | $C_{ent}$ | $C_{exit}$ | $B_{en}$ | $B_{ex}$ | $R_a$ |
|---|---|---|---|---|---|
| 1 | 0.23 | 1.92 | 6.299 | 0.960 | 0.952 |
| 2 | 0.24 | 2.47 | 8.531 | 0.970 | 0.959 |
| 3 | 0.22 | 1.35 | 2.237 | 0.940 | 0.931 |
| 4 | 0.28 | 1.86 | 2.346 | 0.938 | 0.930 |
| 5 | 0.45 | 2.05 | 3.377 | 0.930 | 0.924 |
| 6 | 0.33 | 1.84 | 3.648 | 0.963 | 0.955 |
| 7 | 0.58 | 1.11 | 20.901 | 0.950 | 0.948 |
| 8 | 0.41 | 1.06 | 19.687 | 0.978 | 0.970 |
| 9 | 0.3 | 2.1 | 6.964 | 0.949 | 0.941 |
| 10 | 0.2 | 2.84 | 7.612 | 0.950 | 0.945 |
| 11 | 0.21 | 2.09 | 6.486 | 0.970 | 0.966 |
| 12 | 0.2 | 1.65 | 7.640 | 0.950 | 0.940 |
| 13 | 0.3 | 1.78 | 7.825 | 0.980 | 0.972 |
| 14 | 0.49 | 2.02 | 7.654 | 0.977 | 0.969 |
| 15 | 0.22 | 2.15 | 8.775 | 0.960 | 0.951 |
| 16 | 0.23 | 2.34 | 4.181 | 0.973 | 0.965 |
| 17 | 0.17 | 2.16 | 9.796 | 0.970 | 0.961 |
| 18 | 0.17 | 2.41 | 6.487 | 0.967 | 0.959 |
| 19 | 0.16 | 2.24 | 7.756 | 0.972 | 0.958 |
| 20 | 0.17 | 2.45 | 9.564 | 0.970 | 0.962 |

Table 4.4: Drilling responses for AISI 316

| Exp. No. | $C_{ent}$ | $C_{exit}$ | $B_{en}$ | $B_{ex}$ | $R_a$ |
|---|---|---|---|---|---|
| 1 | 0.842 | 0.8944 | 0.37 | 0.6709 | 1.3978 |
| 2 | 0.930 | 0.9022 | 0.20 | 1.7304 | 2.5224 |
| 3 | 0.926 | 0.8736 | 0.26 | 0.6853 | 1.6436 |
| 4 | 0.962 | 0.8732 | 0.16 | 2.9268 | 2.0196 |
| 5 | 0.957 | 0.8665 | 0.39 | 0.9213 | 8.4075 |
| 6 | 0.952 | 0.8975 | 0.35 | 0.9637 | 7.9460 |
| 7 | 0.929 | 0.8906 | 0.33 | 2.3459 | 17.614 |
| 8 | 0.876 | 0.9128 | 0.51 | 2.9749 | 8.0010 |
| 9 | 0.911 | 0.8834 | 0.57 | 1.0671 | 9.6895 |
| 10 | 0.885 | 0.8879 | 0.42 | 1.6954 | 6.0075 |
| 11 | 0.909 | 0.9088 | 0.38 | 1.0848 | 6.2480 |
| 12 | 0.920 | 0.8889 | 0.39 | 2.1101 | 6.1395 |
| 13 | 0.926 | 0.9147 | 0.18 | 1.7783 | 6.5671 |
| 14 | 0.918 | 0.9114 | 0.24 | 1.6068 | 13.0625 |
| 15 | 0.920 | 0.8933 | 0.27 | 1.7736 | 9.0700 |
| 16 | 0.923 | 0.9076 | 0.29 | 1.9023 | 8.5215 |
| 17 | 0.931 | 0.9038 | 0.33 | 1.4690 | 8.0405 |
| 18 | 0.901 | 0.9015 | 0.37 | 1.3556 | 8.1100 |
| 19 | 0.924 | 0.9106 | 0.41 | 1.7992 | 7.7930 |
| 20 | 0.929 | 0.9048 | 0.32 | 1.8194 | 8.1300 |

### 4.5. Results and Discussions

The analysis of variance (ANOVA) analysis is performed to know the statistical significance of the control parameters (spindle speed, feed rate and drill bit diameter) on the drilling responses such as burr height at entry ($B_{en}$), burr height at exit ($B_{ex}$), surface roughness ($R_a$), circularity at entry ($C_{ent}$) and circularity at exit ($C_{exit}$) as shown in Table 4.5, 4.6, 4.7, 4.8 and 4.9 respectively for Ti6Al4V. The coefficient of determination ($R^2$) for $B_{en}$, $B_{ex}$, $R_a$, $C_{en}$ and $C_{ex}$ are 94.77%, 89.82%, 97.05%, 90.35% and 88.04% respectively. All the terms present in the ANOVA are not significant; hence they are pooled as shown in Tables 4.5, 4.8 and 4.9 for few responses.

Table 4.5 shows that A, B, C, A×C and B×C are significant for burr height at entry, Table 4.6 shows that A, B, A×C, $B^2$ and $C^2$ are significant terms for burr height at exit. Table 4.7 shows A, A×C, B×C, $A^2$ and $B^2$ are significant terms for the surface roughness. Tables 4.8 and 4.9 suggest that the terms A, A×C, B×C, $A^2$, and $C^2$ are statistically significant terms for circularity at entry and exit at significance level of 0.05.

Table 4.5: Pooled ANOVA for burr height at entry (Ti6Al4V)

| Source | Sum of Squares | df | Mean Square | F Value | p-value Prob> F | |
|---|---|---|---|---|---|---|
| Model | 0.2480 | 6 | 0.0413 | 39.2885 | < 0.0001 | significant |
| A-Spindle speed | 0.0071 | 1 | 0.0071 | 6.82470 | 0.02150 | |
| B-Feed rate | 0.0052 | 1 | 0.0053 | 5.02660 | 0.04300 | |
| C-Drill diameter | 0.0980 | 1 | 0.0980 | 93.1299 | < 0.0001 | |
| A×C | 0.0162 | 1 | 0.0162 | 15.3934 | 0.00170 | |
| B×C | 0.0040 | 1 | 0.0040 | 3.84830 | 0.07160 | |
| $C^2$ | 0.1173 | 1 | 0.1173 | 111.5082 | < 0.0001 | |
| Residual | 0.0136 | 13 | 0.0011 | | | |
| Lack of Fit | 0.0094 | 8 | 0.0012 | 1.4109 | 0.3665 | not significant |
| Pure Error | 0.0042 | 5 | 0.0008 | | | |
| Cor Total | 0.2617 | 19 | | | | |

Table 4.6 ANOVA for burr height at exit (Ti6Al4V)

| Source | Sum of Squares | df | Mean Square | F Value | p-value Prob> F | |
|---|---|---|---|---|---|---|
| Model | 3.4665 | 9 | 0.385167 | 9.8009 | 0.0007 | significant |
| A -Spindle speed | 0.2371 | 1 | 0.23716 | 6.0347 | 0.0339 | |
| B -Feed rate | 1.1155 | 1 | 1.11556 | 28.3864 | 0.0003 | |
| C -Drill diameter | 0.1690 | 1 | 0.16900 | 4.3003 | 0.0649 | |
| A×B | 0.0018 | 1 | 0.00180 | 0.0458 | 0.8348 | |
| A×C | 0.2178 | 1 | 0.21780 | 5.5421 | 0.0404 | |
| B×C | 0.0364 | 1 | 0.03645 | 0.9275 | 0.3582 | |
| $A^2$ | 0.1065 | 1 | 0.10652 | 2.7106 | 0.1307 | |
| $B^2$ | 0.4470 | 1 | 0.44702 | 11.375 | 0.0071 | |
| $C^2$ | 0.3829 | 1 | 0.38297 | 9.7452 | 0.0108 | |
| Residual | 0.3929 | 10 | 0.03929 | | | |

| | | | | | | |
|---|---|---|---|---|---|---|
| Lack of Fit | 0.3115 | 5 | 0.06230 | 3.8229 | 0.0837 | not significant |
| Pure Error | 0.0814 | 5 | 0.01629 | | | |
| Cor Total | 3.8594 | 19 | | | | |

Table 4.7: ANOVA for surface roughness (Ti6Al4V)

| Source | Sum of Squares | df | Mean Square | F Value | p-value Prob> F | |
|---|---|---|---|---|---|---|
| Model | 429.1685 | 6 | 71.52808 | 71.2412 | < 0.0001 | significant |
| A-Spindle speed | 0.4183 | 1 | 0.418325 | 0.41665 | 0.5298 | |
| B-Feed rate | 70.0698 | 1 | 70.06980 | 69.7888 | < 0.0001 | |
| C-Drill diameter | 115.7952 | 1 | 115.7952 | 115.3309 | < 0.0001 | |
| A×B | 1.6260 | 1 | 1.626036 | 1.6195 | 0.2254 | |
| A×C | 1.3478 | 1 | 1.347836 | 1.3424 | 0.2674 | |
| B×C | 239.9112 | 1 | 239.9112 | 238.9491 | < 0.0001 | |
| Residual | 13.0523 | 13 | 1.004026 | | | |
| Lack of Fit | 6.9953 | 8 | 0.874418 | 0.7218 | 0.6758 | not significant |
| Pure Error | 6.0569 | 5 | 1.211399 | | | |
| Cor Total | 442.2208 | 19 | | | | |

Table 4.8: Pooled ANOVA for circularity at entry (Ti6Al4V)

| Source | Sum of Squares | df | Mean Square | F Value | P-value Prob> F | |
|---|---|---|---|---|---|---|
| Model | 0.0035 | 8 | 0.000447 | 12.873 | 0.0001 | significant |
| A-Spindle speed | 0.0005 | 1 | 0.000508 | 14.637 | 0.0028 | |
| B-Feed rate | 0.0001 | 1 | 0.000129 | 3.7108 | 0.0803 | |
| C-Drill diameter | 9.41E-06 | 1 | 9.41E-06 | 0.2710 | 0.6130 | |
| A×C | 0.0003 | 1 | 0.000347 | 9.9960 | 0.0091 | |
| B×C | 0.0009 | 1 | 0.000935 | 26.929 | 0.0003 | |
| $A^2$ | 0.0008 | 1 | 0.000896 | 25.784 | 0.0004 | |
| $C^2$ | 0.0001 | 1 | 0.000157 | 4.5080 | 0.0573 | |
| $B^2$ | 0.0003 | 1 | 0.00033 | 9.5020 | 0.0104 | |
| Residual | 0.0003 | 11 | 3.47E-05 | | | |
| Lack of Fit | 0.0003 | 6 | 4.49E-05 | 1.9900 | 0.2336 | not significant |
| Pure Error | 0.0001 | 5 | 2.26E-05 | | | |
| Cor Total | 0.0039 | 19 | | | | |

Table 4.9: Pooled ANOVA for circularity at exit (Ti6Al4V)

| Source | Sum of Squares | df | Mean Square | F Value | P-value Prob> F | |
|---|---|---|---|---|---|---|
| Model | 0.0032 | 7 | 0.000453 | 12.624 | 0.0001 | significant |
| A-Spindle speed | 0.0004 | 1 | 0.000424 | 11.805 | 0.0049 | |
| B-Feed rate | 9.18E-05 | 1 | 9.18E-05 | 2.5570 | 0.1358 | |
| C-Drill diameter | 4.28E-05 | 1 | 4.28E-05 | 1.1940 | 0.2961 | |
| A×C | 0.0003 | 1 | 0.000262 | 7.3040 | 0.0192 | |
| B×C | 0.0009 | 1 | 0.000995 | 27.704 | 0.0002 | |
| $A^2$ | 0.0013 | 1 | 0.001262 | 35.144 | < 0.0001 | |
| $C^2$ | 0.0002 | 1 | 0.000182 | 5.073 | 0.0438 | |
| Residual | 0.0004 | 12 | 3.59E-05 | | | |
| Lack of Fit | 0.0003 | 7 | 4.44E-05 | 1.843 | 0.2594 | not significant |

| | | | |
|---|---|---|---|
| Pure Error | 0.0001 | 5 | 2.41E-05 |
| Cor Total | 0.0036 | 19 | |

The surface plots helps to understand the effectiveness of control parameters on drilling responses of Ti6Al4V. Figure 4.7 indicates that burr height at entry ($B_{en}$) decreases with the increase of feed rate for any value of the drill diameter. Similarly, burr height at entry goes on decreasing slightly with increase of drill diameter for a particular value of feed rate. Figure 4.8 shows that the burr height at exit ($B_{ex}$) increases initially and then decreases with feed rate for any value of drill diameter. Same trend is observed when drill diameter increases for any particular value of feed rate. Figure 4.9 indicates that the surface roughness gradually increases with the increase of spindle speed for any value of feed rate. However, surface roughness increases rapidly with the increase of feed rate for any value of spindle speed.

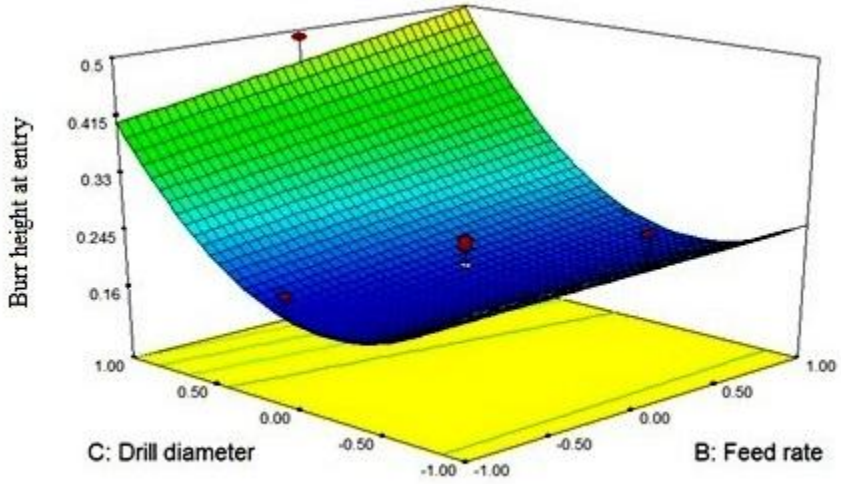


Figure 4.7: Surface plot for burr height at entry (Ti6Al4V)

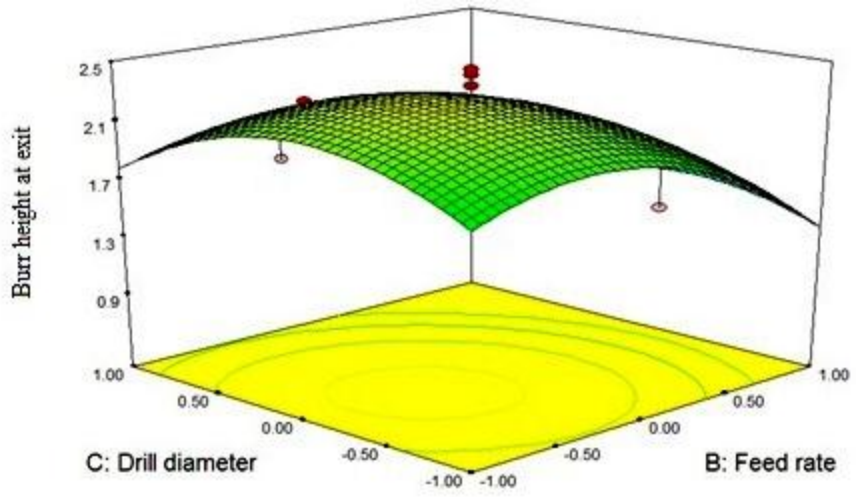


Figure 4.8: Surface plot for burr height at exit (Ti6Al4V)

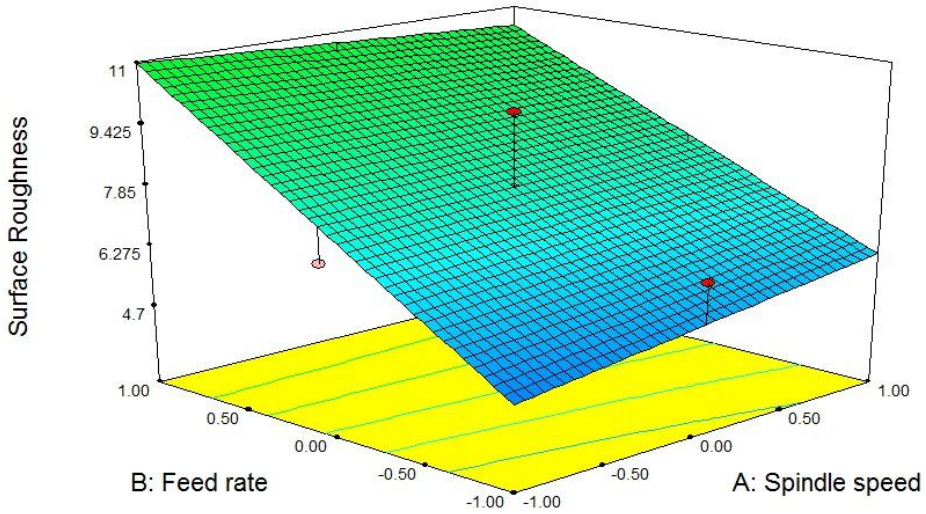


Figure 4.9: Surface plot for surface roughness (Ti6Al4V)

Similarly, the ANOVA is carried out to know the adequacy and statistical significance of the control parameters (spindle speed, feed rate and drill bit diameter) on burr height at entry ($B_{en}$), burr height at exit ($B_{ex}$), surface roughness ($R_a$), $C_{ent}$ and $C_{exit}$ for drilling of AISI 316. The coefficient of determination ($R^2$) for $B_{en}$, $B_{ex}$, $R_a$, $C_{ent}$ and $C_{exit}$ are 85.38%, 93.81%, 94.45%, 86.79% and 90.04% respectively. Table 4.10 shows that C, A×B and$C^2$ are significant for burr height at entry. Table 4.11 shows that A, B, A×B, A×C and B×C are significant terms for burr height at exit. Table 4.12 shows that A, B, C, A×B, A×C, B×C and $B^2$ are significant terms for the surface roughness. Tables 4.13 shows that A×B, A×C and B×C are significant terms for circularity at entry. Table 4.14

suggest that the terms A, A×C, B×C, $A^2$, and $C^2$ are statistically significant terms for circularity at exit at significance level of 0.05.

Table 4.10: ANOVA for burr height at entry (AISI 316)

| Source | Sum of Squares | df | Mean Square | F Value | p-value Prob> F | |
|---|---|---|---|---|---|---|
| Model | 0.17369 | 9 | 0.0193 | 6.4907 | 0.0036 | significant |
| A-Spindle speed | 0.00784 | 1 | 0.00784 | 2.6368 | 0.1355 | |
| B-Feed rate | 0.00016 | 1 | 0.00016 | 0.0538 | 0.8212 | |
| C-Drill diameter | 0.04225 | 1 | 0.04225 | 14.21 | 0.0037 | |
| A×B | 0.01051 | 1 | 0.01051 | 3.5357 | 0.0895 | |
| A×C | 0.02101 | 1 | 0.02101 | 7.0672 | 0.0240 | |
| B×C | 0.00781 | 1 | 0.00781 | 2.6276 | 0.1361 | |
| $A^2$ | 0.04297 | 1 | 0.04297 | 14.452 | 0.0035 | |
| $B^2$ | 0.00062 | 1 | 0.00062 | 0.2081 | 0.6580 | |
| $C^2$ | 0.0704 | 1 | 0.0704 | 23.678 | 0.0007 | |
| Residual | 0.02973 | 10 | 0.00297 | | | |
| Lack of Fit | 0.01645 | 5 | 0.00329 | 1.2383 | 0.4101 | not significant |
| Pure Error | 0.01328 | 5 | 0.00266 | | | |
| Cor Total | 0.20342 | 19 | | | | |

Table 4.11: ANOVA for burr height at exit (AISI 316)

| Source | Sum of Squares | df | Mean Square | F Value | p-value Prob> F | |
|---|---|---|---|---|---|---|
| Model | 7.4139 | 9 | 0.8238 | 16.8373 | < 0.0001 | significant |
| A-Spindle speed | 2.1166 | 1 | 2.1166 | 43.2629 | < 0.0001 | |
| B-Feed rate | 3.217 | 1 | 3.217 | 65.7545 | < 0.0001 | |
| C-Drill diameter | 0.1042 | 1 | 0.1042 | 2.13027 | 0.1751 | |
| A×B | 0.391 | 1 | 0.391 | 7.99167 | 0.0179 | |
| A×C | 0.8643 | 1 | 0.8643 | 17.6668 | 0.0018 | |
| B×C | 0.6188 | 1 | 0.6188 | 12.6485 | 0.0052 | |
| $A^2$ | 0.0856 | 1 | 0.0856 | 1.75048 | 0.2153 | |
| $B^2$ | 0.0043 | 1 | 0.0043 | 0.08871 | 0.7719 | |
| $C^2$ | 0.05 | 1 | 0.05 | 1.02178 | 0.3359 | |
| Residual | 0.4893 | 10 | 0.0489 | | | |
| Lack of Fit | 0.2479 | 5 | 0.0496 | 1.02739 | 0.4885 | not significant |
| Pure Error | 0.2413 | 5 | 0.0483 | | | |
| Cor Total | 7.9031 | 19 | | | | |

Table 4.12: ANOVA for surface roughness (AISI 316)

| Source | Sum of Squares | df | Mean Square | F Value | p-value Prob> F | |
|---|---|---|---|---|---|---|
| Model | 261.018 | 9 | 29.0021 | 18.919 | < 0.0001 | significant |
| A-Spindle speed | 15.0207 | 1 | 15.0207 | 9.7985 | 0.0107 | |
| B-Feed rate | 7.91388 | 1 | 7.91388 | 5.1625 | 0.0464 | |
| C-Drill diameter | 167.122 | 1 | 167.122 | 109.02 | < 0.0001 | |
| A×B | 12.2515 | 1 | 12.2515 | 7.9921 | 0.0179 | |
| A×C | 16.7479 | 1 | 16.7479 | 10.925 | 0.0079 | |
| B×C | 11.3252 | 1 | 11.3252 | 7.3878 | 0.0216 | |

| | | | | | | |
|---|---|---|---|---|---|---|
| $A^2$ | 1.9033 | 1 | 1.9033 | 1.2416 | 0.2912 | |
| $B^2$ | 17.0049 | 1 | 17.0049 | 11.093 | 0.0076 | |
| $C^2$ | 3.53868 | 1 | 3.53868 | 2.3084 | 0.1596 | |
| Residual | 15.3296 | 10 | 1.53296 | | | |
| Lack of Fit | 14.3013 | 5 | 2.86026 | 13.908 | 0.0059 | not significant |
| Pure Error | 1.02831 | 5 | 0.20566 | | | |
| Cor Total | 276.348 | 19 | | | | |

Table 4.13: ANOVA for circularity at entry (AISI 316)

| **Source** | **Sum of Squares** | **df** | **Mean Square** | **F Value** | **p-value Prob> F** | |
|---|---|---|---|---|---|---|
| Model | 0.0125 | 9 | 0.0014 | 7.3012 | 0.0023 | significant |
| A-Spindle speed | 0.0002 | 1 | 0.0002 | 0.8408 | 0.3807 | |
| B-Feed rate | 5E-05 | 1 | 5E-05 | 0.278 | 0.6095 | |
| C-Drill diameter | 0.0002 | 1 | 0.0002 | 1.112 | 0.3165 | |
| A×B | 0.0012 | 1 | 0.0012 | 6.569 | 0.0282 | |
| A×C | 0.0041 | 1 | 0.0041 | 21.759 | 0.0009 | |
| B×C | 0.006 | 1 | 0.006 | 31.794 | 0.0002 | |
| $A^2$ | 0.0004 | 1 | 0.0004 | 2.2417 | 0.1652 | |
| $B^2$ | 5E-05 | 1 | 5E-05 | 0.2365 | 0.6372 | |
| $C^2$ | 0.0004 | 1 | 0.0004 | 1.9264 | 0.1953 | |
| Residual | 0.0019 | 10 | 0.0002 | | | |
| Lack of Fit | 0.0013 | 5 | 0.0003 | 2.296 | 0.1914 | not significant |
| Pure Error | 0.0006 | 5 | 0.0001 | | | |
| Cor Total | 0.0144 | 19 | | | | |

Table 4.14: ANOVA for circularity at exit (AISI 316)

| **Source** | **Sum of Squares** | **df** | **Mean Square** | **F Value** | **p-value Prob> F** | |
|---|---|---|---|---|---|---|
| Model | 0.0034 | 9 | 0.00038 | 10.0465 | 0.0006 | significant |
| A-Spindle speed | 0.0004 | 1 | 0.00042 | 11.2209 | 0.0074 | |
| B-Feed rate | 9E-05 | 1 | 9.2E-05 | 2.43082 | 0.1500 | |
| C-Drill diameter | 4E-05 | 1 | 4.3E-05 | 1.13451 | 0.3119 | |
| A×B | 4E-05 | 1 | 3.6E-05 | 0.95648 | 0.3511 | |
| A×C | 0.0003 | 1 | 0.00026 | 6.94237 | 0.0250 | |
| B×C | 0.001 | 1 | 0.00099 | 26.3334 | 0.0004 | |
| $A^2$ | 0.0009 | 1 | 0.00094 | 24.9075 | 0.0005 | |
| $B^2$ | 8E-05 | 1 | 7.7E-05 | 2.04177 | 0.1835 | |
| $C^2$ | 0.0002 | 1 | 0.00022 | 5.77329 | 0.0371 | |
| Residual | 0.0004 | 10 | 3.8E-05 | | | |
| Lack of Fit | 0.0002 | 5 | 4E-05 | 1.13407 | 0.4468 | not significant |
| Pure Error | 0.0002 | 5 | 3.5E-05 | | | |
| Cor Total | 0.0038 | 19 | | | | |

Similarly, the surface plots have been developed to carefully analyze the effect of the control parameters on process responses during drilling of AISI 316. Figure 4.10 shows that burr height at entry increases initially and then decreases as spindle speed

increases for a particular value of feed rate. The burr height at entry decreases with increase of feed rate for any value of spindle speed. Figure 4.11 represents that the burr height at exit increases with increase in spindle speed for any value of drill diameter. Burr height at exit increases with increase of drill diameter for any value of spindle speed. Figure 4.12 indicates that the surface roughness initially increases and then decreases with the increase of spindle speed for any value of feed rate. Similarly, it shows that surface roughness initially increases briskly and then decreases with feed rate for any value of spindle speed.

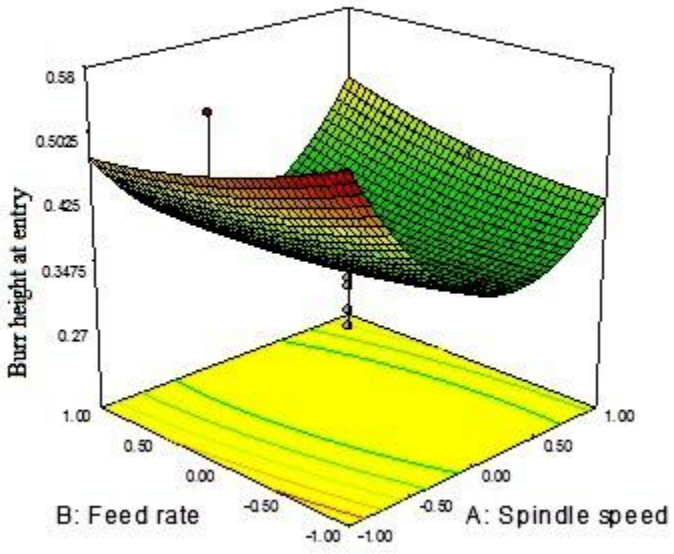


Figure 4.10: Surface plot for burr height at entry (AISI 316)

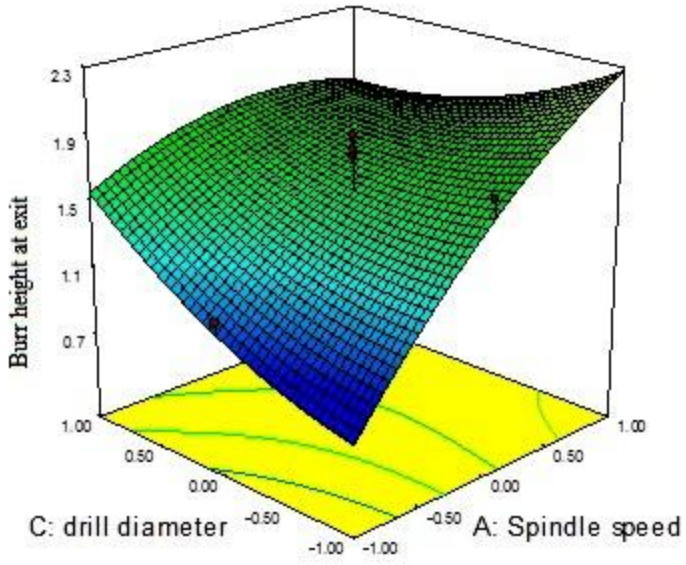


Figure 4.11: Surface plot for burr height at exit (AISI 316)

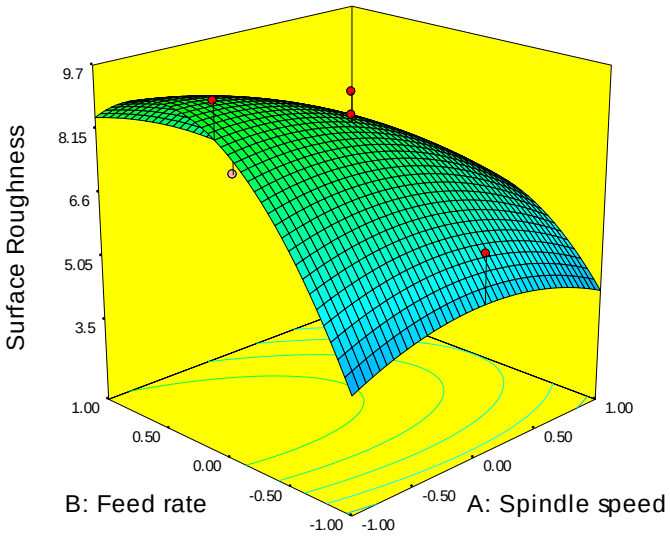


Figure 4.12: Surface plot for surface roughness (AISI 316)

### 4.5.1. Comparison of responses

To compare the process responses for two different types of work pieces such as Ti6Al4V and AISI 316, circularity at entry is shown in Figure 4.13 for all the experimental

runs. It is observed that circularity at entry is maximum (Figure 4.13) for Ti6Al4V as compared to AISI 316. It (Figure 4.13) also indicates that the circularity at entry for the Ti6Al4V is relatively higher than AISI 316 in most of the cases when the hole is drilled with same parametric condition. Figure 4.14 shows that circularity at the exit of drilled holes is relatively closer for both the work pieces (Ti6Al4V and AISI 316) but circularity at exit is comparatively higher for AISI 316 than Ti6Al4V. The comparative study for the burr height at entry during drilling of Ti6Al4V and AISI 316 indicates that the burr height at entry is less for Ti6Al4V in most of the cases as compared to AISI 316 (Figure 4.15). In most of the experiment runs, it is observed that burr height at exit for the Ti6Al4V is higher than AISI 316 (Figure 4.16). Figure 4.17 shows that the surface roughness of the drilled is higher for AISI 316 than Ti6Al4V.

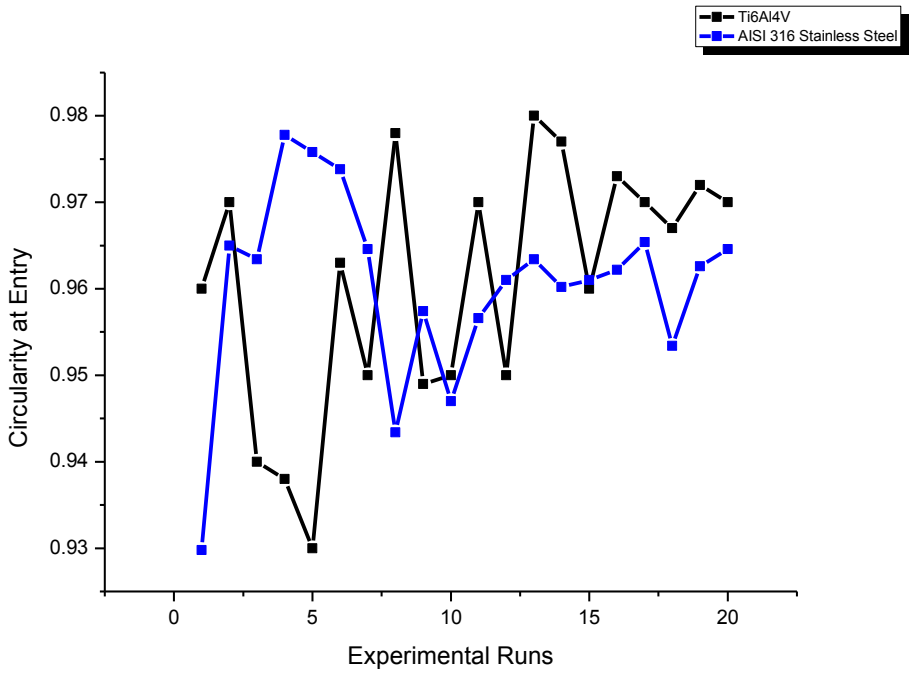


Figure 4.13: Comparison of circularity at entry for all experimental runs between Ti6Al4V and AISI 316

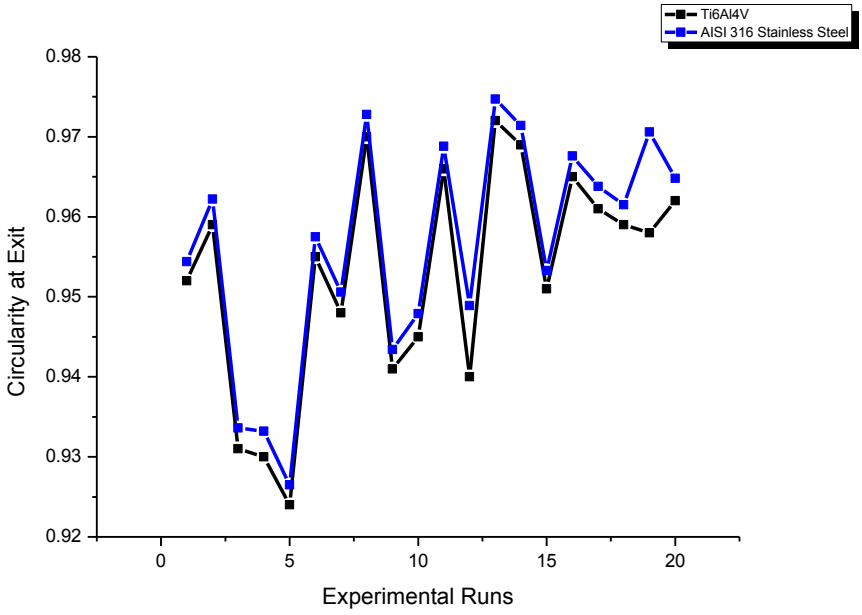


Figure 4.14: Comparison of circularity at exit for all experimental runs between Ti6Al4V and AISI 316

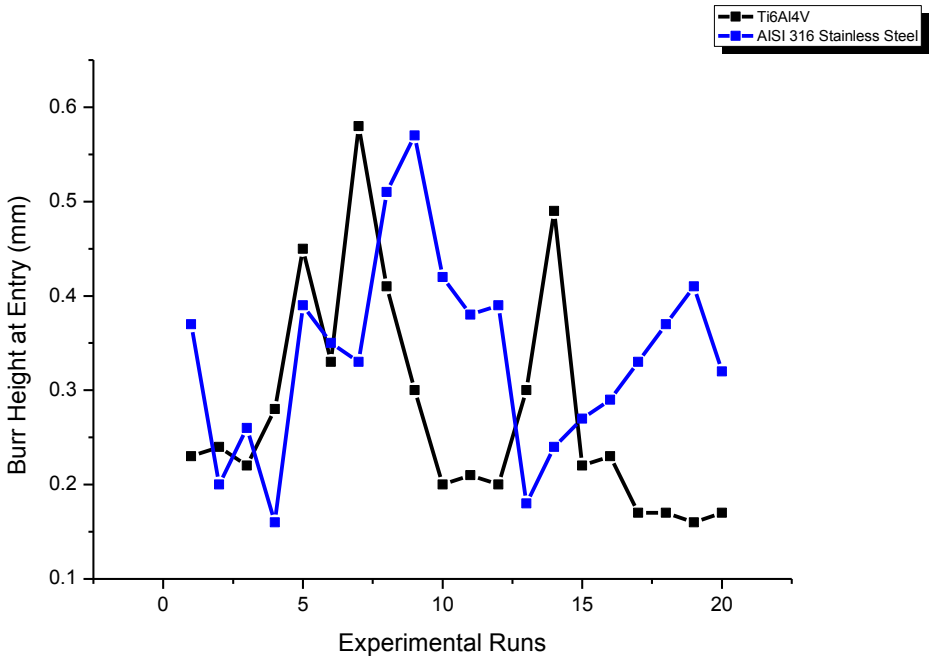


Figure 4.15: Comparison of burr height at entry for all experimental runs between Ti6Al4V and AISI 316

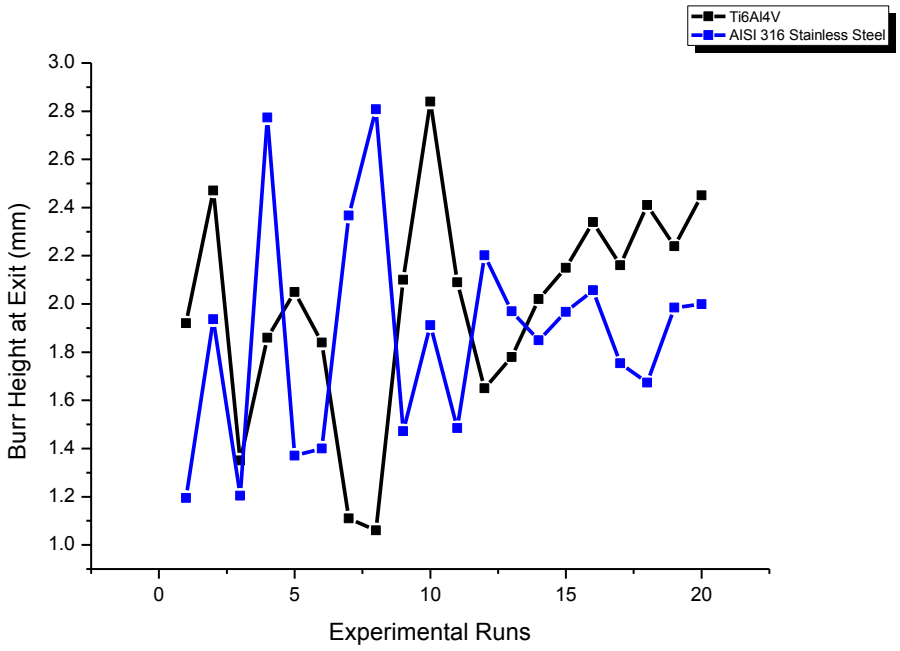


Figure 4.16: Comparison of burr height at exit for all experimental runs between Ti6Al4V and AISI 316

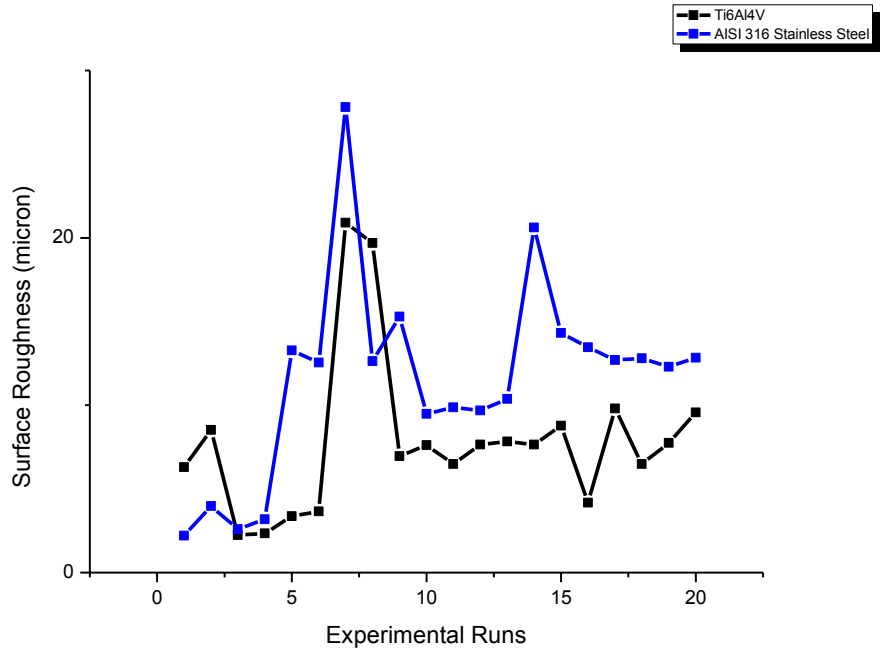


Figure 4.17: Comparison of surface roughness for all experimental runs between Ti6Al4V and AISI 316

### 4.5.2. Multi-response optimization using SIR-TOPSIS

For obtaining best parametric condition for simultaneous optimization of burr height at entry, burr height at exit and surface roughness, these responses are included in the

decision matrix of SIR method. Let the $A_1$, $A_2$, $A_3$, ……., $A_{20}$ are 20 number of experimental runs as the alternatives which are evaluated against three criteria $g_1$ (burr height at entry), $g_2$ (burr height at exit) and $g_3$ (surface roughness). The decision matrix and the generalized criteria were shown in Table 4.15 and 4.16.

Table 4.15: The decision matrix (Ti6Al4V)

| **Alternatives** | **Criteria** | | |
|---|---|---|---|
| | $g_1$(min) | $g_2$(min) | $g_3$(min) |
| $A_1$ | 0.23 | 1.92 | 6.2990 |
| $A_2$ | 0.24 | 2.47 | 8.5305 |
| $A_3$ | 0.22 | 1.35 | 2.2370 |
| $A_4$ | 0.28 | 1.86 | 2.3460 |
| $A_5$ | 0.45 | 2.05 | 3.3770 |
| $A_6$ | 0.33 | 1.84 | 3.6475 |
| $A_7$ | 0.58 | 1.11 | 20.9007 |
| $A_8$ | 0.41 | 1.06 | 19.6870 |
| $A_9$ | 0.30 | 2.10 | 6.9640 |
| $A_{10}$ | 0.20 | 2.84 | 7.6120 |
| $A_{11}$ | 0.21 | 2.09 | 6.4860 |
| $A_{12}$ | 0.20 | 1.65 | 7.6400 |
| $A_{13}$ | 0.30 | 1.78 | 7.8250 |
| $A_{14}$ | 0.49 | 2.02 | 7.6540 |
| $A_{15}$ | 0.22 | 2.15 | 8.7750 |
| $A_{16}$ | 0.23 | 2.34 | 4.1810 |
| $A_{17}$ | 0.17 | 2.16 | 9.7960 |
| $A_{18}$ | 0.17 | 2.41 | 6.4865 |
| $A_{19}$ | 0.16 | 2.24 | 7.7560 |
| $A_{20}$ | 0.17 | 2.45 | 9.5640 |
| Criterion type | Type I | Type I | Type I |

Table 4.16: The decision matrix (AISI 316)

| **Alternatives** | **Criteria** | | |
|---|---|---|---|
| | $g_1$(min) | $g_2$(min) | $g_3$(min) |
| $A_1$ | 0.37 | 0.6709 | 1.3978 |
| $A_2$ | 0.2 | 1.7304 | 2.5224 |
| $A_3$ | 0.26 | 0.6853 | 1.6436 |
| $A_4$ | 0.16 | 2.9268 | 2.0196 |
| $A_5$ | 0.39 | 0.9213 | 8.4075 |
| $A_6$ | 0.35 | 0.9637 | 7.9460 |
| $A_7$ | 0.33 | 2.3459 | 17.614 |
| $A_8$ | 0.51 | 2.9749 | 8.0010 |
| $A_9$ | 0.57 | 1.0671 | 9.6895 |
| $A_{10}$ | 0.42 | 1.6954 | 6.0075 |
| $A_{11}$ | 0.38 | 1.0848 | 6.2480 |
| $A_{12}$ | 0.39 | 2.1101 | 6.1395 |
| $A_{13}$ | 0.18 | 1.7783 | 6.5671 |
| $A_{14}$ | 0.24 | 1.6068 | 13.0625 |

| | | | |
|---|---|---|---|
| $A_{15}$ | 0.27 | 1.7736 | 9.0700 |
| $A_{16}$ | 0.29 | 1.9023 | 8.5215 |
| $A_{17}$ | 0.33 | 1.469 | 8.0405 |
| $A_{18}$ | 0.37 | 1.3556 | 8.1100 |
| $A_{19}$ | 0.41 | 1.7992 | 7.7930 |
| $A_{20}$ | 0.32 | 1.8194 | 8.1300 |
| Criterion type | Type I | Type I | Type I |

S-matrix and I-matrix will be calculated using equations 4.2 and 4.3. Following is the S-matrix and I-matrix of Ti6Al4V

$$S = \begin{bmatrix} 9 & 12 & 14 \\ 8 & 1 & 5 \\ 10 & 17 & 19 \\ 6 & 13 & 18 \\ 2 & 10 & 17 \\ 4 & 14 & 15 \\ 0 & 18 & 0 \\ 3 & 19 & 2 \\ 7 & 8 & 11 \\ 14 & 0 & 8 \\ 13 & 9 & 13 \\ 14 & 16 & 6 \\ 5 & 15 & 13 \\ 1 & 11 & 3 \\ 11 & 7 & 3 \\ 9 & 4 & 9 \\ 16 & 6 & 5 \\ 17 & 3 & 11 \\ 19 & 5 & 6 \\ 17 & 2 & 7 \end{bmatrix} \quad \text{and} \quad I = \begin{bmatrix} 9 & 7 & 5 \\ 11 & 18 & 14 \\ 7 & 2 & 0 \\ 13 & 6 & 1 \\ 17 & 9 & 2 \\ 15 & 5 & 3 \\ 18 & 1 & 19 \\ 16 & 0 & 18 \\ 12 & 11 & 8 \\ 4 & 19 & 11 \\ 6 & 10 & 6 \\ 4 & 3 & 13 \\ 14 & 4 & 6 \\ 16 & 8 & 16 \\ 7 & 12 & 16 \\ 9 & 15 & 8 \\ 3 & 13 & 13 \\ 1 & 16 & 7 \\ 0 & 14 & 12 \\ 1 & 17 & 11 \end{bmatrix}$$

Following is the S-matrix and I-matrix for AISI 316

$$S = \begin{bmatrix} 7 & 19 & 19 \\ 17 & 10 & 16 \\ 15 & 18 & 18 \\ 19 & 2 & 17 \\ 4 & 17 & 5 \\ 9 & 15 & 10 \\ 10 & 2 & 0 \\ 2 & 0 & 9 \\ 1 & 15 & 2 \\ 2 & 10 & 15 \\ 6 & 14 & 13 \\ 4 & 3 & 14 \\ 18 & 7 & 12 \\ 16 & 11 & 1 \\ 14 & 8 & 3 \\ 13 & 4 & 4 \\ 11 & 12 & 8 \\ 7 & 13 & 7 \\ 3 & 6 & 11 \\ 12 & 5 & 6 \end{bmatrix} \quad \text{and} \quad I = \begin{bmatrix} 9 & 0 & 0 \\ 2 & 9 & 3 \\ 4 & 1 & 1 \\ 0 & 14 & 2 \\ 11 & 2 & 13 \\ 8 & 3 & 9 \\ 7 & 15 & 16 \\ 16 & 17 & 10 \\ 16 & 4 & 15 \\ 15 & 8 & 4 \\ 11 & 5 & 6 \\ 12 & 14 & 5 \\ 2 & 11 & 6 \\ 3 & 7 & 15 \\ 5 & 10 & 13 \\ 6 & 14 & 14 \\ 5 & 7 & 11 \\ 9 & 6 & 11 \\ 13 & 12 & 8 \\ 6 & 13 & 11 \end{bmatrix}$$

For the aggregation procedure TOPSIS method has been used to calculate the S-flows and I-flows using the equation 4.8 and 4.13 respectively. Here, three decision criteria are considered to have equal weights, $w_j = 1/3$ (j = 1, 2 and 3). In order check the sensitivity of the method, eleven distances with $\lambda$ = 1, 2, . . . . .,11 are considered. The r-flow values (equation 4.14) for the decision matrix of both the work pieces (Ti6Al4V and AISI 316) are calculated and presented in Table 4.17 and 4.18.

Table 4.17: r-flow values and block distance ranges from (λ = 1, 2, ……..,11) (Ti6Al4V)

| r- flow values for alternatives | λ | | | | | | | | | | |
|---|---|---|---|---|---|---|---|---|---|---|---|
| | 1 | 2 | 3 | 4 | 5 | 6 | 7 | 8 | 9 | 10 | 11 |
| $A_1$ | 0.625 | 0.6204 | 0.6163 | 0.6128 | 0.6100 | 0.6077 | 0.6058 | 0.6044 | 0.6032 | 0.6023 | 0.6016 |
| $A_2$ | 0.2456 | 0.2726 | 0.2861 | 0.2937 | 0.2982 | 0.3012 | 0.3032 | 0.3045 | 0.3054 | 0.3061 | 0.3065 |
| $A_3$ | 0.8364 | 0.7847 | 0.7594 | 0.7453 | 0.7370 | 0.7316 | 0.7280 | 0.7254 | 0.7235 | 0.7221 | 0.7210 |
| $A_4$ | 0.6491 | 0.6158 | 0.6010 | 0.5931 | 0.5885 | 0.5857 | 0.5839 | 0.5828 | 0.5820 | 0.5816 | 0.5812 |
| $A_5$ | 0.5088 | 0.5062 | 0.5039 | 0.5023 | 0.5014 | 0.5008 | 0.5004 | 0.5003 | 0.5001 | 0.5001 | 0.5000 |
| $A_6$ | 0.5893 | 0.5684 | 0.5513 | 0.5396 | 0.5319 | 0.5266 | 0.5228 | 0.5200 | 0.5179 | 0.5163 | 0.5150 |
| $A_7$ | 0.3214 | 0.4037 | 0.4319 | 0.4462 | 0.4548 | 0.4605 | 0.4646 | 0.4677 | 0.4701 | 0.4719 | 0.4735 |
| $A_8$ | 0.4138 | 0.4492 | 0.4739 | 0.4876 | 0.4958 | 0.5013 | 0.5051 | 0.5079 | 0.5101 | 0.5117 | 0.5131 |
| $A_9$ | 0.4561 | 0.4575 | 0.4592 | 0.4610 | 0.4629 | 0.4648 | 0.4664 | 0.4680 | 0.4693 | 0.4705 | 0.4715 |
| $A_{10}$ | 0.3929 | 0.4237 | 0.4290 | 0.4304 | 0.4310 | 0.4312 | 0.4314 | 0.4314 | 0.4315 | 0.4315 | 0.4315 |
| $A_{11}$ | 0.6140 | 0.6095 | 0.6047 | 0.5999 | 0.5957 | 0.5919 | 0.5888 | 0.5862 | 0.5840 | 0.5822 | 0.5807 |
| $A_{12}$ | 0.6429 | 0.6154 | 0.5960 | 0.5837 | 0.5757 | 0.5704 | 0.5666 | 0.5638 | 0.5617 | 0.5601 | 0.5588 |
| $A_{13}$ | 0.5789 | 0.5652 | 0.5526 | 0.5431 | 0.5364 | 0.5317 | 0.5283 | 0.5258 | 0.5240 | 0.5226 | 0.5215 |
| $A_{14}$ | 0.2727 | 0.3167 | 0.3415 | 0.3555 | 0.3640 | 0.3695 | 0.3733 | 0.376 | 0.3781 | 0.3798 | 0.3811 |
| $A_{15}$ | 0.3750 | 0.3903 | 0.3997 | 0.4054 | 0.4090 | 0.4113 | 0.4128 | 0.4138 | 0.4145 | 0.4150 | 0.4154 |
| $A_{16}$ | 0.4074 | 0.4143 | 0.4169 | 0.4169 | 0.4155 | 0.4137 | 0.4118 | 0.4100 | 0.4084 | 0.4070 | 0.4057 |
| $A_{17}$ | 0.4821 | 0.4860 | 0.4962 | 0.5057 | 0.5129 | 0.5183 | 0.5222 | 0.5252 | 0.5275 | 0.5294 | 0.5309 |
| $A_{18}$ | 0.5636 | 0.5447 | 0.5357 | 0.5305 | 0.5273 | 0.5254 | 0.5243 | 0.5236 | 0.5232 | 0.5230 | 0.5228 |
| $A_{19}$ | 0.5357 | 0.5248 | 0.5365 | 0.5469 | 0.5542 | 0.5593 | 0.5629 | 0.5655 | 0.5674 | 0.5689 | 0.5701 |
| $A_{20}$ | 0.4727 | 0.4813 | 0.4908 | 0.4972 | 0.5012 | 0.5036 | 0.5050 | 0.5059 | 0.5064 | 0.5067 | 0.5069 |

Table 4.18: r-flow values and block distance ranges from (λ = 1, 2, …….., 11) (AISI 316)

| r- flow values for alternatives | λ | | | | | | | | | | |
|---|---|---|---|---|---|---|---|---|---|---|---|
| | 1 | 2 | 3 | 4 | 5 | 6 | 7 | 8 | 9 | 10 | 11 |
| $A_1$ | 0.8105 | 0.7209 | 0.6903 | 0.6759 | 0.6294 | 0.6622 | 0.6584 | 0.6556 | 0.6534 | 0.6516 | 0.6502 |
| $A_2$ | 0.7241 | 0.6457 | 0.6707 | 0.6569 | 0.6005 | 0.6426 | 0.6387 | 0.6358 | 0.6336 | 0.6320 | 0.6306 |
| $A_3$ | 0.8794 | 0.8457 | 0.8414 | 0.8310 | 0.8333 | 0.8198 | 0.8166 | 0.8144 | 0.8126 | 0.8113 | 0.8103 |
| $A_4$ | 0.6693 | 0.5141 | 0.5710 | 0.5569 | 0.5952 | 0.5431 | 0.5393 | 0.5365 | 0.5344 | 0.5327 | 0.5314 |
| $A_5$ | 0.4569 | 0.4002 | 0.4918 | 0.5037 | 0.5590 | 0.5167 | 0.5204 | 0.5230 | 0.5250 | 0.5265 | 0.5277 |
| $A_6$ | 0.5908 | 0.5294 | 0.5847 | 0.5864 | 0.6248 | 0.5915 | 0.5938 | 0.5958 | 0.5974 | 0.5987 | 0.5998 |
| $A_7$ | 0.2021 | 0.2177 | 0.2896 | 0.3037 | 0.3525 | 0.3171 | 0.3206 | 0.3232 | 0.3252 | 0.3267 | 0.3279 |
| $A_8$ | 0.1691 | 0.1923 | 0.2623 | 0.2757 | 0.3220 | 0.2881 | 0.2913 | 0.2936 | 0.2953 | 0.2966 | 0.2977 |
| $A_9$ | 0.2982 | 0.3024 | 0.4021 | 0.4162 | 0.4766 | 0.4301 | 0.4341 | 0.4370 | 0.4392 | 0.4410 | 0.4424 |
| $A_{10}$ | 0.4573 | 0.3958 | 0.4697 | 0.4664 | 0.5121 | 0.4616 | 0.4603 | 0.4594 | 0.4588 | 0.4584 | 0.4582 |
| $A_{11}$ | 0.5600 | 0.4941 | 0.5502 | 0.5443 | 0.5804 | 0.5353 | 0.5323 | 0.5299 | 0.5281 | 0.5267 | 0.5256 |
| $A_{12}$ | 0.3608 | 0.3238 | 0.4117 | 0.4241 | 0.4807 | 0.4370 | 0.4406 | 0.4433 | 0.4453 | 0.4468 | 0.4480 |
| $A_{13}$ | 0.6238 | 0.5355 | 0.5866 | 0.5805 | 0.6151 | 0.5750 | 0.5737 | 0.5728 | 0.5723 | 0.5719 | 0.5717 |
| $A_{14}$ | 0.4859 | 0.4097 | 0.4806 | 0.4736 | 0.5187 | 0.4655 | 0.4634 | 0.4620 | 0.4610 | 0.4604 | 0.4600 |
| $A_{15}$ | 0.4286 | 0.3700 | 0.4427 | 0.4459 | 0.4949 | 0.4494 | 0.4504 | 0.4511 | 0.4516 | 0.4519 | 0.4522 |
| $A_{16}$ | 0.3398 | 0.2997 | 0.3801 | 0.3919 | 0.4459 | 0.4051 | 0.4090 | 0.4119 | 0.4142 | 0.4160 | 0.4175 |
| $A_{17}$ | 0.5330 | 0.4711 | 0.5291 | 0.5265 | 0.5628 | 0.5218 | 0.5199 | 0.5183 | 0.5170 | 0.5160 | 0.5151 |
| $A_{18}$ | 0.4667 | 0.4097 | 0.4782 | 0.4836 | 0.5312 | 0.4917 | 0.4946 | 0.4968 | 0.4985 | 0.4999 | 0.5010 |
| $A_{19}$ | 0.3350 | 0.2957 | 0.3674 | 0.3754 | 0.4253 | 0.3845 | 0.3873 | 0.3893 | 0.3908 | 0.3919 | 0.3928 |
| $A_{20}$ | 0.3909 | 0.3359 | 0.4054 | 0.4120 | 0.4612 | 0.4215 | 0.4247 | 0.4271 | 0.429 | 0.4305 | 0.4317 |

### 4.5.3. Constrained Harmony Search algorithm

The proposed developed model obtained by equivalence method (SIR-TOPSIS) is used for optimization applying HS algorithm to have optimal parametric setting during drilling of Ti6Al4V. To develop the empirical relationship between control process parameters (Table 3.3) and r-flow values (Table 4.17) obtained from SIR-TOPSIS method, non–linear regression analysis (equation 4.21) has been carried out. The optimization problem is handled by two non-linear equality constraints $C_{ent}$ (circularity at entry) and $C_{exit}$ (circularity at exit) using penalty method. The non-linear equality constraints have been developed by regression analysis of the control parameters and the responses such as $C_{ent}$ and $C_{exit}$. The objective function (for λ=1) and the constraints are expressed below (equation 4.22 and 4.23):

$$\text{Maximize } r-\text{flow} = 1.926 \times A^{-0.146} \times B^{0.081} \times C^{-0.2} \quad (4.21)$$

Subject to:

$$C_{ent} = 0.898 \times (A \times C)^{0.017} \times (B/A)^{-0.005} \times C^{0.001} = 1 \quad (4.22)$$

$$C_{exit} = 0.9 \times (A \times C)^{0.016} \times (B/A)^{-0.005} \times C^{0.011} = 1 \quad (4.23)$$

$$\text{where } 400 \le A \le 600,\ 30 \le B \le 50 \text{ and } 5 \le C \le 7$$

To achieve optimum parametric setting for the process responses, harmony search algorithm has been applied using the objective function (equation 4.21) and constraints equations (equation 4.22 and 4.23) as per the steps discussed in harmony search coded in MATLAB 12.0 environment. The algorithm considers HM size of 6 and maximum iterations number of 1500. As the code is developed for minimization of function, therefore the objective function (r-flow) f(x) is made equivalent by multiplying the objective function by -1. The best fitness value of 0.7971 is obtained for parametric values of 405.2363 rpm of spindle speed, 49.6976 mm/min of feed rate and diameter of 5mm. Sensitivity analysis has been performed by changing the values of block distances (λ) ranging from λ = 1, 2,…..,11. The relationship between process parameters and the r-flow is obtained by nonlinear regression for each value of λ. Optimal fitness value is shown for different values of λ (λ=2, 3, 4,....,11) in Figure 4.18.

Similarly, the analysis has been carried out for drilling of AISI 316. The empirical relationship between process parameters and r-flow values (Table 4.18) has been developed non-linear regression analysis. The developed equation 4.24 has been used as the objective function. Two non-linear equality constraints $C_{ent}$ (circularity at entry) and $C_{exit}$ (circularity at exit) have been handled using penalty method. The non-linear equality constraints have been developed by regression analysis between control parameters and the responses such as $C_{ent}$ and $C_{exit}$. The objective function (for λ=1) and the constraints are expressed below (equation 4.25 and 4.26):

$$\text{Maximize } r-\text{flow} = 10.6 \times A^{0.018} \times B^{-0.44} \times C^{-0.662} \quad (4.24)$$

Subject to:

$$C_{ent} = 0.873 \times (A \times C)^{0.01} \times (B/A)^{0.004} \times C^{0.011} = 1 \quad (4.25)$$

$$C_{exit} = 0.864 \times (A \times C)^{0.018} \times (B/A)^{-0.004} \times C^{-0.003} = 1 \quad (4.26)$$

$$\text{where } 400 \le A \le 600,\ 30 \le B \le 50 \text{ and } 5 \le C \le 7$$

The algorithm considers HM size of 6 and maximum iterations number of 1500. The fitness value of 0.9145 is obtained resulting optimum parametric setting as 592.1492 rpm of spindle speed, 30.2191 mm/min of feed rate and diameter of 5 mm is obtained. Similarly, the algorithm is performed for all the ranges of λ (ranges from λ = 1, 2,….,11) to determine the value of λ at which best fitness is obtained. This is to be noted that empirical relation between process parameters and r-flow is obtained through non-linear regression analysis for each value of λ for optimization purpose. The fitness value obtained in the analysis is plotted in the Figure 4.18 for the drilling of AISI 316.

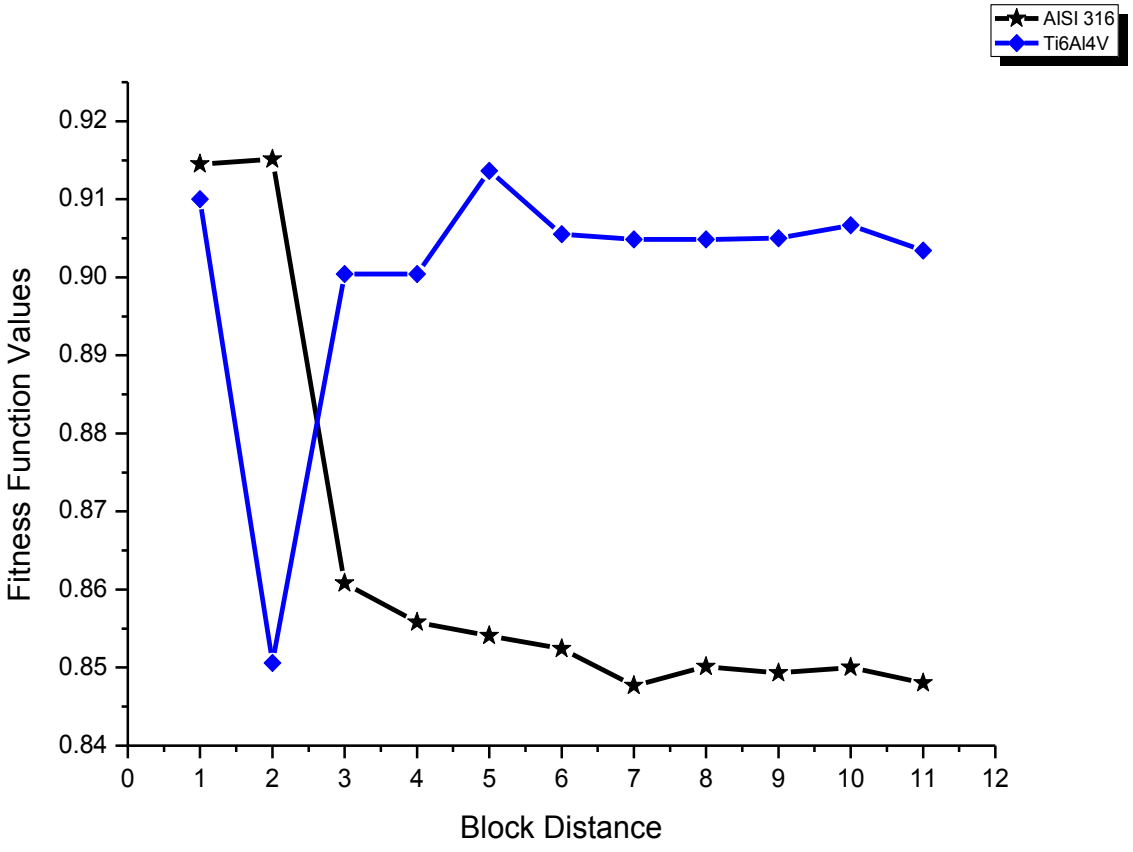


Figure 4.18: Sensitivity for the fitness value

Figure 4.18 shows that highest fitness value is obtained at λ=5 for Ti6Al4V whereas at λ=2 for AISI 316.Comparison of the fitness values obtained for both the workpiece shows that the fitness value obtained for Ti6Al4V is comparatively higher than AISI 316 in overall study of the sensitivity curve. The optimum fitness value and their parametric values of the control parameters obtained in the analysis are listed in Table 4.19.

Table 4.19: Parametric condition and fitness value.

| **Drilled Material** | **Value of Block distance (λ)** | **Spindle speed (RPM)** | **Feed rate (mm/min)** | **Drill bit diameter (mm)** | **Fitness value** |
|---|---|---|---|---|---|
| Ti6Al4V | 5 | 405.2366 | 49.3272 | 5 | 0.8026 |
| AISI 316 | 2 | 592.1471 | 30.2191 | 5 | 0.9151 |

### 4.6. Conclusions

Present chapter highlights the effect of drilling parameters viz. spindle (drilling) speed, feed rate and drill diameter on the performance characteristics such as circularity at entry and exit, burr height at entry and exit and surface roughness during drilling of Ti6Al4V and AISI 316. The comparative study of drilling of Ti6Al4V and AISI 316 indicates that performance characteristics obtained for work piece material Ti6Al4V is superior to that of AISI 316 with respect to circularity at entry, burr height at entry and surface roughness. In present investigation, a hybrid approach for optimization of multiple responses such as burr height at entry and exit and surface roughness using SIR-TOPSIS embedded with HS algorithm is proposed considering circularity at entry and exit as constraints. Since multiple responses are considered, they are converted into an equivalent response (r-flow) using SIR-TOPSIS method. Non-linear regression analysis has carried out to obtain empirical relation between process parameters and r-flow, which is to be maximized. Empirical relations between process parameters and circularity at entry and exit obtained by non-linear regression analysis are used as constraint equations. The constrained optimization problem is solved by HS algorithm to find out optimum parametric setting. The results suggest that hybrid approach can be successfully used for multi-response optimization.

# CHAPTER 5

# EXPERIMENTAL INVESTIGATION OF LASER DRILLING PROCESS

# CHAPTER 5

# EXPERIMENTAL INVESTIGATION OF LASER DRILLING PROCESS

## 5.1. Introduction

Lasers can be successfully used for machining of materials such as metals, composites, ceramics and polymers. In laser drilling, a high energy infrared laser beam (between 0.1-2.0 mm in diameters) is focused on a spot on the work piece resulting in melting, vaporization and chemical degradation throughout the depth of the material. The fluids and degraded materials from the holes are removed by assistant gas or gas jet co-axial to the laser beam. The major advantages in laser machining is that there is no contact between tool and the work materials; thus eliminates the problem of chatter and vibration during machining of small and thin components (Chryssolouris et al. 1988). The substantial advantage achieved in using lasers for machining lies in the fact that it can machine high strength to weight and volume ratio materials. It can be used in machining of complex parts and shapes. The current challenge faced by the tool makers now needs investigation on effect of laser process parameters such as laser power, pulse frequency and flushing pressure on the performance characteristics like heat affected zone (HAZ), taper of the kerf and quality of the surface in laser machining. To meet this challenge, the current chapter presents the details of materials and methods used in laser drilling.

## 5.2. Experimental details

The experiments have been performed on ORION-3015 $CO_2$ laser cutting machine using nitrogen as an assistant gas for cleaning the extra material after machining (flushing) (Figure 5.1). ORION-3015 is carbon dioxide ($CO_2$) laser cutting machine setup having latest design to provide an intelligent and cost effective solution for laser processing needs. It is controlled by Fanuc CNC control features with 9.5" color screen. CADMAN-L 3D software is used for controlling laser processing set up. The laser cutting machine is available at Indian Institute of Technology Guwahati. The laser machine is supplied by LVD Company (Belgium). The specification of the laser cutting machine (ORION-3015) is listed in the Table 5.1. Figure 5.2 shows the work piece and machine setup.

Table 5.1: Laser machine specification

| | |
|---|---|
| Maximum Sheet Size | 60 inch ×120 inch |
| Maximum Sheet Weight | 1250 Ibs |
| X-axis Travel | 121 inch |
| Y-axis Travel | 61 inch |
| Z-axis Travel | 11.5 inch |
| Memory | 2 Mb |

| | |
|---|---|
| Display | Color |
| Maximum Positioning Speed X,Y-axis | 3935 inch |
| Maximum Positioning Speed Z-axis | 700 inch |
| Repetitive Accuracy | ±0.0008 inch |
| Positioning Accuracy | ±0.002 inch |
| Type | Fanuc HF excited $CO_2$ laser |
| Laser Power (± 2 %) | 2500 W |
| Range | 100-2500 W |
| Output Stability | ± 1 % ± 2 % |
| Wave Length | 10,6 µm |
| Laser Gas | 10 l/hour |
| Cooling Water | Sealed circuit |
| Maximum Sheet Size | 120 inch× 60 inch× 0.47 inch |
| Maximum Stack Weight | 5511 lbs. |
| Maximum Stack Height | 3.9 inch |
| Weight | 10582 lbs |


Figure 5.1: $CO_2$ laser cutting machine

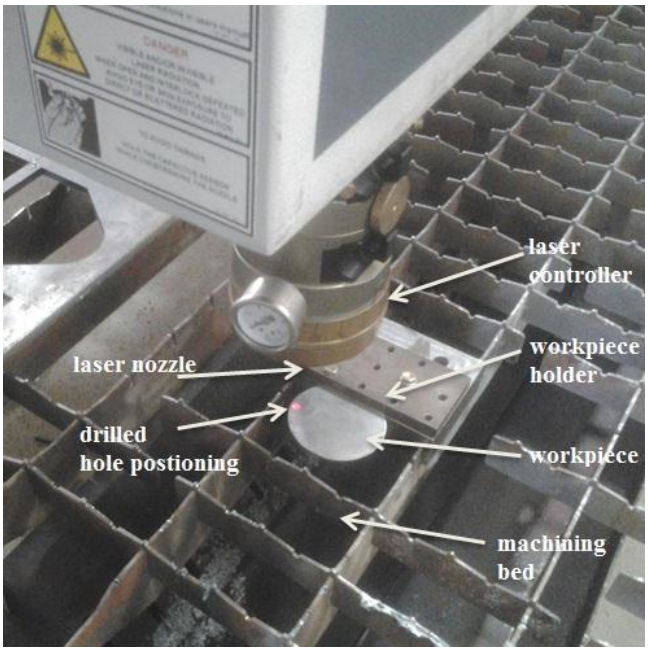

Figure 5. 2 : Work piece setup for laser drilling

The work materials such as Ti6Al4V and AISI 316 of thickness 2 mm are exposed to a focused stationary laser beam with coaxial $CO_2$ gas jet. As the temperature increases, melting of work materials occurs leading to depression at center. The removal of the molten metal has been carried out using $N_2$ as an assistant gas with flushing pressures ranging between 34 to 40 bars. The Figure 5.3 shows the schematic layout of the $CO_2$ laser drilling operation.

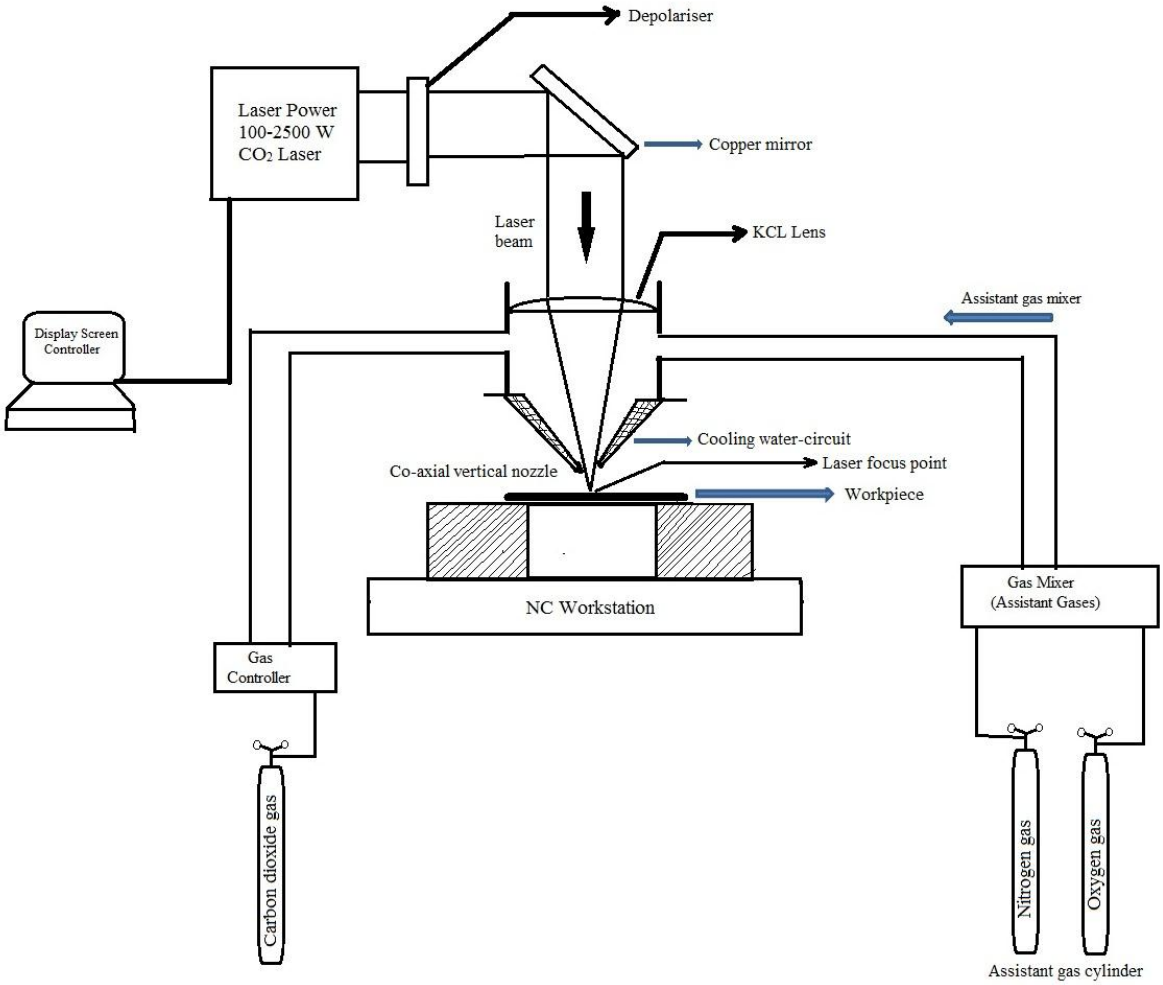


Figure 5.3: Schematic layout of $CO_2$ laser drilling process

The work pieces used for the experimental studies are titanium alloy (Ti6Al4V) and stainless steel (AISI 316). The material AISI 316 is originally in the form of cylindrical bar of length 200 mm and 70 mm diameter. The material is cut into circular plates of 70 mm diameter and 2 mm thickness for laser drilling. Grinding and cleaning of work sample has been done properly to obtain flat and clean top surface. The material Ti6Al4V is originally in the form of rectangular plate of 150 mm × 150 mm and of thickness 2 mm. The work piece is cut into square plate of dimension 50 mm × 50 mm and of thickness 2 mm (Figure 5.4). The material is procured from Manohar Metal Supply Corporation, Mumbai, India

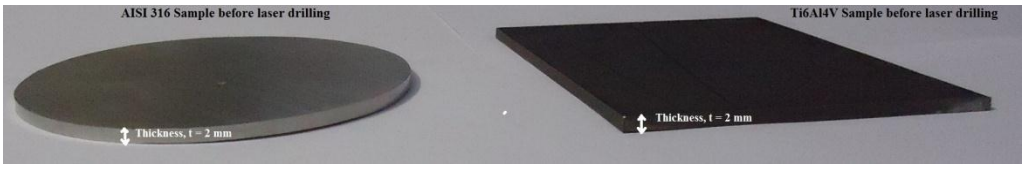


Figure 5.4: The workpieces before machining

Scanning electron microscope (SEM) JEOL JSM-6048LV (having magnification of 8X to 50,000X) shown in Figure 5.5 has been used for scanning electron microscopy with energy dispersive spectroscopy (SEM-EDS). SEM-EDS have been performed to confirm the constituents present in the work material. The image of the sample has been taken at 200 micron (μ) under magnification of 500X in scanning electron microscope (SEM) and the analysis has been done by Energy-dispersive X-ray spectroscopy (Ye and Liu 2005; Hascalik and Caydas 2007; Fasai et al. 2009; Kayali et al. 2013). The SEM-EDS analysis shows that the content of titanium (Ti) is at peak (Figure 5.6) and the other constituents present in the work sample are vanadium (V) and aluminium (Al). The work piece is having Ti of 92% atomic weight, V of 5.35% atomic weight and Al of 2.56% atomic weight. These results confirm that work sample is Ti6Al4V and can be used for further analysis. Similarly, the SEM EDS analysis (Figure 5.7) has been carried out for the other work piece in which major peak level is obtained for Fe (iron) and other constituents are Ni (nickel) and Cr (chromium). The results in atomic weight obtained by the analysis for the sample are 73.31% of Fe, 18.91% of Cr and Ni having 7.78%. The results confirm that the material is AISI 316.


Figure 5.5: Scanning electron microscope JEOL JSM-6048LV

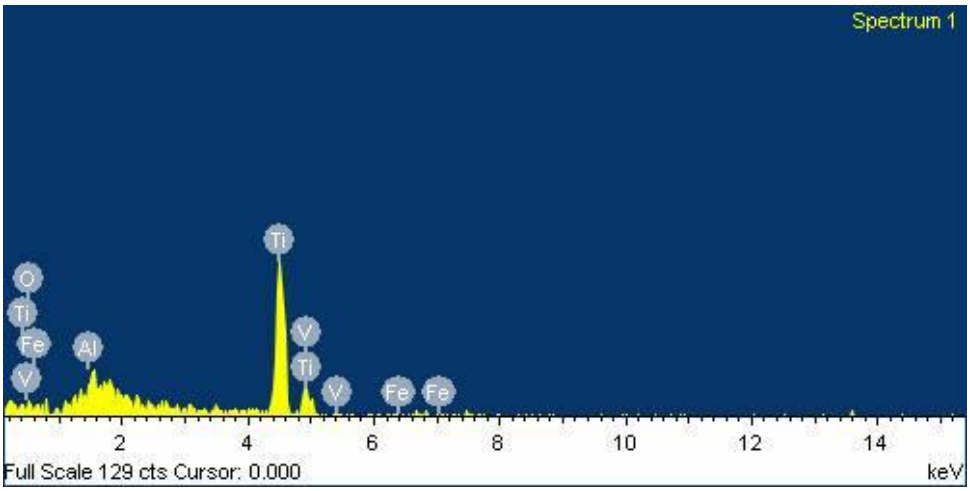


Figure 5.6: SEM-EDS image of Ti6Al4V

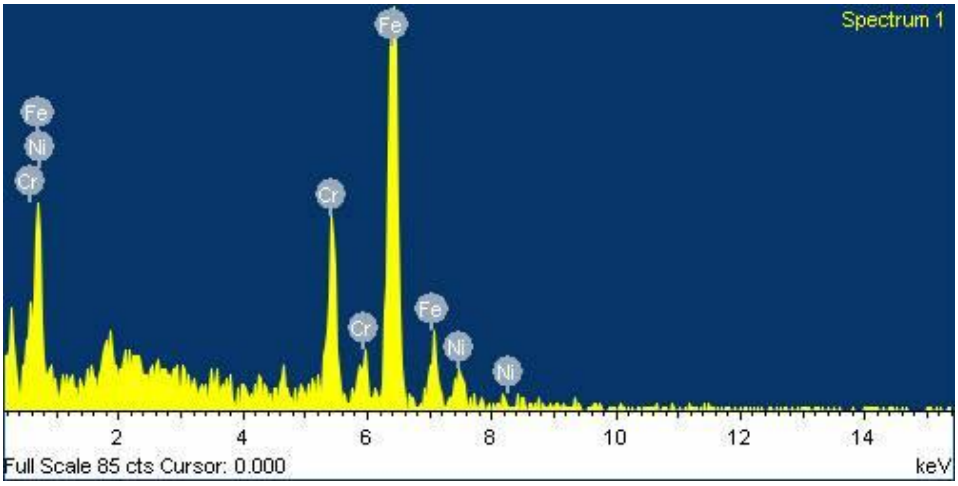


Figure 5.7: SEM-EDS image of AISI 316

In this present investigation, Taguchi method has been employed to understand the effect of control parameters on various laser drilling performance characteristics with less number of experimental runs. The control parameters are selected through an exhaustive literature review (Low et al. 2000; Ghoreishi et al 2002; Brajdic et al. 2008; Reissig et al. 2004; Bandyopadhyay et al. 2005; Sun and Brandt 2013). The control parameters considered are flushing pressure (Pa) of the assistant gas, laser power (W) and frequency (Hz), each at three levels . Taguchi's $L_9$ orthogonal array is used to design the experimental layout (Table 5.2).

Table 5.2: Control parameters and their levels

| Sl. No. | Process parameters | Unit | Levels | | |
|---|---|---|---|---|---|
| | | | Low | Middle | High |
| 1 | Flushing Pressure | Pa | 34 | 37 | 40 |
| 2 | Power | W | 2000 | 2250 | 2500 |
| 3 | Frequency | Hz | 1600 | 1800 | 2000 |

The process performance characteristics (responses) considered is circularity at entry of the kerf, taper of the drilled hole, spatter area and heat affected zone.

Circularity is one of the important metrological parameters used to assess the roundness of circular parts or features. The quality of the drilled hole may be defined in terms of circularity (both at entry and exit). The circularity of the hole is measured by using the ratio of minimum ($r_1$) to maximum ($r_2$) Feret's diameters of the hole (Ghoreishi et al. 2002).The diameters are measured using optical microscope (RADIAL INSTRUMENT with Samsung camera setup, 30-X magnification) shown in Figure 5.8. Farets's diameter is obtained by joining tangents to the maximum points of the surface. The images of hole so acquired are used in image processing toolbox of MATLAB 12.0 to measure the Farret's diameter.

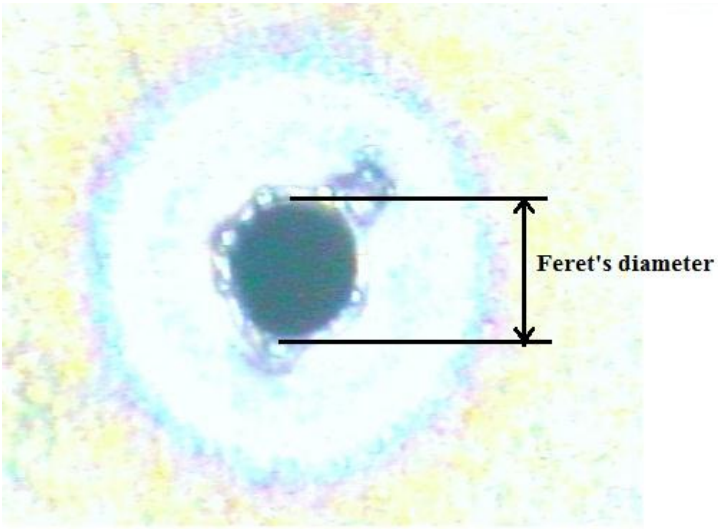


Figure 5.8: Circularity image of laser drilling specimen

Laser cutting process generally produces tapered shape due to the divergence of laser beam (Adams and Hardway 1965). The effect of thickness of the work piece, focal setting and power intensity significantly influence taper of the hole (Yilbas 1997). The Taper is calculated using the following expression (Equation 5.4) where $D_{ent}$ and $D_{exit}$ are the diameters at entry and exit of the hole respectively (Yeo et al. 1994; Ghoreishi 2002). In present study, it is obserevd that diameter at entry ($D_{ent}$) is invariably greater than diameter at exit ($D_{exit}$) (Figure 5.9).

$$\text{Taper} = \frac{D_{ent} - D_{exit}}{2t} \tag{5.1}$$

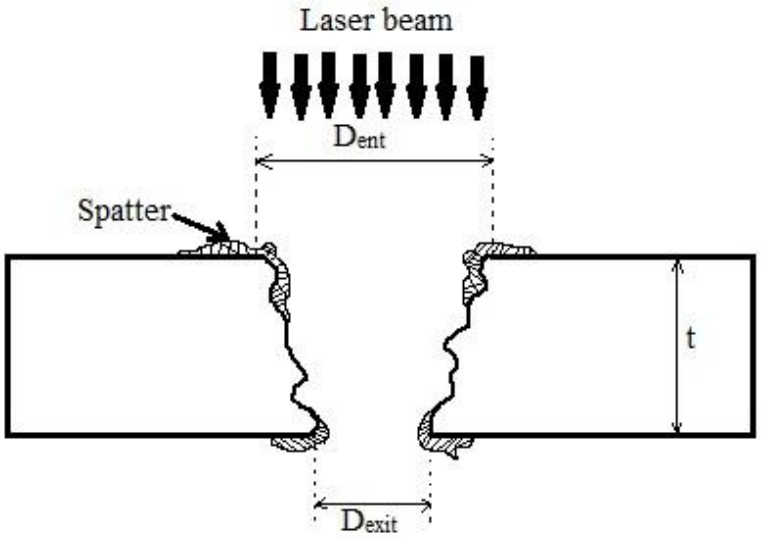


Figure 5.9: Taper formation diagram on workpiece after laser drilling

Spatter is one of the natural defects occurs during laser drilling. It occurs due to the incomplete flushing of the molten material. The remaining material solidifies and adheres around the periphery of the hole (Low et al. 2001). In the present investigation, the spatter formation occurs on the surface of the holes to a greater extent and spatter is consistently more in case of thin work pieces. The extent of spatter formed on Ti6Al4V and AISI 316 materials is significantly different (Figure 5.10). The spatter area is measured using optical microscope (RADIAL INSTRUMENT with Samsung camera setup, 30-X magnification). The images of near the hole so acquired are used in image processing toolbox of MATLAB 12.0 to measure the spatter area.

As laser machining is a thermal process, huge amount of energy is conducted into the work piece leading to change in microstructure, materials properties and phase composition such as changes in grain size and formation of carbide near the heat affected zone (HAZ) (Prusa et al. 1999). The narrow zone formed exactly adjacent to the laser drilled holes is known as HAZ (Figure 5.11). The samples are polished using 100, 200 and 300 microns sand papers and etching is done by NaOH solution to measure the heat affected zone thickness of the drilled hole (Padhee et al. 2011; Kaur et al. 2006; Bharatish et al. 2013; Nageshet al. 2013) shown in Figure 5.10. The HAZ thickness is measured using the equation 5.5 (Kaur et al. 2006).

$$\text{HAZ thickness} = \frac{\text{HAZ diameter} - \text{Drilled hole diameter}}{2} \tag{5.2}$$

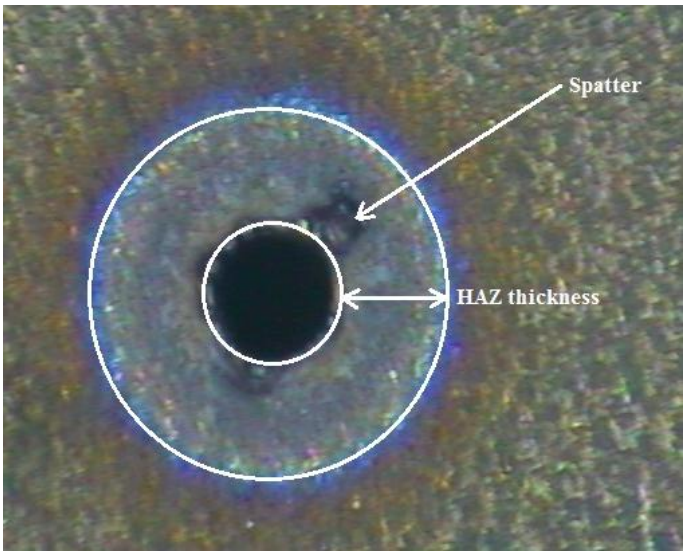

Figure 5.10: HAZ thickness diagram after laser drilling

The performance characteristics (responses) of laser drilling process such as circularity, taper, spatter area and HAZ are summarized in Table 5.3 and 5.4 respectively for Ti6Al4V and AISI 316. The laser drilled samples are shown in Figure 5.11 and Figure 5.12.

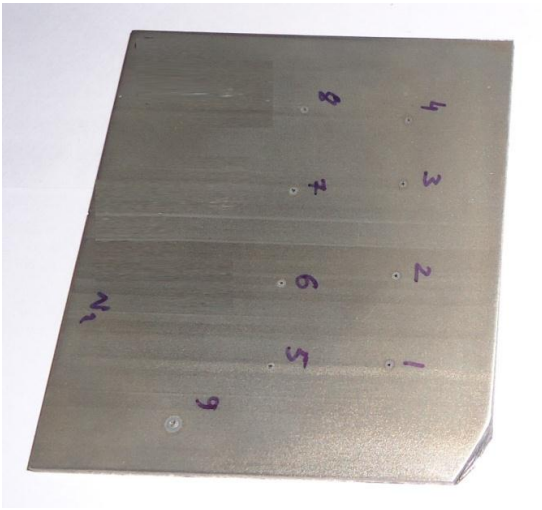
Figure 5.11: Work piece after laser drilling (Ti6Al4V)

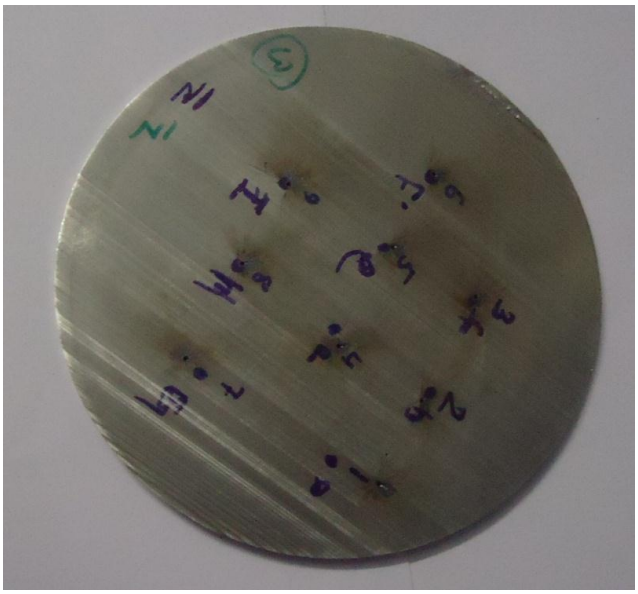

Figure 5.12: Work piece after laser drilling (AISI 316)

Table 5.3: Laser Drilling responses for Ti6Al4V work material

| Experimental Run | Process Parameters | | | Output Responses | | | |
|---|---|---|---|---|---|---|---|
| | Flushing Pressure, Pa | Power, W | Frequency, Hz | Circularity | Taper | Spatter Area, $mm^2$ | HAZ, mm |
| 1 | 34 | 2000 | 1600 | 0.9243 | 0.1177 | 2.8826 | 0.4826 |
| 2 | 34 | 2250 | 1800 | 0.8644 | 0.0722 | 5.5217 | 0.6731 |
| 3 | 34 | 2500 | 2000 | 0.9546 | 0.0421 | 11.175 | 1.1625 |
| 4 | 37 | 2000 | 1800 | 0.9278 | 0.1227 | 3.4438 | 0.6718 |
| 5 | 37 | 2250 | 2000 | 0.8916 | 0.0945 | 3.1613 | 0.6539 |
| 6 | 37 | 2500 | 1600 | 0.8863 | 0.0404 | 4.5964 | 0.5269 |
| 7 | 40 | 2000 | 2000 | 0.8988 | 0.0883 | 4.4011 | 0.4948 |
| 8 | 40 | 2250 | 1600 | 0.8236 | 0.0505 | 6.3280 | 0.4733 |
| 9 | 40 | 2500 | 1800 | 0.8686 | 0.0611 | 9.2811 | 0.9522 |

Table 5.4: Laser Drilling responses for AISI 316 work material

| Experimental Run | Process Parameters | | | Output Responses | | | |
|---|---|---|---|---|---|---|---|
| | Flushing Pressure, Pa | Power, W | Frequency, Hz | Circularity | Taper | Spatter Area, $mm^2$ | HAZ, mm |
| 1 | 34 | 2000 | 1600 | 0.8644 | 0.0834 | 2.8826 | 0.3946 |
| 2 | 34 | 2250 | 1800 | 0.8669 | 0.0429 | 3.6 | 0.5864 |
| 3 | 34 | 2500 | 2000 | 0.8725 | 0.0576 | 1.913 | 0.6334 |
| 4 | 37 | 2000 | 1800 | 0.7536 | 0.0618 | 7.6313 | 0.4627 |
| 5 | 37 | 2250 | 2000 | 0.8218 | 0.0322 | 1.76 | 0.4952 |
| 6 | 37 | 2500 | 1600 | 0.7241 | 0.0632 | 1.664 | 0.3302 |
| 7 | 40 | 2000 | 2000 | 0.9097 | 0.081 | 3.36 | 0.3548 |
| 8 | 40 | 2250 | 1600 | 0.8611 | 0.0774 | 6.328 | 0.3251 |
| 9 | 40 | 2500 | 1800 | 0.7403 | 0.061 | 8.9333 | 0.3138 |

### 5.3. Results and Discussions

To analyze the parametric effect on the process responses during laser drilling operation, analysis of variance (ANOVA) for each drilling response has been performed. ANOVA for taper shows that laser power has higher percentage of contribution (74.12%) on formation of taper during laser drilling of Ti6Al4V (Table 5.5). ANOVA for taper shows that power has contribution of 40.3% on forming taper in laser drilling of AISI 316 (Table 5.6). The main effect plot shows that taper decreases with increases in laser power for the work piece Ti6Al4V (Figure 5.13). The optimal parameter setting for achieving minimum taper are flushing pressure of 40 Pa, laser power of 2500 W and frequency of 1600 Hz. The main effect plot shown in Figure 5.14 for laser drilling of AISI 316 indicates that minimum taper can be achieved at flushing pressure of 37 Pa, laser power of 2250 W and frequency of 1800 Hz.

Table 5.5: ANOVA for taper (Ti6Al4V)

| Source | DF | Seq SS | Adj SS | Adj MS | F | % Contribution |
|---|---|---|---|---|---|---|
| Pressure | 2 | 3.69 | 3.69 | 1.845 | 0.24 | 3.46 |
| Power | 2 | 79.062 | 79.062 | 39.531 | 5.07 | 74.12 |
| Frequency | 2 | 8.314 | 8.314 | 4.157 | 0.53 | 7.79 |
| Residual Error | 2 | 15.603 | 15.603 | 7.802 | | |
| Total | 8 | 106.67 | | | | |

Table 5.6: ANOVA for taper (AISI 316)

| Source | DF | Seq SS | Adj SS | Adj MS | F | % contribution |
|---|---|---|---|---|---|---|
| Pressure | 2 | 15.617 | 15.617 | 7.809 | 4.57 | 26.93 |
| Power | 2 | 23.373 | 23.373 | 11.687 | 6.84 | 40.3 |
| Frequency | 2 | 15.589 | 15.589 | 7.794 | 4.56 | 26.88 |
| Residual Error | 2 | 3.417 | 3.417 | 1.709 | | |
| Total | 8 | 57.996 | | | | |

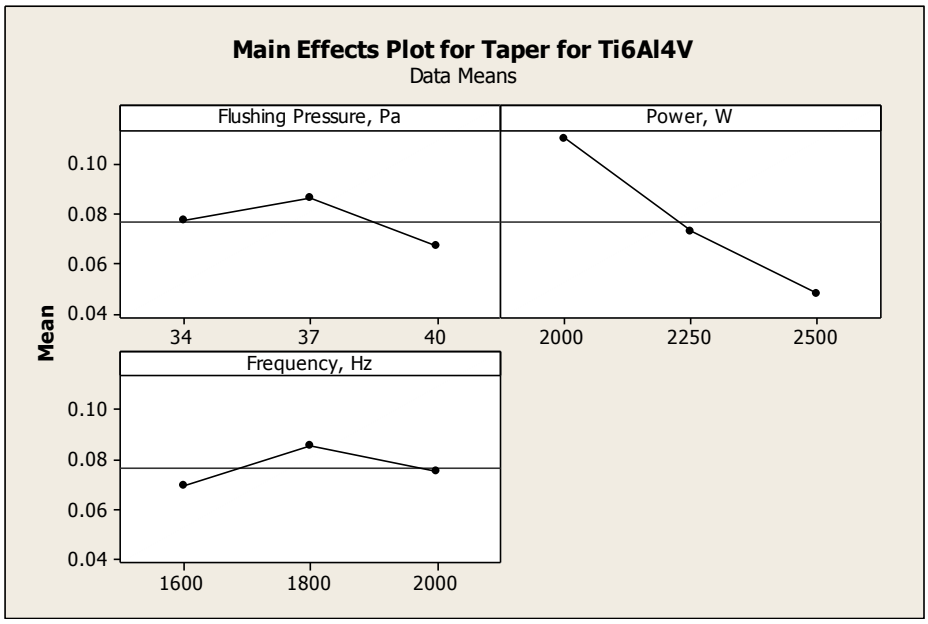


Figure 5.13: Main effect plot for taper (work piece Ti6Al4V)

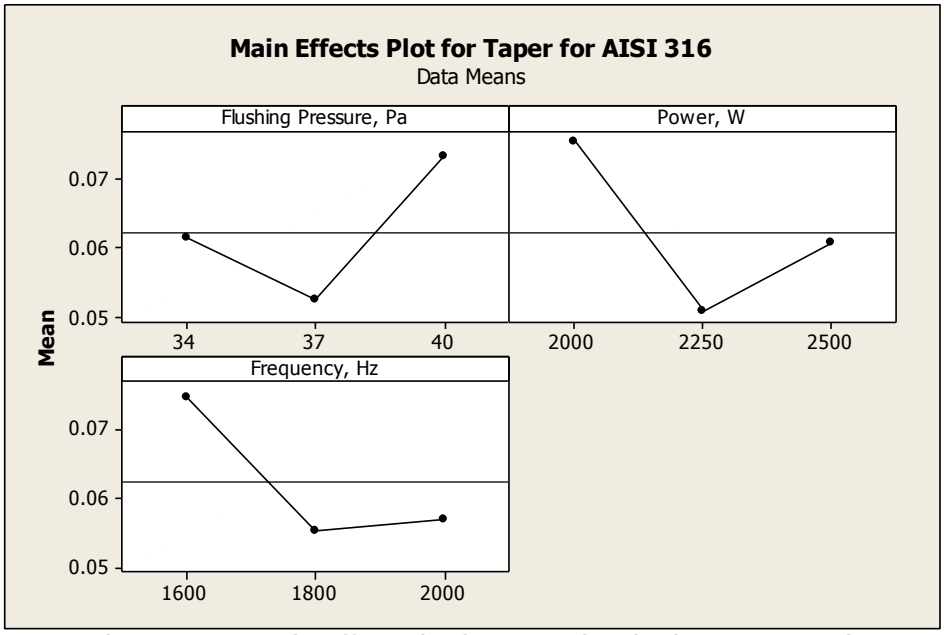


Figure 5.14: Main effect plot for taper (work piece AISI 316)

The comparative study for taper shown in Figure 5.15 suggests taper formed in the work piece AISI 316 is higher as compared to Ti6Al4V in most of the experimental runs. Therefore, Ti6Al4V is preferable to AISI 316 as far as taper is concerned in laser drilling.

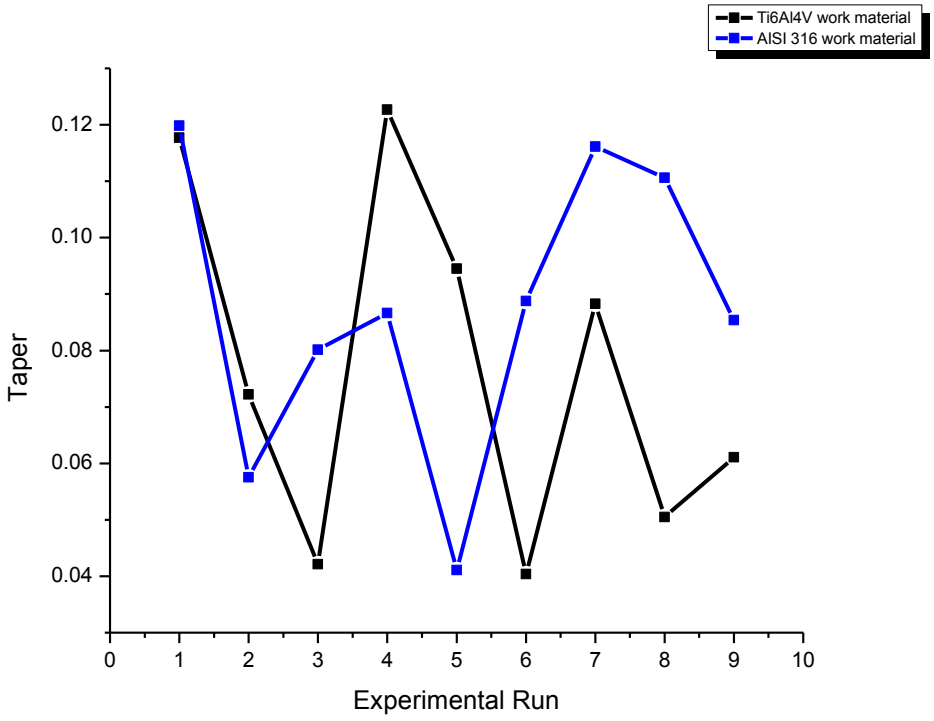


Figure 5.15: Comparative graph of Taper formation after laser drilling of Ti6Al4V and AISI-316

ANOVA for heat affected zone (HAZ) shows that frequency contributes of 41.18% on development of HAZ in laser drilling of Ti6Al4V (Table 5.7). ANOVA for HAZ in laser drilling of AISI 316 shows that flushing pressure has significant percentage of contribution i.e. 58.53% (Table 5.8). The main effect plot shows that HAZ increases with increases in laser power for the work piece Ti6Al4V (Figure 5.16). The optimal parameter setting for achieving minimum HAZ are flushing pressure of 37 Pa, laser power of 2000 W and frequency of 1600 Hz. The main effect plot shown in Figure 5.17 for laser drilling of AISI 316 shows that the HAZ decreases with increases in flushing pressure and HAZ increases with increases in pulse frequency for the workpiece AISI 316. The minimum HAZ can be achieved for laser drilling of AISI 316 at flushing pressure of 40 Pa, laser power of 2000 W and frequency of 1600 Hz.

Table 5.7: ANOVA for HAZ (Ti6Al4V)

| **Source** | **DF** | **Seq SS** | **Adj SS** | **Adj MS** | **F** | **% contribution** |
|---|---|---|---|---|---|---|
| Pressure | 2 | 4.348 | 4.348 | 2.174 | 0.58 | 7.26 |
| Power | 2 | 23.427 | 23.427 | 11.713 | 3.15 | 39.14 |
| Frequency | 2 | 24.65 | 24.65 | 12.325 | 3.32 | 41.18 |
| Residual Error | 2 | 7.436 | 7.436 | 3.718 | | |
| Total | 8 | 59.861 | | | | |

Table 5.8: ANOVA for HAZ (AISI 316)

| Source | DF | Seq SS | Adj SS | Adj MS | F | % contribution |
|---|---|---|---|---|---|---|
| Pressure | 2 | 24.618 | 24.618 | 12.309 | 9.35 | 58.53 |
| Power | 2 | 2.298 | 2.298 | 1.149 | 0.87 | 5.46 |
| Frequency | 2 | 12.508 | 12.508 | 6.254 | 4.75 | 29.74 |
| Residual Error | 2 | 2.633 | 2.633 | 1.317 | | |
| Total | 8 | 42.057 | | | | |

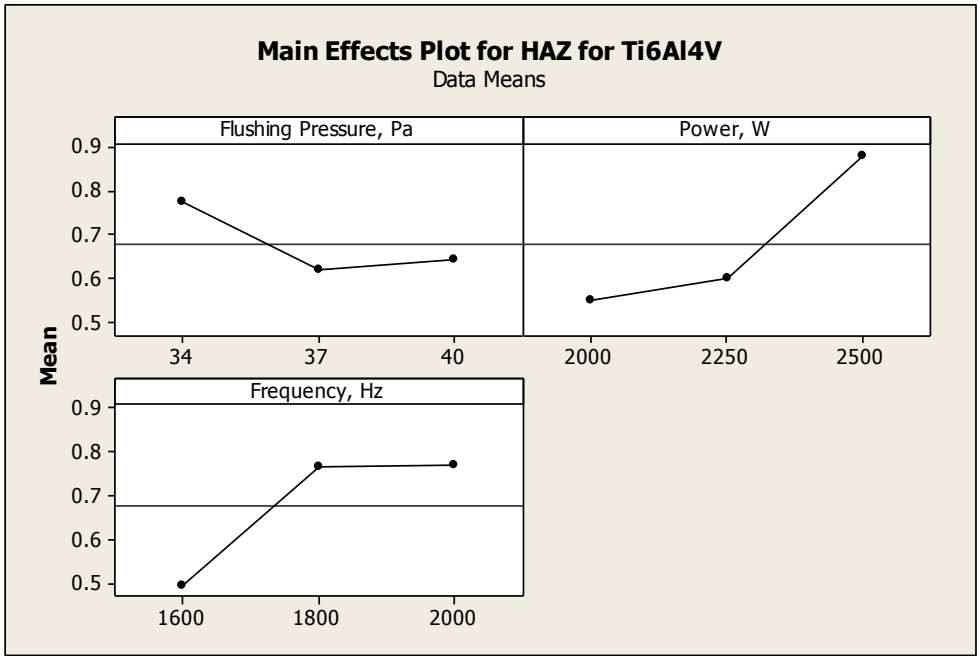


Figure 5.16: Main effect plot for HAZ for the workpiece Ti6Al4V

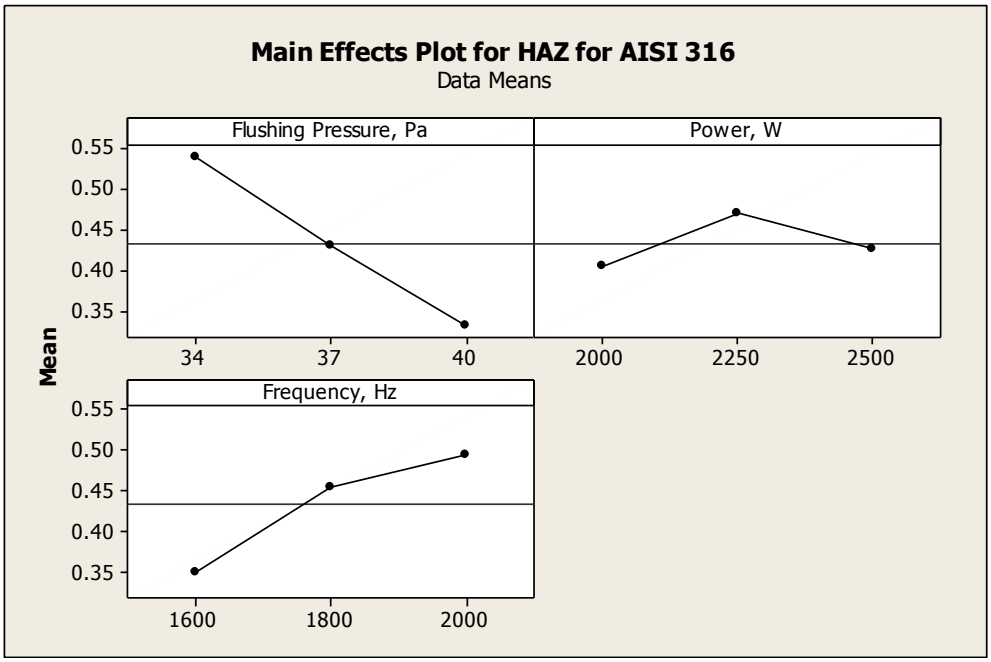


Figure 5.17: Main effect plot for HAZ for the workpiece AISI 316

The comparative study for HAZ shown in Figure 5.18 indicates that HAZ developed for the workpiece AISI 316 is higher as compared to Ti6Al4V in most of the experimental runs. Therefore, Ti6Al4V is preferable over AISI 316 as far as HAZ is concerned in laser drilling.

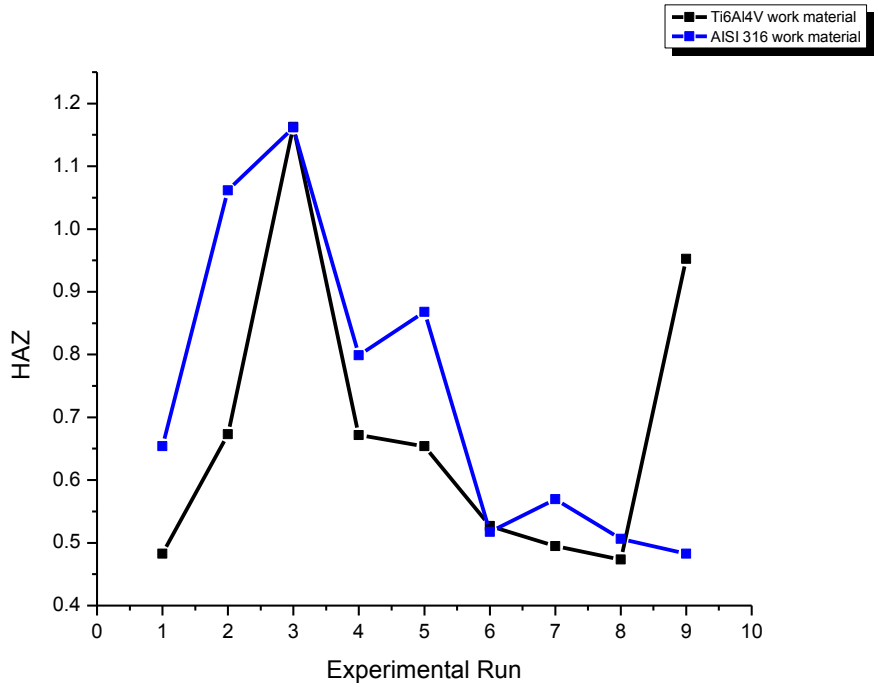


Figure 5.18: Comparison of thickness of HAZ in laser drilling of Ti6Al4V and AISI-316

ANOVA for circularity at entry shows that laser power contributes 45.23% to circularity in laser drilling of Ti6Al4V (Table 5.9) whereas it contributes 44.23% in laser drilling of AISI 316 (Table 5.10). The main effect plot shows that circularity decreases with increases in flushing pressure and increases with increases in pulse frequency for the work piece Ti6Al4V (Figure 5.19). The optimal parameter setting for achieving maximum circularity are flushing pressure of 34 Pa, laser power of 2000 W and frequency of 2000 Hz. The main effect plot shown in Figure 5.20 for laser drilling of AISI 316 indicates that maximum circularity can be achieved at flushing pressure of 34 Pa, laser power of 2250 W and frequency of 2000 Hz.

Table 5.9: ANOVA for circularity (Ti6Al4V)

| Source | DF | Seq SS | Adj SS | Adj MS | F | % contribution |
|---|---|---|---|---|---|---|
| Pressure | 2 | 0.4014 | 0.4014 | 0.2007 | 9.24 | 35.21 |
| Power | 2 | 0.51569 | 0.51569 | 0.25785 | 11.87 | 45.23 |
| Frequency | 2 | 0.21432 | 0.21432 | 0.10716 | 4.93 | 18.8 |
| Residual Error | 2 | 0.04344 | 0.04344 | 0.02172 | | 3.81 |
| Total | 8 | 1.17486 | | | | |

Table 5.10: ANOVA for circularity (AISI 316)

| Source | DF | Seq SS | Adj SS | Adj MS | F | % contribution |
|---|---|---|---|---|---|---|
| Pressure | 2 | 1.8663 | 1.8663 | 0.93315 | 18.08 | 44.23 |
| Power | 2 | 1.0965 | 1.0965 | 0.54825 | 10.62 | 25.99 |
| Frequency | 2 | 1.1536 | 1.1536 | 0.57682 | 11.18 | 27.34 |
| Residual Error | 2 | 0.1032 | 0.1032 | 0.05161 | | |
| Total | 8 | 4.2197 | | | | |

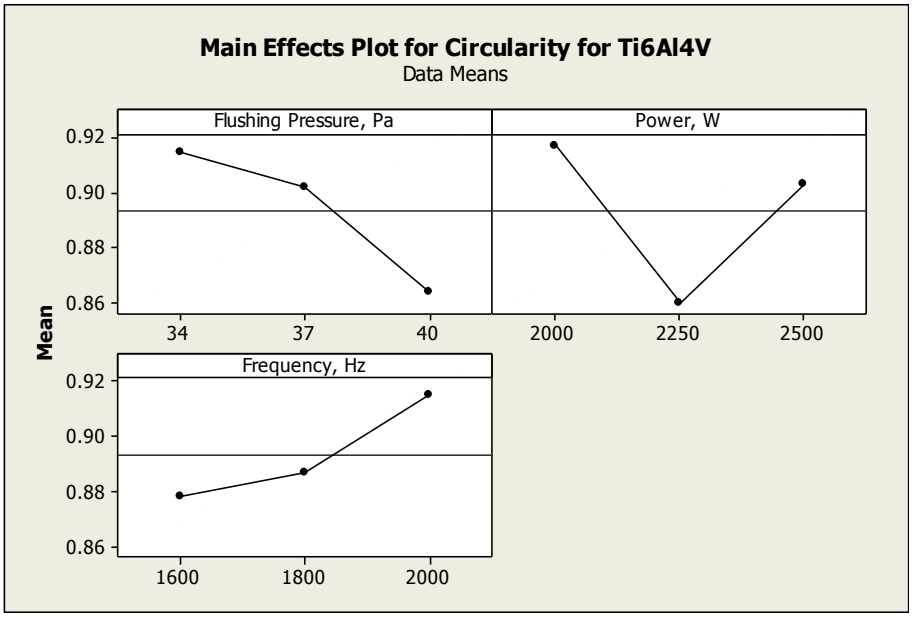


Figure 5.19: Main effect plot for circularity for the workpiece Ti6Al4V

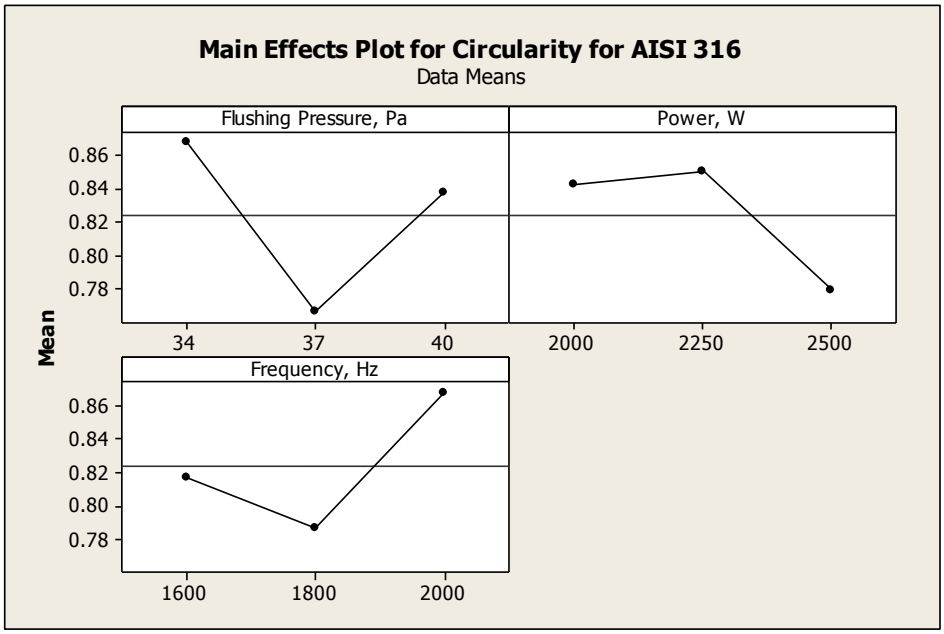


Figure 5.20: Main effect plot for circularity for the workpiece AISI 316

The comparative figure for circularity shown in Figure 5.21 suggests circularity in case of laser drilling of work piece Ti6Al4V is higher as compared to AISI 316 in most of the

experimental runs. Therefore, Ti6Al4V is preferable to AISI 316 as far as circularity is concerned in laser drilling.

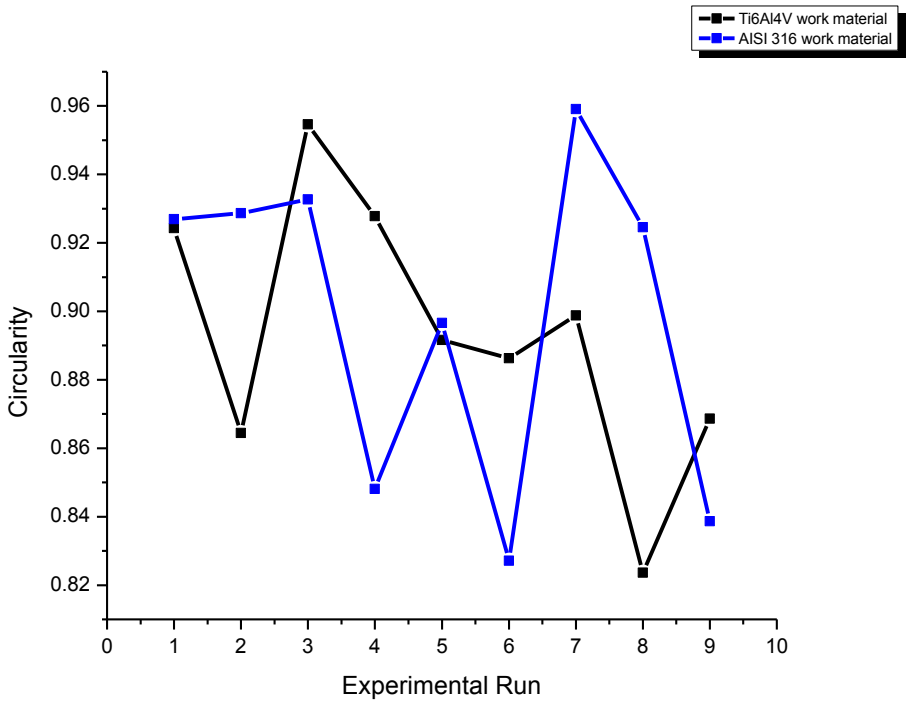


Figure 5.21: Comparison of circularity in laser drilling of Ti6Al4V and AISI-316

ANOVA for spatter area shows that laser power has higher percentage of contribution (54.75%) on spatter area during laser drilling of Ti6Al4V (Table 5.11). ANOVA for spatter area shows that frequency has contribution of 50.38% on spatter in laser drilling of AISI 316 (Table 5.12). The main effect plot shows that spatter area increases monotonously with increases in laser power and pulse frequency for the work piece Ti6Al4V (Figure 5.22). The optimal parameter setting for achieving minimum spatter area are flushing pressure of 37 Pa, laser power of 2000 W and frequency of 1600 Hz. The main effect plot shown in Figure 5.23 for laser drilling of AISI 316 indicates that minimum spatter area can be achieved at flushing pressure of 34 Pa, laser power of 2250 W and frequency of 2000 Hz.

Table 5.11: ANOVA for spatter area (Ti6Al4V)

| Source | DF | Seq SS | Adj SS | Adj MS | F | % contribution |
|---|---|---|---|---|---|---|
| Pressure | 2 | 37.255 | 37.255 | 18.627 | 2.46 | 27.94 |
| Power | 2 | 73.012 | 73.012 | 36.506 | 4.83 | 54.75 |
| Frequency | 2 | 7.975 | 7.975 | 3.988 | 0.53 | 5.98 |
| Residual Error | 2 | 15.116 | 15.116 | 7.558 | | |
| Total | 8 | 133.359 | | | | |

Table 5.12: ANOVA for spatter area (AISI 316)

| Source | DF | Seq SS | Adj SS | Adj MS | F | % contribution |
|---|---|---|---|---|---|---|
| Pressure | 2 | 81.26 | 81.26 | 40.63 | 2.78 | 32.97 |
| Power | 2 | 11.77 | 11.77 | 5.887 | 0.4 | 4.78 |
| Frequency | 2 | 124.15 | 124.15 | 62.077 | 4.25 | 50.38 |
| Residual Error | 2 | 29.24 | 29.24 | 14.619 | | |
| Total | 8 | 246.43 | | | | |

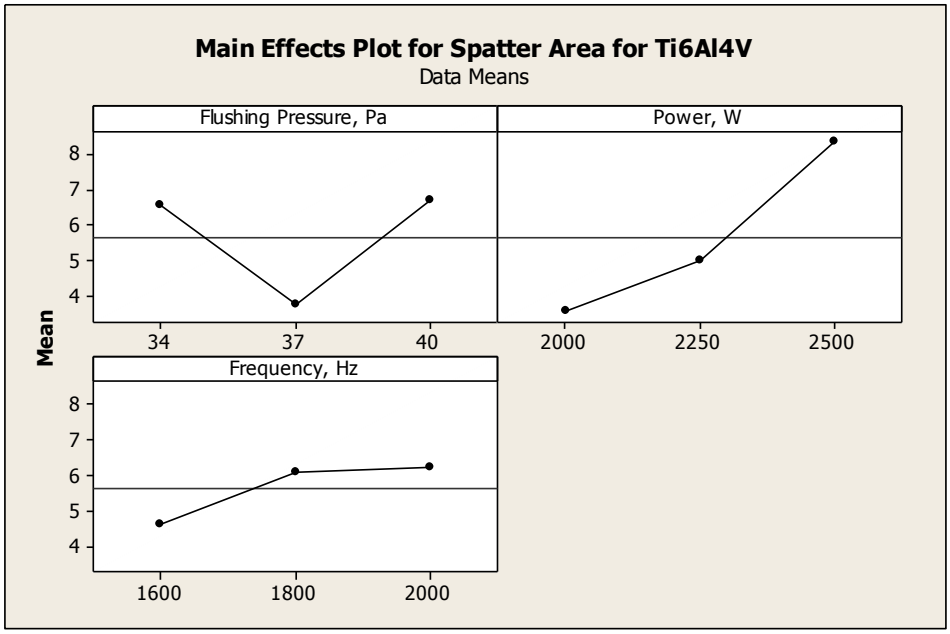


Figure 5.22: Main effect plot for spatter area for the workpiece Ti6Al4V

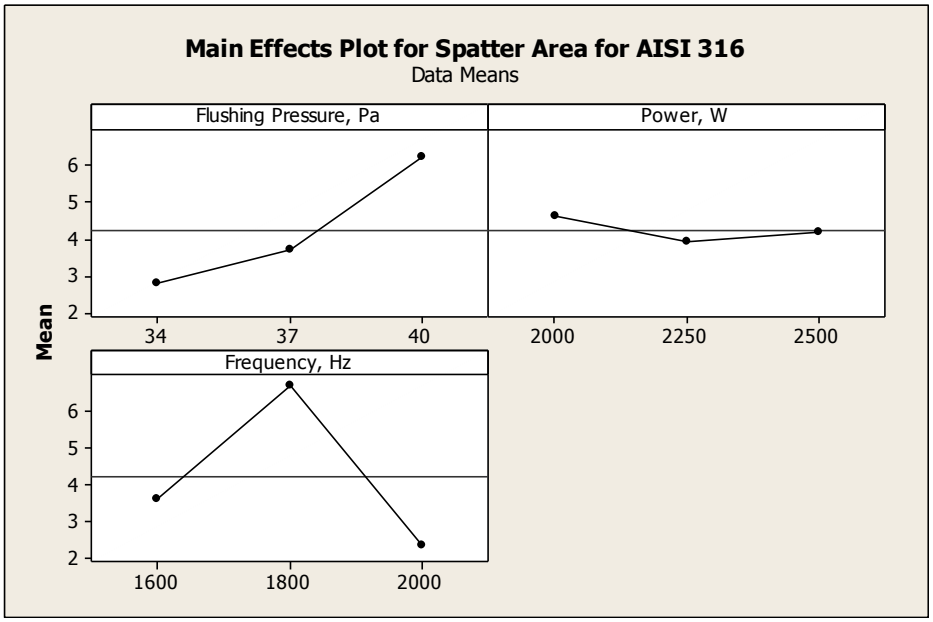


Figure 5.23: Main effect plot for spatter area for the workpiece AISI 316

The comparative analysis (Figure 5.24) for the spatter area formed near the drilled hole in the work piece AISI 316 is higher as compared to Ti6Al4V in most of the experimental runs. Therefore, Ti6Al4V is preferable to AISI 316 as far as taper is concerned in laser drilling.

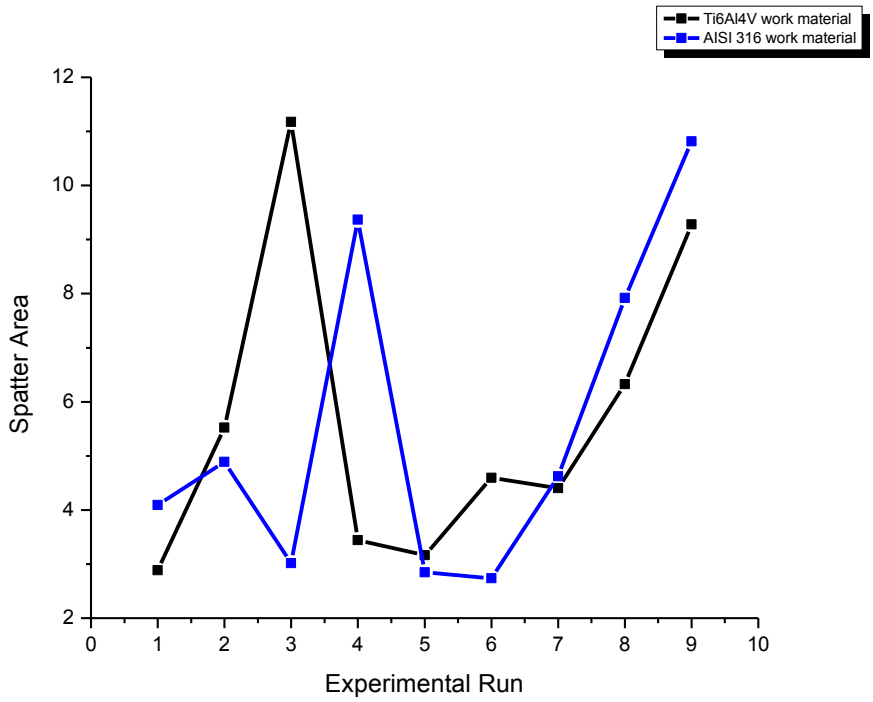


Figure 5.24: Comparative graph of spatter area formed after laser drilling of Ti6Al4V and AISI-316

**5.4. Conclusions**

This chapter describes influence of process parameters on the responses during laser drilling. Analysis of variance for all the responses such as circularity at entry, taper of the hole, spatter area near the drilled area and HAZ shows that laser power and pulse frequency are the most important factors during laser drilling of Ti6Al4V and AISI 316. The comparative study of the responses on the two different work pieces at same parametric level concludes that performance characteristics obtained after laser drilling is superior for Ti6Al4V as compared to AISI 316. The results suggest that Ti6Al4V is a preferable work piece for laser drilling

# CHAPTER 6

# EXECUTIVE SUMMARY AND FINDINGS

# CHAPTER 6

# EXECUTIVE SUMMARY AND FINDINGS

## 6.1. Introduction

The research work focuses on investigating the parametric appraisal during drilling of bio-compatible materials viz. Ti6Al4V and AISI 316. In this study, attempt has been made to develop a numerical model for drilling analysis of the work piece such as Ti6Al4V and AISI 316. To check the adequacy of the developed numerical model, experimental study has been performed (Chapter 3). The responses collected in experimental study are circularity at entry and exit, burr height at entry and exit and surface roughness. To obtain optimum parametric setting for the multiple-responses, a hybrid optimization approach has been adapted using SIR-TOPSIS method embedded with HS algorithm (Chapter 4). The study also investigates the effect of high speed $CO_2$ laser drilling using Ti6Al4V and AISI 316 samples. To understand the effect of control parameters in laser drilling process on the work pieces and to select the preferable work piece, comparative study of performance characteristics on both the work pieces has been performed (Chapter 5). The detailed outcomes and contribution is discussed in the following sections.

## 6.3. Summary of findings

In the research work, chapter 3 illustrates the application of finite element analysis for developing numerical model to predict the drilling performance characteristics. Experiments have been conducted using same parametric setting of the numerical model to validate the model. Table 6.1 shows the mean relative error (equation 3.1) obtained between the experimental and numerically evaluated values. Small mean relative error suggests that the developed numerical model is an adequate model for further analysis.

Table 6.1: Mean relative error of the drilling responses for the different materials

| Materials | Responses | Mean Relative Error (%) |
|---|---|---|
| Ti6Al4V | Circularity at entry | 5.05 |
| | Circularity at exit | 2.95 |
| | Thrust Force | 4.71 |
| | Torque | 4.67 |
| AISI 316 | Circularity at entry | 4.7 |
| | Circularity at exit | 2.51 |

| | |
|---|---|
| Thrust Force | 8.91 |
| Torque | 4.62 |

In chapter 4, a hybrid approach for optimization of multiple responses simultaneously using SIR-TOPSIS embedded with HS algorithm has been proposed. Drilling experiments for Ti6Al4V and AISI 316 work pieces have been conducted using TiN PVD coated drill bit in dry condition. It is observed that feed rate and drill diameter have significant influence on burr height. In case of surface roughness, feed rate and spindle speed are the significant factors. Considering circularity at entry and exit as constraints, the other responses such as burr height at entry and exit and surface roughness are converted into single response known as r-flow using SIR-TOPSIS method. The equation between r-flow value and process parameters is developed by non-linear regression is used as objective function in HS algorithm. The optimum parametric setting and fitness values for the different materials are noted in Table 6.2.

Table 6.2: Parametric output responses and fitness values

| Drilled Material | Spindle speed (RPM) | Feed rate (mm/min) | Drill bit diameter (mm) | Fitness value |
|---|---|---|---|---|
| Ti6Al4V | 405.2366 | 49.3272 | 5 | 0.8026 |
| AISI 316 | 592.1471 | 30.2191 | 5 | 0.9151 |

In chapter 5, $CO_2$ laser is implemented for the drilling of metal alloys such as Ti6Al4V and AISI 316. Analysis of variance for the responses such as circularity, taper of hole, spatter area near the drilled area and HAZ shows that laser power and pulse frequency are the most influencing factors during laser drilling of Ti6Al4V and AISI 316. The results suggest that Ti6Al4V is a preferable workpiece as compared to AISI 316 during laser drilling when above responses are considered. The obtained results also suggest that $CO_2$ laser can also be used for the drilling of metal alloys.

**6.2. Major contribution to research work**

After extensive literature survey and research work, the following contributions are highlighted in the present research work.

- A finite element based numerical model has been developed for predicting the drilling responses of Ti6Al4V and AISI 316 using DEFORM 3D software. The model is validated through experimental observations. The model can be successfully used to predict the performance characteristics in drilling. This can help the tool engineers to reduce the experimental efforts.

- The proposed hybrid approach for multi-response optimization of drilling process using SIR-TOPSIS method with HS algorithm can help the practicing engineers to simultaneously optimize several responses. The method uses one of the efficient multi-criteria decision making method along with a latest evolutionary approach. The proposed method being quite generic can be applied to fields other than drilling.
- The optimization method proposed in the work can easily handle constrained optimization problems.
- As the effect of control parameters on performance characteristics in conventional and laser drilling has been explored in detail, the process parametric setting becomes easy for drilling.
- It is found that behavior of titanium alloy is superior in all the considered performance characteristics both in conventional and laser drilling to stainless steel.
- It is important to note that $CO_2$ laser can be successfully applied for laser drilling of alloys.

**6.4. Limitation of the study**

In spite of several advantages obtained through proposed study, the followings may be treated as limitations since they have not been addressed in this study.

- Machine tool vibration during drilling operation has been neglected.
- Interaction effect of process parameters during laser drilling has been ignored.

**6.5. Future scope**

The present work provides a wide scope for future investigators to explore many aspects of CNC drilling process and laser drilling processes. Followings are some recommendations for future research include:

- The study can be extended to study surface roughness of the hole and burr height using finite element analysis.
- Dimensional accuracy and tool wear may be included as performance characteristics.
- FEM based modeling can be done for laser operation.
- The different types of laser assistant gas can be taken as one of the control parameters in laser machining.
- Drilling study on bio-ceramics having bone-like properties may be conducted.
- The effect of control parameters during laser drilling of bio-ceramics can be studied

Abdel-Hady Gepreel, M., and Niinomi, M. (2013). Biocompatibility of Ti-alloys for long-term implantation. Journal of the mechanical behavior of biomedical materials, 20, 407-415.

Abouridouane, M., Klocke, F., and Lung, D. (2013). Microstructure-based 3D Finite Element Model for Micro Drilling Carbon Steels. Procedia CIRP, 8, 93-98.

Abouridouane, M., Klocke, F., Lung, D., and Adams, O. (2012). Size effects in micro drilling ferritic-pearlitic carbon steels. Procedia CIRP, 3, 91-96.

Adams Jr, C. M., and Hardway, G. (1965). Fundamentals of Laser Beam Machining and Drilling. IEE Transactions on Industry and General Applications, 90-96.

Akman, E., Demir, A., Canel, T., and Sinmazcelik, T. (2009). Laser welding of Ti6Al4V titanium alloys. Journal of materials processing technology, 209(8), 3705-3713.

Alghamdi, H. S., Cuijpers, V. M. J. I., Wolke, J. G. C., Van-den Beucken, J. J. J. P., and Jansen, J. A. (2013). Calcium-phosphate-coated oral implants promote osseointegration in osteoporosis. Journal of dental research, 0022034513505769.

Andriya, N., Rao, P. V., and Ghosh, S. (2012). Dry Machining of Ti-6Al-4V using PVD Coated TiAlN Tools. In Proceedings of the World Congress on Engineering, 3, 1-6.

Armendia, M., Garay, A., Iriarte, L. M., and Arrazola, P. J. (2010). Comparison of the machinabilities of Ti6Al4V and TIMETAL 54M using uncoated WC–Co tools. Journal of Materials Processing Technology, 210(2), 197-203

Arrazola, P. J., Garay, A., Iriarte, L. M., Armendia, M., Marya, S., and Le Maitre, F. (2009). Machinability of titanium alloys (Ti6Al4V and Ti555. 3). Journal of Materials Processing Technology, 209(5), 2223-2230.

Asilturk, I. and Neseli, S. (2012), Multi response optimisation of CNC turning parameters via Taguchi method-based response surface analysis. Measurement, 45(4), 785-794.

Aurich, J. C., Dornfeld, D., Arrazola, P. J., Franke, V., Leitz, L., and Min, S. (2009). Burrs—analysis, control and removal. CIRP Annals-Manufacturing Technology, 58(2), 519-542

Bagci, E., and Ozcelik, B. (2006). Finite element and experimental investigation of temperature changes on a twist drill in sequential dry drilling. The International Journal of Advanced Manufacturing Technology, 28(7-8), 680-687.

Bandyopadhyay, S., Gokhale, H., Sarin Sundar, J. K., Sundararajan, G., and Joshi, S. V. (2005). A statistical approach to determine process parameter impact in Nd: YAG laser drilling of IN718 and Ti-6Al-4V sheets. Optics and Lasers in Engineering, 43(2), 163-182.

Baskar, N., Asokan, P., Prabhaharan, G., and Saravanan, R. (2005). Optimization of machining parameters for milling operations using non-conventional methods. The International Journal of Advanced Manufacturing Technology, 25(11-12), 1078-1088.

Bellows, G., and Kohls, J. B. (1982). Drilling Without Drills. AM. Machinist., 126(3), 173-188.

Bharatish, A., Narasimha Murthy, H.N., Anand, B., Madhusoodana, C.D., Praveena, G.S., Krishna, M. (2013) Characterization of hole circularity and heat affected zone in pulsed $CO_2$ laser drilling of alumina ceramics. Optics and Laser Technology, 53, 22-32.

Bhowmick, S., Lukitsch, M. J., and Alpas, A. T. (2010). Dry and minimum quantity lubrication drilling of cast magnesium alloy (AM60). International Journal of Machine Tools and Manufacture, 50(5), 444-457.

Biswas, A., and Dutta Majumdar, J. (2009). Surface characterization and mechanical property evaluation of thermally oxidized Ti-6Al-4V. Materials Characterization, 60(6), 513-518.

Bouzakis, K. D., Gerardis, S., Katirtzoglou, G., Makrimallakis, S., Bouzakis, A., Cremer, R., and Fuss, H. G. (2009). Application in milling of coated tools with rounded cutting edges after the film deposition. CIRP Annals-Manufacturing Technology, 58(1), 61-64.

Boyer, R. R. (1996). An overview on the use of titanium in the aerospace industry. Materials Science and Engineering: A, 213(1), 103-114.

Brajdic, M., Walther, K., and Eppelt, U. (2008). Analysis of laser drilled deep holes in stainless steel by superposed pulsed Nd: YAG laser radiation. Optics and lasers in engineering, 46(9), 648-655.

Brans, J. P., Vincke, P., and Mareschal, B. (1986). How to select and how to rank projects: The PROMETHEE method. European journal of operational research, 24(2), 228-238.

Cantero, J. L., Tardío, M. M., Canteli, J. A., Marcos, M., and Miguélez, M. H. (2005). Dry drilling of alloy Ti–6Al–4V. International Journal of Machine Tools and Manufacture, 45(11), 1246-1255.

Cao, W., and Hench, L. L. (1996). Bioactive materials. Ceramics international, 22(6), 493-507

Caydas, U., Hascalik, A., Buytoz, O., and Meyveci, A. (2011). Performance evaluation of different twist drills in dry drilling of AISI 304 austenitic stainless steel. Materials and Manufacturing Processes, 26(8), 951-960.

Chen, W. C., and Liu, X. D. (2000). Study on the various coated twist drills for stainless steels drilling. Journal of Materials Processing Technology, 99(1), 226-230.

Chow, H. M., Lee, S. M., and Yang, L. D. (2008). Machining characteristic study of friction drilling on AISI 304 stainless steel. Journal of materials processing technology, 207(1), 180-186.

Chryssolouris, G., Bredt, J., Kordas, S., and Wilson, E. (1988). Theoretical aspects of a laser machine tool. Journal of Manufacturing Science and Engineering, 110(1), 65-70.

Cicek, A., Kivak, T., and Ekici, E. (2013). Optimization of drilling parameters using Taguchi technique and response surface methodology (RSM) in drilling of AISI 304 steel with cryogenically treated HSS drills. Journal of Intelligent Manufacturing, 1-11.

Cobos, C., Leon, E., and Mendoza, M. (2013). A harmony search algorithm for clustering with feature selection. Revista Facultad de Ingenieria, (55), 153-164.

Constantin, C., Mihai Croitoru, S. M., Constantin, G., and Florinel Bisu, C. (2010). 3D FEM analysis of cutting processes. In Proc. Of the 3rd WSEAS International Conference on Visualization, Imaging and Simulation, Faro, Portugal (41-46).

Corduan, N., Himbart, T., Poulachon, G., Dessoly, M., Lambertin, M., Vigneau, J., and Payoux, B. (2003). Wear mechanisms of new tool materials for Ti-6AI-4V high performance machining. CIRP Annals-Manufacturing Technology, 52(1), 73-76.

Cus, F., and Balic, J. (2003). Optimization of cutting process by GA approach. Robotics and Computer-Integrated Manufacturing, 19(1), 113-121.

Dewidar, M. M., Khalil, K. A., and Lim, J. K. (2007).Processing and mechanical properties of porous 316L stainless steel for biomedical applications. Transactions of Nonferrous Metals Society of China, 17(3), 468-473.

Dornfeld, D. A., Kim, J. S., Dechow, H., Hewson, J., and Chen, L. J. (1999). Drilling burr formation in titanium alloy, Ti-6AI-4V. CIRP Annals-Manufacturing Technology, 48(1), 73-76.

El-Abd, M. (2013). An improved global-best harmony search algorithm. Applied Mathematics and Computation, 222, 94-106.

El-Taweel, T. A., Abdel-Maaboud, A. M., Azzam, B. S., and Mohammad, A. E. (2009). Parametric studies on the $CO_2$ laser cutting of kevlar-49 composite. The International Journal of Advanced Manufacturing Technology, 40(9-10), 907-917.

Fasasi, A. Y., Mwenifumbo, S., Rahbar, N., Chen, J., Li, M., Beye, A. C., Arnold, C.B., and Soboyejo, W. O. (2009). Nano-second UV laser processed micro-grooves on Ti6Al4V for biomedical applications. Materials Science and Engineering: C, 29(1), 5-13.

Ferreira, J. R., Coppini, N. L., and Levy Neto, F. (2001). Characteristics of carbon–carbon composite turning. Journal of Materials Processing Technology, 109(1), 65-71.

Fleck, C., and Eifler, D. (2010). Corrosion, fatigue and corrosion fatigue behaviour of metal implant materials, especially titanium alloys. International journal of fatigue, 32(6), 929-935

Fluhrer, J. (2006). Deform 3D User's Manual Version 6.0. Scientific Forming Technologies Corporation, Columbus, OH.

Gaitonde, V. N., Karnik, S. R., Achyutha, B. T., and Siddeswarappa, B. (2007). Methodology of Taguchi optimization for multi-objective drilling problem to minimize burr size. The International Journal of Advanced Manufacturing Technology, 34(1-2), 1-8.

Gaitonde, V. N., Karnik, S. R., Achyutha, B. T., and Siddeswarappa, B. (2008). Genetic algorithm-based burr size minimization in drilling of AISI 316L stainless steel. Journal of materials processing technology, 197(1), 225-236.

Gaitonde, V. N., Karnik, S. R., Achyutha, B. T., and Siddeswarappa, B. (2008). Taguchi optimization in drilling of AISI 316L stainless steel to minimize burr size using multi-performance objective based on membership function. Journal of materials processing technology, 202(1), 374-379.

Gaitonde, V. N., Karnik, S. R., Siddeswarappa, B., and Achyutha, B. T. (2008). Integrating Box-Behnken design with genetic algorithm to determine the optimal parametric combination for minimizing burr size in drilling of AISI 316L stainless steel. The International Journal of Advanced Manufacturing Technology, 37(3-4), 230-240.

Gandarias, A., Lopez de Lacalle, L. N., Aizpitarte, X., and Lamikiz, A. (2008). Study of the performance of the turning and drilling of austenitic stainless steels using two coolant techniques. International Journal of Machining and Machinability of Materials, 3(1), 1-17.

Gao, F., Tian, X., Liu, S., and Li, B. (2012). The Simulation on Drilling of Carbon Fiber Reinforced Plastic Composites. In Proceedings of the 2012 International Conference on Computer Application and System Modeling. Atlantis Press.

Gao, X. J., Li, H., Liu, Q., Zou, P., and Liu, F. (2011). Simulation of stainless steel drilling mechanism based on Deform-3D. Advanced Materials Research, 160, 1685-1690.

Gao, X. J., Zou, P., Liu, Q., and Gao, H. H. (2011). Study on the Effects of the Geometrical Parameter of Twist Drill on the Drilling Performance of Stainless Steel. Advanced Materials Research, 189, 2251-2254.

Garcia-Alonso, M. C., Saldana, L., Valles, G., Gonzalez-Carrasco, J. L., Gonzalez-Cabrero, J., Martınez, M. E., Gil-Garay, E., and Munuera, L. (2003). In vitro corrosion behaviour and osteoblast response of thermally oxidised Ti6Al4V alloy. Biomaterials, 24(1), 19-26.

Gardner, J. D., and Dornfeld, D. (2006). Finite element modeling of drilling using DEFORM. Laboratory for Manufacturing and Sustainability.

Geetha, M., Singh, A. K., Asokamani, R., and Gogia, A. K. (2009). Ti based biomaterials, the ultimate choice for orthopaedic implants–a review. Progress in Materials Science, 54(3), 397-425.

Ghoreishi, M., Low, D. K. Y., and Li, L. (2002). Comparative statistical analysis of hole taper

and circularity in laser percussion drilling. International Journal of Machine Tools and Manufacture, 42(9), 985-995.

Gittens, R. A., Olivares-Navarrete, R., Tannenbaum, R., Boyan, B. D., and Schwartz, Z. (2011). Electrical implications of corrosion for osseointegration of titanium implants. Journal of dental research, 90(12), 1389-1397.

Gorsse, S., and Miracle, D. B. (2003). Mechanical properties of Ti-6Al-4V/TiB composites with randomly oriented and aligned TiB reinforcements. Acta Materialia, 51(9), 2427-2442.

Guo, Y. B., and Caslaru, R. (2011). Fabrication and characterization of micro dent arrays produced by laser shock peening on titanium Ti–6Al–4V surfaces. Journal of Materials Processing Technology, 211(4), 729-736.

Haq, A. N., Karthikeyan, K., Sivakumar, K., and Saravanan, R. (2006). Particle swarm optimization (PSO) algorithm for optimal machining allocation of clutch assembly. The International Journal of Advanced Manufacturing Technology, 27(9-10), 865-869.

Hascalik, A., and Caydas, U. (2007). Electrical discharge machining of titanium alloy (Ti–6Al–4V). Applied Surface Science, 253(22), 9007-9016.

Hench, L. L. (1998). Biomaterials: a forecast for the future. Biomaterials, 19(16), 1419-1423.

Hench, L. L., and Ethridge, E. C. Biomaterials: an interfacial approach. 1982. Academic, New York.

Homsy, C. A., Ansevin, K. D., O'bannon, W., Thompson, S. A., Hodge, R., and Estrella, M. E. (1970). Rapid in vitro screening of polymers for biocompatibility. Journal of Macromolecular Science - Chemistry, 4(3), 615-634.

Hong, S. Y., and Ding, Y. (2001). Cooling approaches and cutting temperatures in cryogenic machining of Ti-6Al-4V. International Journal of Machine Tools and Manufacture, 41(10), 1417-1437.

Jeon, Y., and Lee, C. M. (2012). Current research trend on laser assisted machining. International Journal of Precision Engineering and Manufacturing, 13(2), 311-317.

Jha, A. K., Singh, S. K., Swathi Kiranmayee, M., Sreekumar, K., and Sinha, P. P. (2010). Failure analysis of titanium alloy (Ti6Al4V) fastener used in aerospace application. Engineering Failure Analysis, 17(6), 1457-1465.

Kadirgama, K., Abou-El-Hossein, K. A., Mohammad, B., Al-Ani, H., and Noor, M. M. (2008). Cutting force prediction model by FEA and RSM when machining Hastelloy C-22HS with 90 holder. Journal of Scientific and Industrial Research, 67, 421-427.

Karnik, S. R., and Gaitonde, V. N. (2008). Development of artificial neural network models to study the effect of process parameters on burr size in drilling. The International Journal of

Advanced Manufacturing Technology, 39(5-6), 439-453.
Karnik, S. R., Gaitonde, V. N., and Davim, J. P. (2008). A comparative study of the ANN and RSM modeling approaches for predicting burr size in drilling. The International Journal of Advanced Manufacturing Technology, 38(9-10), 868-883.
Karpat, Y., and Ozel, T. (2008). Process simulations for 3D turning using uniform and variable microgeometry PCBN tools. International Journal of Machining and Machinability of Materials, 4(1), 26-38.
Kayali, Y., Buyuksagis, A., Gunes, I., and Yalcin, Y. (2013). Investigation of corrosion behaviors at different solutions of boronized AISI 316L stainless steel. Protection of Metals and Physical Chemistry of Surfaces, 49(3), 348-358.
Kilickap, E. (2010). Modeling and optimization of burr height in drilling of Al-7075 using Taguchi method and response surface methodology. The International Journal of Advanced Manufacturing Technology, 49(9-12), 911-923.
Kilickap, E., and Huseyinoglu, M. (2010). Selection of optimum drilling parameters on burr height using response surface methodology and genetic algorithm in drilling of AISI 304 stainless steel. Materials and Manufacturing Processes, 25(10), 1068-1076.
Kivak, T., Samtas, G., and Cicek, A. (2012). Taguchi method based optimisation of drilling parameters in drilling of AISI 316 steel with PVD monolayer and multilayer coated HSS drills. Measurement, 45(6), 1547-1557.
Ko, S. L., Chang, J. E., and Kaipakjian, S. (2003). Development of drill geometry for burr minimization in drilling. CIRP Annals-Manufacturing Technology, 52(1), 45-48.
Ko, S. L., Chang, J. E., and Yang, G. E. (2003). Burr minimizing scheme in drilling. Journal of Materials Processing Technology, 140(1), 237-242.
Kolahan, F., and Liang, M. (1996). A tabu search approach to optimization of drilling operations. Computers and industrial engineering, 31(1), 371-374.
Kolahan, F., and Liang, M. (2000). Optimization of hole-making operations: a tabu-search approach. International Journal of Machine Tools and Manufacture, 40(12), 1735-1753
Kosaraju, S., and Anne, V. G. (2013). Optimal machining conditions for turning Ti-6Al-4V using response surface methodology. Advances in Manufacturing, 1(4), 329-339.
Kuar, A. S., Doloi, B., and Bhattacharyya, B. (2006). Modelling and analysis of pulsed Nd: YAG laser machining characteristics during micro-drilling of zirconia ($ZrO_2$). International Journal of Machine Tools and Manufacture, 46(12), 1301-1310.
Kudla, L. A. (2011). Fracture phenomena of microdrills in static and dynamic conditions. Engineering fracture mechanics, 78(1), 1-12.

Kumar Pandey, A., and Kumar Dubey, A. (2012). Simultaneous optimization of multiple quality characteristics in laser cutting of titanium alloy sheet. Optics and Laser Technology, 44(6), 1858-1865.

Kumar, S., and Satsangi, P. S. (2013). Multiple-response optimization of turning machining by the taguchi method and the utility concept using uni-directional glass fiber-reinforced plastic composite and carbide (k10) cutting tool. Journal of Mechanical Science and Technology, 27(9), 2829-2837.

Kuram, E., and Ozcelik, B. (2014). Micro Milling. In Modern Mechanical Engineering (pp. 325-365). Springer Berlin Heidelberg.

Kurt, M., Bagci, E., and Kaynak, Y. (2009). Application of Taguchi methods in the optimization of cutting parameters for surface finish and hole diameter accuracy in dry drilling processes. The International Journal of Advanced Manufacturing Technology, 40(5-6), 458-469.

Kyratsis, P., Bilalis, N., and Antoniadis, A. (2011). CAD-based simulations and design of experiments for determining thrust force in drilling operations. Computer-Aided Design, 43(12), 1879-1890.

Lee, K. S., and Geem, Z. W. (2005). A new meta-heuristic algorithm for continuous engineering optimization: harmony search theory and practice. Computer methods in applied mechanics and engineering, 194(36), 3902-3933.

Lee, S. M., Chow, H. M., Huang, F. Y., and Yan, B. H. (2009). Friction drilling of austenitic stainless steel by uncoated and PVD AlCrN-and TiAlN-coated tungsten carbide tools. International Journal of Machine Tools and Manufacture, 49(1), 81-88.

Leone, C., Genna, S., Caprino, G., and De Iorio, I. (2010). AISI 304 stainless steel marking by a Q-switched diode pumped Nd: YAG laser. Journal of Materials Processing Technology, 210(10), 1297-1303.

Leyens, C., and Peters, M. (2003). Titanium and titanium alloys (p. 187). Wiley-VCH, Weinheim.

Li, P., Kangasniemi, I., Groot, K., and Kokubo, T. (1994). Bonelike Hydroxyapatite Induction by a Gel-Derived Titania on a Titanium Substrate. Journal of the American Ceramic Society, 77(5), 1307-1312.

Li, R., Riester, L., Watkins, T. R., Blau, P. J., and Shih, A. J. (2008). Metallurgical analysis and nanoindentation characterization of Ti–6Al–4V workpiece and chips in high-throughput drilling. Materials Science and Engineering: A, 472(1), 115-124.

Li, Y., Wong, C., Xiong, J., Hodgson, P., and Wen, C. E. (2010). Cytotoxicity of titanium and titanium alloying elements. Journal of dental research, 89(5), 493-497.

Liao, H. C. (2006). Multi-response optimization using weighted principal component. The International Journal of Advanced Manufacturing Technology, 27(7-8), 720-725.

Lin, C., Kang, S. K., and Ehmann, K. F. (1995). Helical micro-drill point design and grinding. Journal of Manufacturing Science and Engineering, 117(3), 277-287.

Lin, T. R., and Shyu, R. F. (2000). Improvement of tool life and exit burr using variable feeds when drilling stainless steel with coated drills. The International Journal of Advanced Manufacturing Technology, 16(5), 308-313.

Lin, Y. K., and Yeh, C. T. (2012). Multi-objective optimization for stochastic computer networks using NSGA-II and TOPSIS. European Journal of Operational Research, 218(3), 735-746.

Low, D. K. Y., Li, L., and Byrd, P. J. (2000). The effects of process parameters on spatter deposition in laser percussion drilling. Optics and Laser Technology, 32(5), 347-354.

Low, D. K. Y., Li, L., Corfe, A. G., and Byrd, P. J. (2001). Spatter-free laser percussion drilling of closely spaced array holes. International Journal of Machine Tools and Manufacture, 41(3), 361-377.

Lutjering, G., and Wiliams, J. G. (2003). Titanium Springer-Verlag. Berlin Heidelberg.

Mahdavi, M., Fesanghary, M., and Damangir, E. (2007). An improved harmony search algorithm for solving optimization problems. Applied mathematics and computation, 188(2), 1567-1579.

Majumdar, D., and Manna, I. (2011). Laser material processing. International Materials Reviews, 56(5-6), 341-388.

Mandal, N., Doloi, B., Mondal, B., and Das, R. (2011). Optimization of flank wear using Zirconia Toughened Alumina (ZTA) cutting tool: Taguchi method and Regression analysis. Measurement, 44(10), 2149-2155.

Manjarres, D., Landa-Torres, I., Gil-Lopez, S., Del Ser, J., Bilbao, M. N., Salcedo-Sanz, S., and Geem, Z. W. (2013). A survey on applications of the harmony search algorithm. Engineering Applications of Artificial Intelligence, 26(8), 1818-1831.

Marasi, A., (2013). Modeling the effects of cutting parameters on the main cutting force of Ti6Al4V alloy by using hybrid approach. International Journal of Advanced Engineering Applications, 2 (5), 6-14.

Marzouk, M. (2008). A superiority and inferiority ranking model for contractor selection. Construction Innovation: Information, Process, Management, 8(4), 250-268.

Meena, V. K., and Azad, M. S. (2012). Grey relational analysis of micro-EDM machining of Ti-6Al-4V alloy. Materials and Manufacturing Processes, 27(9), 973-977.

Minagar, S., Berndt, C. C., Wang, J., Ivanova, E., and Wen, C. (2012). A review of the

application of anodization for the fabrication of nanotubes on metal implant surfaces. Acta biomaterialia, 8(8), 2875-2888.

Mishra, S., and Yadava, V. (2013). Modeling and optimization of laser beam percussion drilling of thin aluminum sheet. Optics and Laser Technology, 48, 461-474.

Montgomery, D. C. (2009). Factorial experiments. Design and analysis of experiments, 7th edn. Hoboken, NJ: John Wiley and Sons, Inc.

Montgomery, D.C., 2003. Design and Analysis of Experiments. John Wiley and Sons, New York.

Muhammad, R., Ahmed, N., Shariff, Y. M., and Silberschmidt, V. V. (2012). Finite-element analysis of forces in drilling of Ti-alloys at elevated temperature. Solid State Phenomena, 188, 250-255.

Murr, L. E., Quinones, S. A., Gaytan, S. M., Lopez, M. I., Rodela, A., Martinez, E. Y., Hernandez, D. H., Martinez, E., Medina, F., and Wicker, R. B. (2009). Microstructure and mechanical behavior of Ti–6Al–4V produced by rapid-layer manufacturing, for biomedical applications. Journal of the mechanical behavior of biomedical materials, 2(1), 20-32.

Murr, L. E., Quinones, S. A., Gaytan, S. M., Lopez, M. I., Rodela, A., Martinez, E. Y., Hernandez, D. H., Martinez, E., Medina, F., and Wicker, R. B. (2009). Microstructure and mechanical behavior of Ti–6Al–4V produced by rapid-layer manufacturing, for biomedical applications. Journal of the mechanical behavior of biomedical materials, 2(1), 20-32.

Myers, R. H., and Montgomery, D. C. (1995). Response surface methodology: process and product optimization using designed experiments Wiley. New York.

Nagesh, S., Narasimha Murthy, H.N., Krishna, M., and Basavaraj, H. (2013) Parametric study of $CO_2$ laser drilling of carbon nano-powder/vinylester/glass nano-composites using design of experiments and grey relational analysis. Optics and Laser Technology, 48, 480-488.

Navarro, M., Michiardi, A., Castano, O., and Planell, J. A. (2008). Biomaterials in orthopaedics. Journal of the Royal Society Interface, 5(27), 1137-1158.

Oldani, C., and Dominguez, A. (2012). Titanium as a Biomaterial for Implants. Recent Advances in Arthroplasty, Dr. Samo Fokter (Ed.), Intech, Croatia.

Omran, M. G., and Mahdavi, M. (2008). Global-best harmony search. Applied Mathematics and Computation, 198(2), 643-656.

Outeiro, J. C., Dias, A. M., Lebrun, J. L., and Astakhov, V. P. (2002). Machining residual stresses in AISI 316L steel and their correlation with the cutting parameters. Machining science and technology, 6(2), 251-270.

Outeiro, J. C., Pina, J. C., M'saoubi, R., Pusavec, F., and Jawahir, I. S. (2008). Analysis of

residual stresses induced by dry turning of difficult-to-machine materials. CIRP Annals-Manufacturing Technology, 57(1), 77-80.

Padhee, S., Nayak, N., Panda, S. K., Dhal, P. R., and Mahapatra, S. S. (2012). Multi-objective parametric optimization of powder mixed electro-discharge machining using response surface methodology and non-dominated sorting genetic algorithm. Sadhana, 37(2), 223-240.

Padhee, S., Pani, S., and Mahapatra, S. S. (2011). A parametric study on laser drilling of Al/SiCp metal-matrix composite. Proceedings of the Institution of Mechanical Engineers, Part B: Journal of Engineering Manufacture, 226 (1), 76-91.

Perez, J., Llorente, J. I., and Sanchez, J. A. (2000). Advanced cutting conditions for the milling of aeronautical alloys. Journal of Materials Processing Technology, 100(1), 1-11.

Pilny, L., De Chiffre, L., Piska, M., and Villumsen, M. F. (2012). Hole quality and burr reduction in drilling aluminium sheets. CIRP Journal of Manufacturing Science and Technology, 5(2), 102-107.

Pittala, G. M., and Monno, M. (2011). A new approach to the prediction of temperature of the workpiece of face milling operations of Ti-6Al-4V. Applied Thermal Engineering, 31(2), 173-180.

Poutord, A., Rossi, F., Poulachon, G., M'Saoubi, R., and Abrivard, G. (2013). Local Approach of Wear in Drilling Ti6Al4V/CFRP for Stack Modelling. Procedia CIRP, 8, 315-320.

Pradhan, M. K. (2013). Estimating the effect of process parameters on MRR, TWR and radial overcut of EDMed AISI D2 tool steel by RSM and GRA coupled with PCA. The International Journal of Advanced Manufacturing Technology, 68(1-4), 591-605.

Prusa, J. M., Venkitachalam, G., and Molian, P. A. (1999). Estimation of heat conduction losses in laser cutting. International Journal of Machine Tools and Manufacture, 39(3), 431-458.

Qi, L., Wang, X., and Meng, M. Q. (2014). 3D finite element modeling and analysis of dynamic force in bone drilling for orthopedic surgery. International journal for numerical methods in biomedical engineering. doi: 10.1002/cnm.2631.

Rahim, E. A., and Sharif, S. (2006). Investigation on tool life and surface integrity when drilling Ti-6Al-4V and Ti-5Al-4V-Mo/Fe. JSME International Journal Series C, 49(2), 340-345.

Rajamurugan, T. V., Shanmugam, K., Rajakumar, S., and Palanikumar, K. (2012). Modelling and analysis of thrust force in drilling of GFRP Composites using Response Surface Methodology (RSM). Procedia Engineering, 38, 3757-3768.

Rajmohan, T., and Palanikumar, K. (2012). Optimization of machining parameters for surface roughness and burr height in drilling hybrid composites. Materials and Manufacturing

Processes, 27(3), 320-328.
Ramesh, S., Karunamoorthy, L., and Palanikumar, K. (2008). Fuzzy modeling and analysis of machining parameters in machining titanium alloy. Materials and Manufacturing Processes, 23(4), 439-447.
Ramesh, S., Karunamoorthy, L., and Palanikumar, K. (2008). Surface roughness analysis in machining of titanium alloy. Materials and Manufacturing Processes, 23(2), 174-181.
Ratner, B. D. (Ed.). (2004). Biomaterials science: an introduction to materials in medicine. Academic press.
Reissig, L., Volkl, R., Mills, M. J., and Glatzel, U. (2004). Investigation of near surface structure in order to determine process-temperatures during different machining processes of Ti6Al4V. Scripta materialia, 50(1), 121-126.
Rivera-Denizard, O., Diffoot-Carlo, N., Navas, V., and Sundaram, P. A. (2008). Biocompatibility studies of human fetal osteoblast cells cultured on gamma titanium aluminide. Journal of Materials Science: Materials in Medicine, 19(1), 153-158.
Routara, B. C., Mohanty, S. D., Datta, S., Bandyopadhyay, A., and Mahapatra, S. S. (2010). Combined quality loss (CQL) concept in WPCA-based Taguchi philosophy for optimization of multiple surface quality characteristics of UNS C34000 brass in cylindrical grinding. The International Journal of Advanced Manufacturing Technology, 51(1-4), 135-143.
Sakurai, K., Adachi, K., and Ogawa, K. (1992). Low frequency vibratory drilling of Ti-6Al-4V alloy, Keikinzoku, 42(11), 633–637.
Sakurai, K., Adachi, K., Niba, R., and Ogawa, K. (1992). Drilling of Ti--6 Al--4 V Alloy. Journal of Japan Institute of Light Metals (Japan), 42(7), 389-394.
Mohanty, S. (2011), Micro-drilling of biocompatible materials, Graduate Studies of Texas A and M University, Master Thesis.
Sha, Z. H., Wang, F., and Zhang, S. F. (2013). Drilling Simulation of Carbon Fiber Reinforced Plastic Composites Based on Finite Element Method. Advanced Materials Research, 690, 2519-252.
Shelton, J. A., and Shin, Y. C. (2010). Comparative evaluation of laser-assisted micro-milling for AISI 316, AISI 422, TI-6AL-4V and Inconel 718 in a side-cutting configuration. Journal of Micro-mechanics and Micro-engineering, 20(7), 075012.
Shoujin Sun and Milan Brandt, Nontraditional Machining Processes, J. P. Davim (ed.), Chapter 2, Laser Beam Machining, 35-96.
Shuja, S. Z., and Yilbas, B. S. (2014). Flow and heat transfer characteristics of assisting gas impingining onto an alumina coated hole in relation to laser drilling. Optics and Laser

Technology, 59, 123-130.

Shyha, I., Soo, S. L., Aspinwall, D., and Bradley, S. (2010). Effect of laminate configuration and feed rate on cutting performance when drilling holes in carbon fibre reinforced plastic composites. Journal of materials processing technology, 210(8), 1023-1034.

Siddiquee, A. N., Khan, Z. A., and Mallick, Z. (2010). Grey relational analysis coupled with principal component analysis for optimisation design of the process parameters in in-feed centreless cylindrical grinding. The International Journal of Advanced Manufacturing Technology, 46(9-12), 983-992.

Singh, A., Datta, S., Mahapatra, S. S., Singha, T., and Majumdar, G. (2013). Optimization of bead geometry of submerged arc weld using fuzzy based desirability function approach. Journal of Intelligent Manufacturing, 24(1), 35-44.

Singh, I., Bhatnagar, N., and Viswanath, P. (2008). Drilling of uni-directional glass fiber reinforced plastics: Experimental and finite element study. Materials and Design, 29(2), 546-553.

Soreng, A. (2011). Performance of multilayer coated tool in dry machining of AISI 316 austenitic stainless steel (Doctoral dissertation).

Strenkowski, J. S., Hsieh, C. C., and Shih, A. J. (2004). An analytical finite element technique for predicting thrust force and torque in drilling. International Journal of Machine Tools and Manufacture, 44(12), 1413-1421.

Strenkowski, J. S., Shih, A. J., and Lin, J. C. (2002). An analytical finite element model for predicting three-dimensional tool forces and chip flow. International Journal of Machine Tools and Manufacture, 42(6), 723-731.

Sun, Q., Gao, B., Yang, C. C., and Chen, B. B. (2012). FEA of Micro-Hole Drilling in Stainless Steel Based on DEFORM-3D. Advanced Materials Research, 531, 566-570.

Tam, C. M., Tong, T. K., and Wong, Y. W. (2004). Selection of concrete pump using the superiority and inferiority ranking method. Journal of construction engineering and management, 130(6), 827-834.

Tamirisakandala, S., Bhat, R. B., Miracle, D. B., Boddapati, S., Bordia, R., Vanover, R., and Vasudevan, V. K. (2005). Effect of boron on the beta transus of Ti–6Al–4V alloy. Scripta materialia, 53(2), 217-222.

Tamura, S., Matsumura, T., and Arrazola, P. J. (2012). Cutting Force Prediction in Drilling of Titanium Alloy. Journal of Advanced Mechanical Design, Systems, and Manufacturing, 6(6), 753-763.

Tansel, I., Rodriguez, O., Trujillo, M., Paz, E., and Li, W. (1998). Micro-end-milling—I. Wear

and breakage. International Journal of Machine Tools and Manufacture, 38(12), 1419-1436.
Tong, L. I., Chen, C. C., and Wang, C. H. (2007). Optimization of multi-response processes using the VIKOR method. The International Journal of Advanced Manufacturing Technology, 31(11-12), 1049-1057.
Tosun, N. (2006). Determination of optimum parameters for multi-performance characteristics in drilling by using grey relational analysis. The International Journal of Advanced Manufacturing Technology, 28(5-6), 450-455.
Valarmathi, T. N., Palanikumar, K., and Sekar, S. (2012). Modeling of thrust force in drilling of plain medium density fiberboard (MDF) composite panels using RSM. Procedia Engineering, 38, 1828-1835.
Vamsi Krishna, B., Xue, W., Bose, S., and Bandyopadhyay, A. (2008). Functionally graded Co–Cr–Mo coating on Ti–6Al–4V alloy structures. Acta biomaterialia, 4(3), 697-706.
Velumania, S., Navaneethakrishnanb, P., Jayabalc, S., and Smartd, D. R. (2013). Mathematical modeling and prediction of the thrust force and torque in drilling of sisal/glass-vinyl ester hybrid composite using the RSM, MLPNN, RBFN and ENN methods. Indian Journal of Engineering and Materials Sciences, 20(4), 289-298.
Wang, J., De Boer, J., and De Groot, K. (2004). Preparation and characterization of electrodeposited calcium phosphate/chitosan coating on Ti6Al4V plates. Journal of dental research, 83(4), 296-301.
Wang, T., Ke, Y. S., and Zhou, Y. D. (2012). The Simulation of the Influence of Honed Edge Radius on the Cutting Force and Torque in Drilling 42CrMo with K-Grade Carbide Drill Bit. Applied Mechanics and Materials, 130, 1779-1784.
Welsch, G., Boyer, R., and Collings, E. W. (Eds.). (1993). Materials properties handbook: titanium alloys. ASM international.
Weyland, D. (2010). A rigorous analysis of the harmony search algorithm: How the research community can be misled by a “novel” methodology. International Journal of Applied Metaheuristic Computing (IJAMC), 1(2), 50-60.
Xu, X. (2001). The SIR method: A superiority and inferiority ranking method for multiple criteria decision making. European Journal of Operational Research, 131(3), 587-602.
Yan, Y., Ji, L., Bao, Y., and Jiang, Y. (2012). An experimental and numerical study on laser percussion drilling of thick-section alumina. Journal of Materials Processing Technology, 212(6), 1257-1270.
Yang, K., and Ren, Y. (2010). Nickel-free austenitic stainless steels for medical applications. Science and Technology of Advanced Materials, 11(1), 014105. doi:10.1088/1468-69 1.

Yang, X. S. (2009). Harmony search as a metaheuristic algorithm. In Music-inspired harmony search algorithm (pp. 1-14). Springer Berlin Heidelberg.

Ye, H. Z., and Liu, X. Y. (2005). Microstructure and tensile properties of Ti6Al4V/AM60B magnesium matrix composite. Journal of alloys and compounds, 402(1), 162-169.

Yeo, C. Y., Tam, S. C., Jana, S., and Lau, M. W. (1994). A technical review of the laser drilling of aerospace materials. Journal of Materials Processing Technology, 42(1), 15-49.

Yilbas, B. S. (1997). Parametric study to improve laser hole drilling process. Journal of Materials Processing Technology, 70(1), 264-273.

Yoon, H. S., Wu, R., Lee, T. M., and Ahn, S. H. (2011). Geometric optimization of micro drills using Taguchi methods and response surface methodology. International Journal of Precision Engineering and Manufacturing, 12(5), 871-875.

Wadhwa, S., Madaan, J., and Chan, F. T. S. (2009). Flexible decision modeling of reverse logistics system: A value adding MCDM approach for alternative selection. Robotics and Computer-Integrated Manufacturing, 25(2), 460-469.

Zain, A. M., Haron, H., and Sharif, S. (2010). Application of GA to optimize cutting conditions for minimizing surface roughness in end milling machining process. Expert Systems with Applications, 37(6), 4650-4659.

**List of Publications**

**International Conferences**

1. **S. Chatterjee**, C. P. Mohanty and **S. S. Mahapatra**, Evaluation of two-body abrasive wear using FIS and ANN, International Conference on Advanced Materials and Manufacturing, kanyakumari, 2013.
2. **S. Chatterjee**, **S. S. Mahapatra**, C. P. Mohanty and D. K. Bagal, Parametric effect of process parameters in drilling of bio-compatible material, NIRMA 3rd International conference, Ahmedabad, India, 2013.
2. **S. Chatterjee**, **S. S. Mahapatra**, K. Abhishek and R. K. Yadav, Optimizaion of drilling process parameters by harmony search algorithm, IEEE International conference on recent advances and innovations in engineering, Jaipur, 2014.
3. C. P. Mohanty, **S. S. Mahapatra**, **S. Chatterjee** and P.C. Padhi, An experimental investigation on machinablity of inconel-718 super alloy, International conference on advancement in polymeric material, Bhubaneswar, 2014.
4. **Suman Chatterjee**, Kumar Abhishek, Rajiv Kumar Yadav, Siba Sankar Mahapatra and Saurav Datta, NSGA-II Approach of Optimization to Study the Effects of Drilling Parameters in AISI-304 Stainless Steel, 12th Global Congress on Manufacturing and Management, VIT University, Vellore, 2014. (Accepted)
5. **Suman Chatterjee,** Arpan Kumar Mondal and **Siba Sankar Mahapatra**, Combined Approach for Studying the Parametric Effects on Quality of Holes Using RSM and PCA in Drilling of AISI-304 Stainless Steel, 5th International and 26th All India Manufacturing Technology, Design and Research Conference AIMTDR 2014. (Accepted)

**International Journals**

6. Kumar Abhishek, Saurav Datta, **Suman Chatterjee** and **Siba Sankar Mahapatra**, Parametric Optimization in Turning of CFRP (epoxy) Composites: A Case Experimental Research with Exploration of HS Algorithm, Applied Mechanics and Materials, Vol. 619 (2014) pp 54-57.
7. **S. Chatterjee**, **S. S. Mahapatra**, C. P. Mohanty and D. K. Bagal, Parametric effect of process parameters in drilling of bio-compatible material, Procedia Engineering, 2014. (Accepted).
8. **Suman Chatterjee**, **Siba Sankar Mahapatra** and Kumar Abhishek, An Improved Harmony Search Algorithm for Optimization of Parameters in Drilling of Titanium Alloys, Journal of Advanced Research. (Communicated).